THREE DIMENSIONAL FINITE ELEMENT MODELING FOR THE SPUDCAN PENETRATION INTO CLAYEY SEABED

A THESIS SUBMITTED TO
THE GRADUATE SCHOOL OF NATURAL AND APPLIED SCIENCES
OF
MIDDLE EAST TECHNICAL UNIVERSITY

BY

VOLKAN EMREN

IN PARTIAL FULFILLMENT OF THE REQUIREMENTS
FOR
THE DEGREE OF THE MASTER OF SCIENCE
IN
CIVIL ENGINEERING

JULY 2015

Approval of the thesis:

THREE DIMENSIONAL FINITE ELEMENT MODELING FOR THE SPUDCAN PENETRATION INTO CLAYEY SEABED

submitted by **VOLKAN EMREN** in partial fulfillment of the requirements for the degree of **Master of Science in Civil Engineering Department, Middle East Technical University** by,

Prof.Dr. M. Gülbin Dural Ünver
Dean, Gradute School of **Natural and Applied Sciences** _____

Prof.Dr. Ahmet Cevdet Yalçıner
Head of Department, **Civil Engineering** _____

Asst. Prof. Dr. Nejan Huvaj Sarıhan
Supervisor, **Civil Engineering Dept., METU** _____

Examining Committee Members:

Prof. Dr. Tekin GÜLTOP
Civil Engineering Dept., Çankaya University _____

Asst. Prof. Dr. Nejan HUVAJ SARIHAN
Civil Engineering Dept., METU _____

Prof. Dr. Kağan TUNCAY
Civil Engineering Dept., METU _____

Assoc. Prof. Dr. Mete KÖKEN
Civil Engineering Dept., METU _____

Asst. Prof. Dr. Onur PEKCAN
Civil Engineer Dept., METU _____

Date: 24.07.2015

I hereby declare that all information in this document has been obtained and presented in accordance with academic rules and ethical conduct. I also declare that, as required by these rules and conduct, I have fully cited and referenced all material and results that are not original to this work.

Name, Last name : Volkan, EMREN
Signature :

ABSTRACT

THREE DIMENSIONAL FINITE ELEMENT MODELING FOR THE SPUDCAN PENETRATION INTO CLAYEY SEABED

Emren, Volkan
M.Sc., Department of Civil Engineering
Supervisor: Asst. Prof. Dr. Nejan Huvaj Sarıhan

July 2015, 108 pages

The penetration of the foundation for "jack-up rig" type offshore oil platform (spudcan) into a uniform clayey seabed is studied with three dimensional finite element modeling (Abaqus 6.14) using Coupled Eulerian Lagrangian method. Although there exists some analytical methods (InSafeJIP etc.) for the calculation of the spudcan bearing capacity, they frequently underestimate or overestimate the bearing capacity due to simplifications involved. For the spudcan geometry and soil properties used in this study, based on the 3D FEM analyses, the required penetration depth for a target bearing capacity of spudcans can be reduced by 2 to 4 m. Rate of increase of the bearing capacity with depth is larger in 3D FEM analyses as compared to InSafeJIP method, which may also result in significant savings, however this finding is limited for the spudcan geometry and soil properties used in this study. A systematic parametric study is conducted for the variables that affect the spudcan penetration resistance. These parameters were spudcan diameter (7.5 to 15 m), spudcan cone angle (90 to 150 degrees), roughness of spudcan surface (roughness coefficient of 0 to 1.0), undrained shear strength of clay (20 to 80 kPa), spudcan penetration depths (3 to 20 m), and the spacing between two adjacent spudcans (spacing/diameter ratio of 1.5 to 3.0). Based on these results, spudcan size, cone tip angle etc. can be selected, for each case, to provide required penetration resistance and/or to reduce the required penetration depth.
Understanding the relations between the factors and penetration resistance based on this study, may provide a significant step in enhancing the safe and economical design and successful penetration operation of spudcans. However, it should not be forgotten that, the key is to have extensive and correct information and interpretation about the subsoil profile and material properties.

Keywords: offshore oil platform, spudcan penetration, finite element method, coupled Eulerian Lagrangian

ÖZ

AÇIK DENİZ PETROL PLATFORM TEMELLERİNİN KİLLİ ZEMİNLERE PENETRASYONUNUN 3 BOYUTLU SONLU ELEMANLAR MODELİ

Emren, Volkan
Yüksek Lisans, İnşaat Mühendisliği Bölümü
Tez Yöneticisi: Yard. Doç. Dr. Nejan Huvaj Sarıhan

Temmuz 2015, 108 sayfa

Bu tezde *jack-up* tipi açık deniz petrol platform temellerinin (*spudcan*) üniform killi deniz tabanına penetrasyonu 3 boyutlu sonlu elemanlar modeli (Abaqus 6.14) ile Bağlı Euler – Lagranj Metodu kullanılarak çalışılmıştır. Kılavuzlarda bazı analitik metodlar yer alsa da, bu temellerin taşıma kapasiteleri, metodların kullandığı bazı basitleştirmeler nedeniyle sık sık olduğundan az ya da çok tahmin edilmektedir. Bu çalışmada kullanılan spudcan geometrisi ve zemin özellikleri için, 3 boyutlu sonlu elemanlar metodu analiz sonuçları göz önüne alındığında, hedeflenen taşıma kapasiteleri için gerekli olan penetrasyon derinlikleri 2 ile 4 metre aralığında azaltılabilinir. Ayrıca 3 boyutlu sonlu elemanlar metodu analizlerinde penetrasyon derinliğine bağlı *spudcan* taşıma kapasitesi artış oranı, InSafeJIP metodlarına oranla daha fazladır ve bu da önemli tasarruflar ile sonuçlanabilir, fakat bu sonuç yalnızca bu çalışmadaki spudcan geometrisi ve zemin özellikleri için geçerlidir. *Spudcan* penetrasyon direncini etkileyen faktörler için sistematik parametrik çalışmalar yapılmıştır. Bu parametreler temelin çapı (7.5 ile 15 m arası), temel koniklik açısı (90 ile 150 derece arası), *spudcan* yüzey pürüzlülük katsayısı (0 ile 1. arası), kilin drenajsız kesme dayanımı (20 ile 80 kPa arası), spudcan penetrasyon derinliği (3 ile 20 m arası), ve iki komşu *spudcan* arasındaki uzaklıktır (uzaklık/çap oranı 1.5 ile 3.0 arası). Bu sonuçlara bağlı olarak, temel büyüklükleri, koniklik açıları gibi parametreler farklı durumlar için gerekli penetrasyon direncini sağlamak ve derinliğini azaltmak için seçilebilir. Bu çalışma ile yukarıda bahsedilen faktörler ve penetrasyon direnci arasındaki ilişkiyi anlamak, bu tip temellerin güvenli ve ekonomik dizayn ve başarılı uygulama süreçlerini arttırma konusunda önemli bir adım olabilir. Ancak, unutulmamalıdır ki, kilit nokta zemin profili ve malzeme özellikleri hakkında kapsamlı ve doğru bilgiye sahip olmaktır.

Anahtar Kelimeler: Açık Deniz Petrol Platformu, *Spudcan* Penetrasyonu, Sonlu Elemanlar Metodu, Bağlı Euler – Lagranj

To My Family

ACKNOWLEDGEMENTS

I am grateful to my supervisor, Asst. Prof. Dr. Nejan Huvaj, whose expertise, understanding, generous guidance, and smiling face made it possible for me to work on a topic that was of great interest to me. It was a pleasure working with her.

I am hugely indebted to Prof. Dr. Kağan Tuncay for finding time to reply my questions, for being ever so kind to show interest in my research, and for giving his precious and kind advice regarding the topic of my thesis. Sir, words can never be enough to thank your kindness.

I am highly indebted, and throughly grateful to my dearie friend, Ezgi Budak for giving the right advice at the right time and for being a source of motivation. Ezgi, I will not forget what you have done for me so far, and I do not think I can ever repay the debt I owe you.

I would also like to express my special gratitude to Begüm Güray for being a paragon in my life with her unending patience, love, and support. Begüm, I do not think I will meet someone like you ever again.

I wish to thank my family; my mother Nilgün Emren, my father İzzet Emren, and my sister Selinay Emren for their great encouragement about the next steps of my academic life. I am grateful for their understanding and patience in every minute of this period.

I would like to express my gratitude to all faculty members of Civil Engineering Department of Cankaya University for providing me such peaceful work environment, and giving me their precious advice about the career that I am searching for.

Finally, I would like to thank all the instructors in METU. I learned much throughout my undergraduate, and graduate studies.

TABLE OF CONTENTS

LIST OF FIGURES

LIST OF TABLES

CHAPTER 1

INTRODUCTION

As the demand for oil increases day by day, it is required to explore it even in the offshore locations. For this purpose, offshore platforms are used to produce oil. This production process includes the extraction of the oil from the drilled wells, and the transitory storage of the oil before its journey to markets.

Design, construction, and maintenance of offshore oil platforms, and their dismissal from the site are the main considerations in offshore geotechnical engineering. This branch of civil engineering is different from the onshore engineering since these are large structures standing over considerable heights in water, and their service life are ranging between 25 to 50 years (Dean, 2010).

Exploration of offshore oil and natural gas is one of the major operations in the oil and gas industry. Depth of water is one of the main criteria that determines the type of structure to be used in order to reach the product. These structures can be categorized into several types (McLendon, 2010):

- Fixed Platforms
- Compliant Towers
- Semi-submersible
- Floating Platforms
- Tension Leg Platforms
- Jack-up Rigs
- Spar

In this thesis, the main focus will be on the jack-up rigs. (Figure 1.1) Their floating platforms are brought to its location by ships, and their legs are lowered down into the seabed with rates in the range of e.g. 0.01m/s (*Maersk Interceptor*, n.d.) to 1.7 m/s (Tho, Leung, Chow, & Swaddiwudhipong, 2012). After the legs are stabilized, the platform elevates above the surface of the water. It is possible to adjust the height of these platforms. This type of offshore oil platforms is used in relatively shallow depths up to 150m (Dean, 2010) since it is not practical to reach greater depths for the legs. They are considered to be safer than any other transportable legs as their platforms are located above the water, which provides resistance against environmental effects.

Figure 1.1 The ASTRA Jack-up Rig ("Jack-up rigs," n.d.)

As it can be seen from Figure 1.1, jack-up oil platforms typically have three legs, and they are in the form of lattice steel trusses. These legs are the ones that carry the weight of the rig. Furthermore, with the help of their foundations, i.e. spudcans, weight and other external forces from the platform is distributed over a large area. A spudcan typically have a polygonal shape, and for simplified calculations it can be idealized as a cone shape. Moreover, thanks to its pointy end, it can penetrate into seabed, easily. Their diameter can range from 10 to 25 m ("Punch-Through of Jack-Up Spudcan Foundation in Sand Overlying Clay," 2008). In Figure 1.2, typical spudcan shapes are presented in order to give some idea about typical shapes and sizes.

Figure 1.2 a) A Spudcan ("WIND CARRIER - SPUDCAN," 2011), b) a Spudcan Equipped with Truss-worked Leg ("UWA team to investigate new footings for mobile drilling rigs | Energy and Minerals Institute," n.d.)

While jack-up oil platforms are in service, they confront severe environmental conditions. One of the main issues is the axial load due to the weight of the rig that the legs should carry. Moreover, lateral loads and cyclic loads due to continuous waves and wind are also of concern about these structures. Ship impacts are also one of the issues that the system should stand against.

Although, there are numerous burdens that a jack-up type oil platform should carry in service, may be, the most critical problem emerges immediately after spudcans start their journeys into the seabed. Penetration process includes major risks, and therefore, should be analyzed and conducted, carefully.

This thesis aims to shed light on the penetration process of spudcan type foundations into clayey seabed with realistic three dimensional finite element simulations.

1.1 Problem Statement

Jack-up oil platforms are one of the most common types of structure that are used for oil and natural gas production due to their several advantages such as relative cheapness, mobility, and ease of operation. Several investigations regarding their penetration and service life behavior have been carried out by numerous researchers, and will be mentioned in Chapter 2 of this thesis. Because of the complexity of the interaction between spudcan and the seabed, the problem involves a considerable number of variables. These variables include spudcan diameter, cone angle, roughness of spudcan surface, strength properties of soil, and so forth. The difficulty of the process and the large number of variables make it a grand challenge to develop spudcan penetration design guidelines. Although there exist some analytical methods (SNAME, InSafeJIP etc.) for calculations, they frequently underestimate or overestimate the spudcan bearing capacity due to simplifications involved in the guidelines. Therefore the results based on such simplistic guidelines can sometimes be on the unsafe side (e.g. can result in disasters) or they could be on the very safe side (e.g. resulting in uneconomical designs, i.e. requiring too much penetration for developing sufficient bearing capacity).

Investigation of the aforementioned factors and understanding the relations between them will provide a significant step in enhancing the safe and economical design and successful penetration operation of spudcans. It should not be forgotten that, the key element with utmost importance is to have extensive and correct information and interpretation about the subsoil profile and their material properties.

1.2 Research Objectives

The fundamental objective of this thesis is to investigate the penetration of spudcan type foundations into cohesive seabed by carrying out three dimensional finite element simulations. In order to achieve this objective, following steps will be taken:

(1) Determination of geometrical properties, and the applied boundary constraints (such as dimensions of the finite element model, boundary conditions, mesh resolution, and mesh properties.) for the three dimensional finite element modeling of spudcan penetration.
(2) Verification of the three dimensional finite element model accuracy.
(3) Investigation of the required spudcan penetration depth for different soil strength levels.
(4) Simulating the penetration process with different spudcan parameters, and analyzing their effects.

1.3 Scope

This thesis focuses on the spudcan foundations' penetration behavior into cohesive sea bottom soil by the use of three dimensional finite element software Abaqus 6.14 with Coupled Eulerian Lagrangian (CEL) method. Literature is discussed in Chapter 2. In Chapter 3, the basic concept of the Coupled Eulerian Lagrangian (CEL) Method is presented, and the justifications of its use for this problem, determination of simulation size, and boundary conditions are elaborated. Thereafter, in Chapter 4, theoretical

methods aiming at the penetration of spudcan foundations presented in InSafeJIP (Osborne et al., 2011) are discussed, and our numerical models are compared with them. In Chapter 5, a parametric study is performed to investigate spudcan penetration under a vast variety of conditions. Last of all, in Chapter 6, conclusions and suggestions for future studies are presented.

CHAPTER 2

LITERATURE REVIEW

A jack-up rig is one of the best alternatives among its rivals in oil production industry since it can be removed from a certain location, and be transported to another one when it is necessary,. In addition to its mobility, it allows exploration of oil for water depths up to 130 m (Tho et al., 2012). Different from the conventional construction of onshore shallow foundations, a spudcan type foundation self-penetrates into sea bottom by the application of a vertical load until it reaches the necessary resistance, and stability.

Spudcan penetration process can be divided into two main categories namely shallow and deep penetrations. In case of shallow penetration, the spudcan rests just above the mudline or slightly below it after a small amount of vertical penetration. Generally, shallow penetration is sufficient where the soil profile mainly consists of dense sand or stiff clay. However, when the seabed consists of weaker soils, or when the loads are relatively larger, deep penetration may be required in order to achieve stability.

Deep or shallow, penetration of spudcan foundations always involves considerable risks. Several oil platform accidents were recorded in history (Figure 2.1). Accidents occurred not only during the service life but also before the production of oil started. If the required penetration depth is not accurately estimated, and site investigations are not conducted at a sufficient level, there are significant risks of failure of spudcan foundation at the setup stage. These are illustrated in Figure 2.2. In order to bypass the danger of failure during penetration, one should study the seabed site characteristics carefully. Both in-situ, and lab tests should be conducted in order to predetermine the penetration location, and the required depth of penetration. Some numerical calculations can also be made for this determination. However, since the embedment procedure ends

up with large deformation of the soil profile, classical small strain - small deformation finite element analysis is not suited to this problem. Even more advanced large deformation – large strain approaches may not accurately model the penetration process because of the critical deterioration of the solution accuracy due to extreme mesh distortion. A method which doesn't suffer from mesh distortion and that can handle large deformations – large strains would be the ideal choice for spudcan penetration modeling. We use the Coupled Eulerian Lagrangian Method as it has these qualifications and has been successfully used for penetration simulations in various fields (J. Zhang et al., 2013).

Figure 2.1 Jack-up Rig Disaster ("Arabdrill 19 AD19 - Oil Rig Disasters - Offshore Drilling Accidents," 2002)

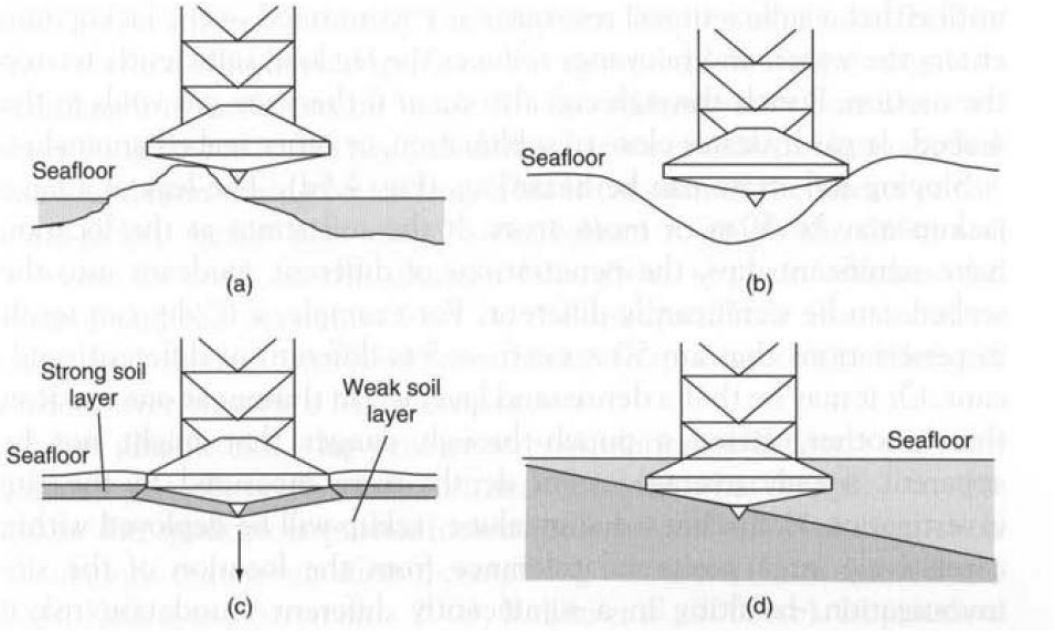

Figure 2.2 Examples of different difficult site conditions (a) Rock Outcrop (b) Softened Remolded Volumes due to Previous Jack-up Extractions (c) Punch-through Failure (d) Sloping in the Separation of Soil Materials (Dean, 2010)

Today, it is indisputable that our civilization needs fossil fuels, and due to the increasing consumption, there is an ever increasing stress on the oil industry. Acquiring them in a cheaper and easier way is the main desire. For shallow offshore drilling, jack-up oil rigs seem to be the one of the best choices. An accurate design of spudcan foundation will decrease the likelihood of accidents at the setup phase which may result in loss of lives and money. Therefore, considerable number of studies has been made for this purpose by various researchers, and will be mentioned in the upcoming pages. Researches on this topic can be divided into two main categories, which are numerical, and experimental methods.

2.1 Numerical Studies

There are some conventional simplified hand calculation methods indicated in InSafeJIP (Osborne et al., 2011) which will be discussed in Chapter 4. However, their

applicability is limited and numerical methods allows realistic simulations of complex problems with no constraints on shape, boundary or behavior of the system. Advanced numerical methods which can handle large strain – large deformation problems without running into mesh distortion issues allow realistic simulation of spudcan penetration into soil. Most popular methods used recently are the Coupled Eulerian Lagrangian (CEL) Method, and the Arbitrary Eulerian Lagrangian (ALE) Method. In addition to these, for the cases that does not require significant embedment depths (such as the small amount of penetration into very dense sand), conventional Finite Element Methods may also be used to solve these problems.

Elkadi, Lottumand, & Luger (2014) investigated the extreme impact forces in case of a touchdown of the spudcan into seabed with the help of the CEL Method implemented in the Abaqus software. In their study, the spudcan is modeled as a 3D rigid solid Lagrangian body and the soil is modeled as a 3D Eulerian body, and the foundation is placed into the Eulerian domain. However, Eulerian elements cannot occupy the same space with the Lagrangian elements. Therefore, initial Eulerian meshes that the spudcan is being held should initially be defined as void.

General contact algorithm was used between the spudcan and the seabed soil, with penalty algorithm based on friction. The writers did not give further information about the contact algorithm; therefore, it is not possible to assume the friction coefficient between these bodies. Only the half of the soil body was modeled because of the symmetry with given dimensions.

Baskarp sand (Elkadi et al., 2014) was used for the analysis in the paper, and the material properties are given in Table 2.1.

Table 2.1 Baskarp Sand Material Properties (Elkadi et al., 2014)

Material Property		
Young's Modulus	54000	kPa
Poisson's Ratio	0.35	-
Angle of Internal Friction	41	Degrees
Dilatancy Angle	9	Degrees

Elkadi et al (2014) gave a prescribed velocity to the spudcan to model the penetration process and observed the reaction forces on a reference of the spudcan in x, y, and z directions. Finally, they compared the calculated values with the measured data obtained in a centrifugal test, and showed that these values are similar.

Qiu & Henke (2011) also used Coupled Eulerian Lagrangian Method in the Abaqus software in order to model the spudcan penetration into seabed. (Figure 2.3) He modeled only the one fourth of the soil body because of the symmetry conditions, and studied two models both with uniform and with layered soil profiles. As in (Elkadi et al., 2014), displacement controlled mechanism is simulated.

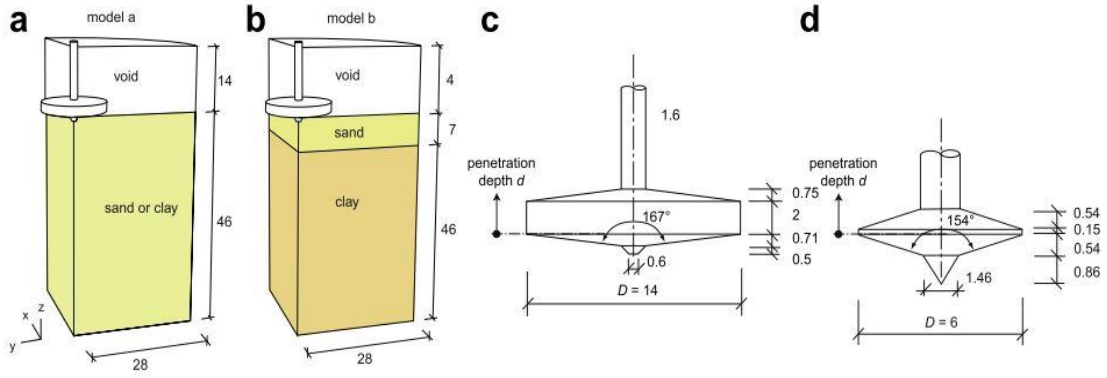

Figure 2.3 Numerical Model for Spudcan Penetration in a) Sand or Clay b) Sand overlying Clay; spudcan geometry used in c) Craig and Chua d) Teh et. Al (units in m)

In their study, they take clay as an elasto-plastic material obeying the Tresca Failure Criterion with the dilation and friction angle of 0º. The clay is assumed to be undrained with 0.49 Poisson's Ratio. Constant stiffness ratio (E_U/C_U) of 500 is adopted. On the other hand, they define sand as elasto-plastic material obeying the Mohr-Coulomb Failure Criterion with 0º dilation angle for loose sand, and φ-30º dilation angle for dense sand.

The study also looked into the determination of the effect of the coarseness of mesh, and penetration velocity. Three meshes with different coarseness have been used for the study. Mesh A has 10918 elements, mesh B consists of 48360 elements and mesh C has 259308 elements. Moreover, some calculations have been made with penetration velocities of 0.25 m/s, 0.5 m/s and 1 m/s. Their results are shown in Figure 2.4.

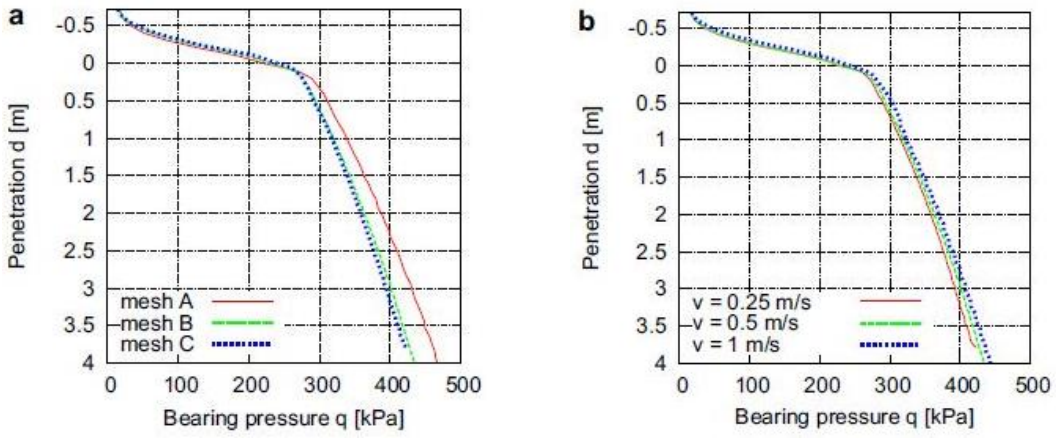

Figure 2.4 Penetration vs Bearing Pressure Curves in Uniform Clay Layer for a) different mesh coarseness b) different penetration velocities (Qiu & Henke, 2011)

From this figure, Qiu & Henke (2011) decided to use mesh B and the penetration velocity of 0.5 m/s in order to consider both accuracy and efficiency of the analysis. The study also looked into the effects of the soil-spudcan interface roughness for penetrating a spudcan into uniform clay and sand. This interface has been modeled as fully smooth, fully rough and taking into account that friction coefficient is 0.5 (Figure 2.5).

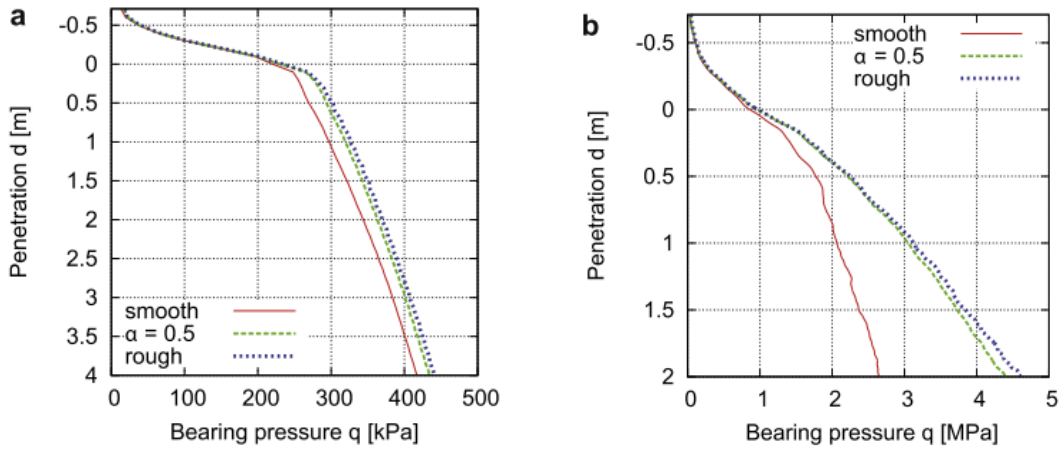

Figure 2.5 Penetration vs Bearing Pressure Curves of a Spudcan for Different Friction Coefficients between Spudcan and Soil for a) uniform clay b) uniform sand (Qiu & Henke, 2011)

They have done all these studies for both uniform clay, and uniform sand layers. The clay was modeled as elasto-plastic material, and the failure criterion was Tresca while the sand was modeled with Mohr-Coulomb failure criterion. After determining the properties of the model, the writer compares the results of his 3D numerical model with the centrifuge data, and showed their consistency.

Y. Zhang, Wang, Cassidy, & Bienen (2014) presented a study which is based on the effects of the size and shape of the surface of spudcan footing in soft clay. They considered for soil sensitivity, values between 1 and 5, and for embedment depths of the spudcan up to 3 diameters are used. The authors claimed that under combined loading, most numerical studies for embedded objects are not realistic since the spudcan foundations were assumed wished-in-place, and the bearing capacity was found for an undisturbed soil profile; however, in reality the footing installation changes the strength of the soil markedly because the soil displaces in large amounts, and remolding causes softening and reduction in the strength of the soil. Hence, the authors aimed to use a realistic soil profile for the numerical model to determine the bearing capacity of a spudcan footing correctly. For this purpose, they used large deformation finite element

approach for the continuous spudcan penetration simulation. Then the soil strength profile was constructed three dimensionally, and under combined loading small-strain finite element analyses were conducted to calculate the capacity of the spudcan. At the end of the analyses, the authors concluded that the combined bearing capacity was reduced compared with wished-in place foundation capacity, and they found that as sensitivity of soil increases, the capacity decreases. Moreover, while as the penetration depth increases, the combined bearing capacity surface increases, the surface eccentricity decreases. Furthermore, a simple expression related with the bearing capacity factor is proposed.

Hossain & Randolph, (2009) completed a study at which they combine centrifuge model testing, and large deformation finite element analysis results dealing with the spudcan penetration behavior into single clay layer. In their study, continuous failure mechanism of the soil that starts with the formation of surface heave during shallow penetration, and ends up with the backfilling of the soil over the foundation. They conducted a parametric study that validates the model against experimental test data. They also compared their results with the approaches that are suggested in the SNAME design code (SNAME, 2008) by presenting some dimensionless charts, and bearing capacity factors from their analyses. They proposed new approaches for spudcan penetration into single clay layer with constant, and linearly changing undrained shear strength at full preload. The results of the traditional small strain analyses for the pre-penetrated spudcans were matched with the results of the large deformation analyses for continuously penetrating spudcan from the seabed in homogeneous clay layer. Another result of their study is that the spudcan base roughness was found to be highly dominant in determination of the bearing capacity factor. Last of all, it was concluded that the methods suggested in SNAME guideline overestimates the required penetration depth.

Chi, Aubeny, & Zimmerman (2009) provides an analysis of the spudcan foundations with the assessment of preloading, bearing capacity, and the displacement. According to the analyses presented in their study, during preloading, spudcan penetrates into soft clay five times deeper than it does in sand. They concluded that the settlement because

of the preloading is much more critical in clay than in sand; although, a spudcan can penetrate into clay with high undrained shear strength as twice deep as that into sand with low friction angle. They shared the following graphs for this purpose (Figure 2.6).

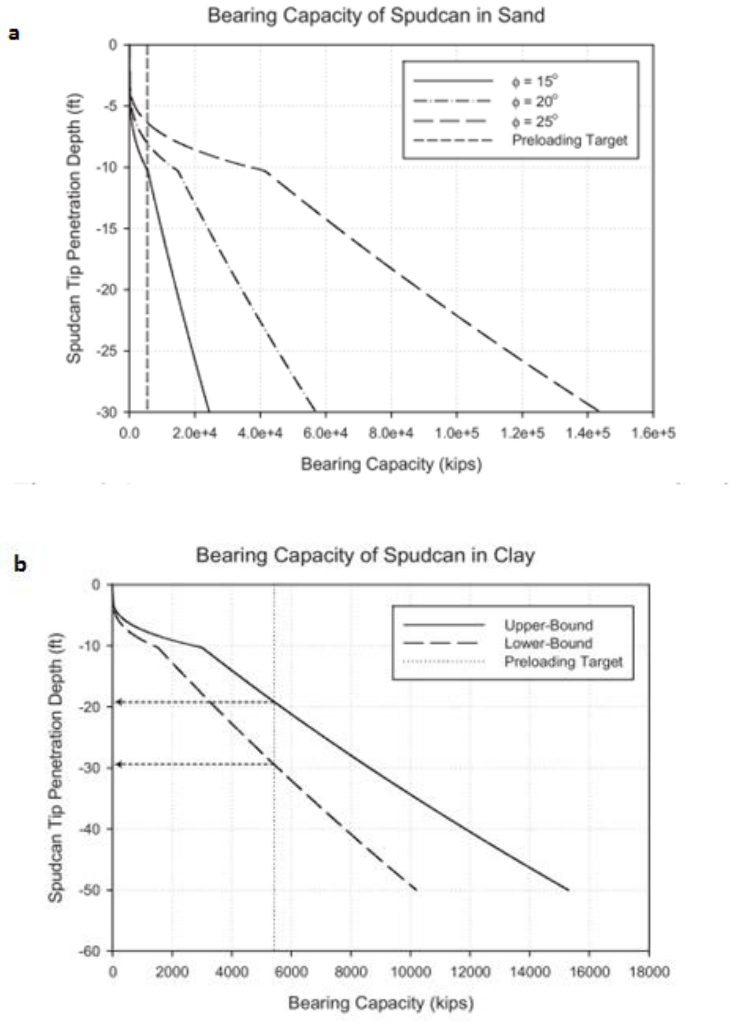

Figure 2.6 Penetration Prediction during Preloading (a) Sand, (b) Clay (Chi et al., 2009)

Yu, Hu, Liu, Randolph, & Kong (2012) studied something different which is called "punch-through failure". This might happen if the seabed that the spudcan is penetrating into consists of a stiffer layer underlain by a softer layer, e.g. a sand overlying a soft

clay. This type of soil profile can cause unexpected drop in bearing capacity as the spudcan penetrates into the soil profile, and can cause failure in offshore oil platforms. Typical bearing capacity vs penetration depth graph for this type of seabed is given in Figure 2.7.

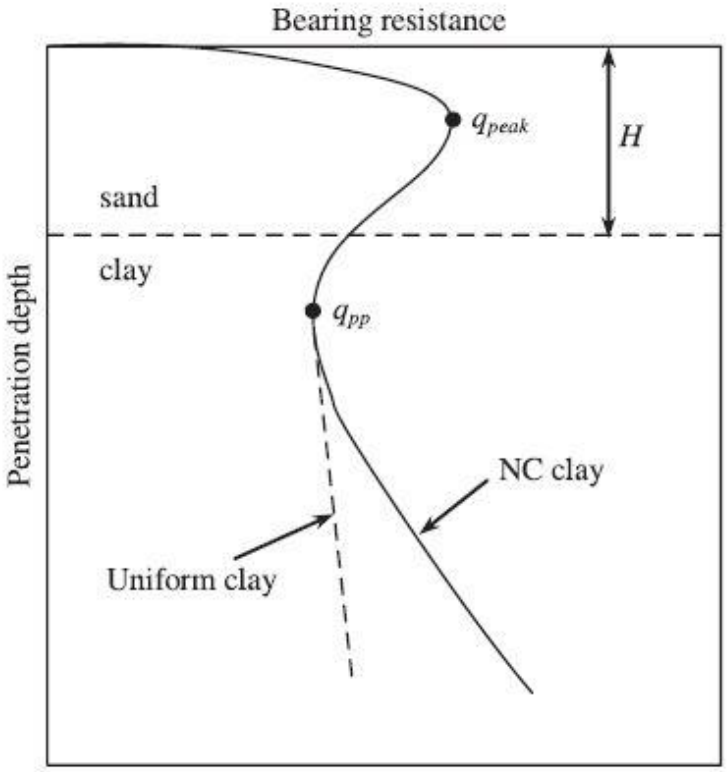

Figure 2.7 Typical Resistance to Penetration Case for Sand Overlying Clay (Yu et al., 2012)

In this Figure,

- q_{peak}: peak resistance in sand layer
- q_{pp}: post peak penetration in clay layer

Yu et al. (2012) used the Remeshing and Interpolating Technique with Small Strain Approach (RITSS) in order to simulate the punch-through behavior during the embedment of a spudcan. As the name implies, this method is leaning against incremental small strain simulations in order to achieve the large deformations with the

help of remeshing, frequently. Also, the interpolation of material properties and stresses are the other requirements of this technique.

The writer has conducted a parametric study on the problem geometry in order to eliminate the negative effects of the geometry of the soil, and the properties of both sand and clay. As a conclusion, he has compared his results with the centrifugal lab test findings, and showed their consistency.

Yi, Lee, Goh, Zhang, & Wu (2012) presented a study about generation of excess pore pressures during the embedment of offshore spudcan foundations. For three different effective stress constitutive models generated by the use of subroutine VUMAT, the analysis was completed by ABAQUS/Explicit. Eulerian approach was adopted in their analysis. The results reveal that the penetration resistance, and the pore pressure generation depend on the value of undrained shear strengths (C_u) by different constitutive models. Furthermore, the results also prove that the Eulerian type of formulation is consistent for many different effective-stress constitutive models. Furthermore, if C_u profile of the mudline is well-defined, so will be the pore pressure response and the penetration resistance. It is not possible to choose the constitutive model that will be used certainly; although, the response of pore pressure is seriously affected by this choice. Both the computational studies and measurements in experimental studies prove the generation of excess pore pressure in significant levels around the spudcan as it penetrates into the ground, and as the excess pore pressure dissipates, the soil strength increases significantly in the long term, therefore the critical condition is the spudcan penetration stage into the cohesive seabed.

Yu et al. (2012) has done a large deformation finite element study for the embedment resistance of spudcans on layered soils which consist of loose sand overlying clay soils. Mohr Coulomb failure criteria with constant strength parameters is adopted for all the analyses since comparison of the numerical models with the experimental data shows that it simulates the behavior well for loose sands. Tresca model, on the other hand, is adopted for clay layer. There is a parametric study for the punch-through behavior in their study. Their parametric study involves the effects of undrained shear strength of

the clay, as well as the friction angle and thickness of the sand layer on penetration resistance of the spudcan. It is concluded in the study that one of the design guidelines, SNAME, underestimates the reaction forces developed on the spudcan surface, significantly.

This paper defines the peak bearing capacity and post-peak bearing capacity values. These are the maximum bearing capacities before a spudcan penetrates into the clay, and after it completely penetrates into clay, respectively. They conclude that on a thin sand layer underlined by a clay layer, initial peak resistance value is not important, especially if the clay has a high undrained shear strength. In these kind of situations, punch-through risk is less. For a thick sand underlined by clay, however, this risk presents significantly even if the clay has high or low undrained shear strength values. The risk of punch-through increases as the friction angle, and thickness of sand increases, and shear strength of the clay decreases.

J. Zhang et al. (2013) have proposed a study on the spudcan penetration process based on centrifugal model tests, and their numerical results well agree with the experimental results. They found that soil flow failures such as surface heave, formation of cavity, and backfill occur during penetration. They have concluded their paper as follows:

- As the strength ratio of the stiff and soft clay decreases, volume of the stiff block stuck under the spudcan decreases,
- As the continuity and uniformity of the stiff clay layer above the spudcan increases while it is being penetrated, the cavity depth at which soil starts to flow onto spudcan increases,
- As the soil unit weight increases, the amount of stiff soil backfill onto spudcan increases, and the cavity depth decreases,

The pressure generated under the spudcan increases first, then decreases due to punch-through, and increases sharply from inside to outside. Therefore, the assumption that the pressure at the spudcan is distributed linearly on its bottom doesn’t agree with this fact.

M.S. Hossain & Randolph (2010a) investigated the penetration process of a spudcan type foundation into layered soil consisting of strong clay overlying weak clay by using large deformation finite element method. This type of soil profile has potential punch-through risk because of the reduction in the local maximum penetration resistance that is achieved during the penetration. They compared their numerical findings with their physical model study that showed results of the centrifuge model test of the same problem, and they caught a good agreement between these. They conducted parametric studies by taking different layer thicknesses, base roughness coefficients for spudcan, and strength ratios into account. According to M.S. Hossain & Randolph (2010a) punch-through risk increases when the bearing resistance reduces as the spudcan approaches the interface between two layers. Furthermore, punch-through occurs for all cases if the strength ratio is below 0.6.

Lee & Randolph (2011) has developed a methodology that estimates spudcan resistance during penetration from field cone penetration, and T-bar test data. The study focuses on how varieties in consolidation conditions affect the penetration behavior and on penetrometer testing. For this aim, a correlation model is developed taking various parameters into account in order to reflect different ratios of embedment resistance and rate of penetration for different consolidation conditions. In order to describe ratio of penetration resistance, they introduced a consolidation index, and by using it, they developed soil classification charts that are based on consolidation.

A procedure of design, and an example of the proposed methodology based on penetrometer were presented in their study. Results from centrifuge tests, and from literature were used to compare the results of their study. They confirmed that the methodology produced during this study matches very well for different degrees of consolidation during penetration.

Tho et al. (2012) used Coupled Eulerian Lagrangian (CEL) technique in order to simulate the penetration of a spudcan foundation into seabed that consists of different type of soil strata. FEM mesh of the model was kept the same for the analyses, and for the first part of the paper, they presented the requirement of mesh density (Figure 2.8),

penetration rate (Figure 2.9), and other factors that influence the computation time. In Figure 2.8, they presented penetration resistance versus penetration depth graphs for four different mesh densities which are also given. In the study, Mesh 3 was chosen for the analysis. In Figure 2.9, for three different penetration velocities, same graphs were sketched. For the sake of analysis, 0.3344 m/s was chosen to be the penetration rate for the spudcan. After determining the model requirements, and optimizing the computation time, model applicability was validated with the published experimental data presented in different papers.

Mesh	Number of elements	Number of degrees of freedom in the model
1	55,610	179,430
2	133,239	420,018
3	355,298	1,101,534
4	456,884	1,411,983

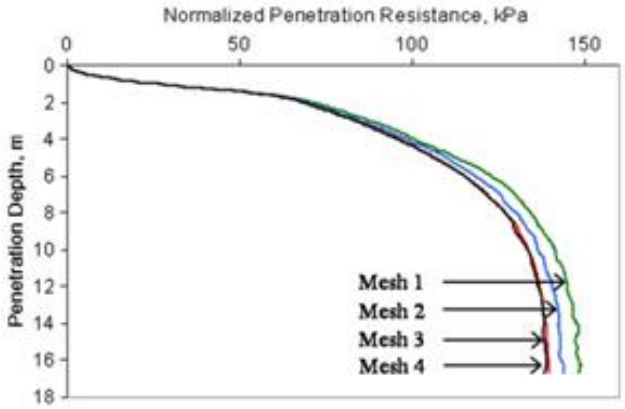

Figure 2.8 Normalized Penetration Resistance vs Penetration Depth for 4 Different Mesh Densities (Tho et al., 2012)

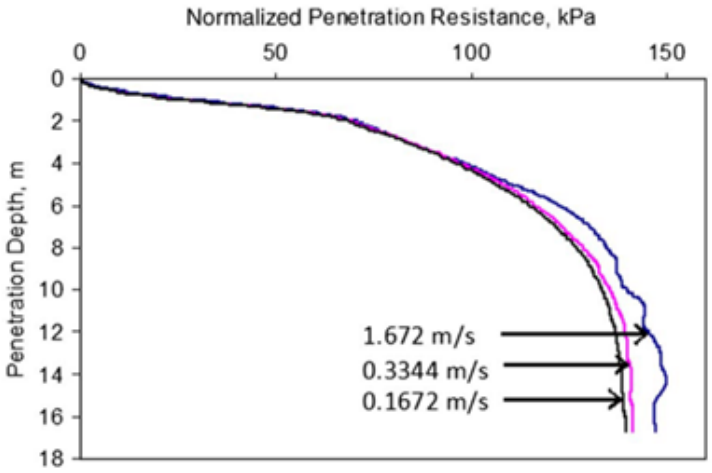

Figure 2.9 Normalized Penetration Resistance vs Penetration Depth for 3 Different Penetration Rates (Tho et al., 2012)

Clay with constant, and linearly increasing strength as well layered soils consists of stiff soil overlying soft clay were used in order to validate the results with experimental findings. Both for flow mechanism, and load-penetration response, simulations agree well with the experimental ones, and Figure 2.10, and Figure 2.11 show this agreement.

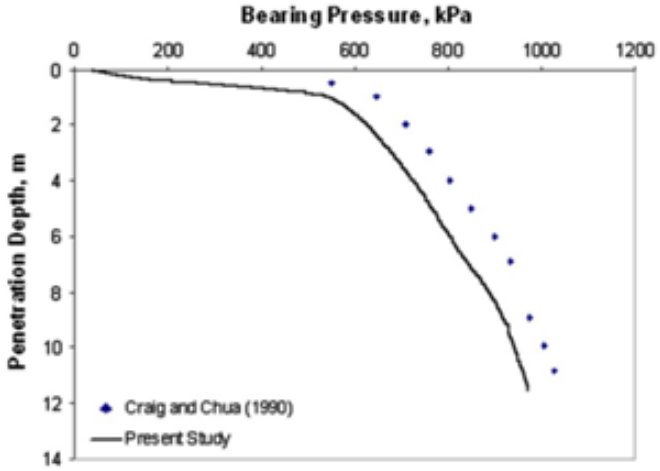

Figure 2.10 Bearing Pressure vs Penetration Depth for Clay with Constant Strength (Tho et al., 2012)

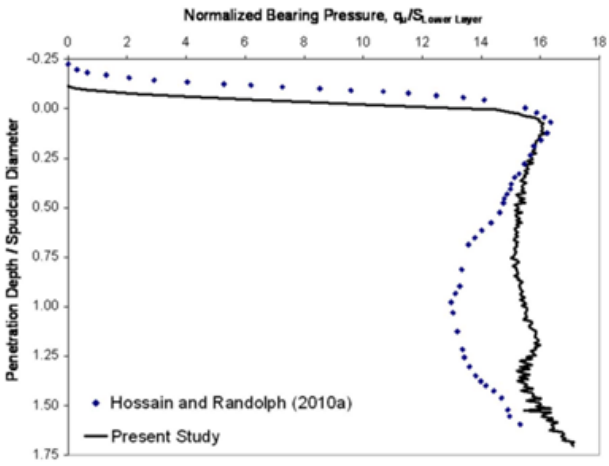

Figure 2.11 Load – Penetration Curves for Stiff Clay overlying Soft Clay Profile (Tho et al., 2012)

2.2 Experimental Studies

Craig & Chua (1991) carried out experiments to deep penetration on sand and clay of spudcan foundations. They examined $c_u/\gamma B$ which is a dimensionless term, where c_u, γ and B stand for the undrained shear strength of the lower clay layer, the unit weight of the upper soil layer and the foundation width, respectively. Some tests had been performed on strip footings and some of them on circular models; some models had been made by using either dry sand or saturated sand. Results from these tests have revealed that the self-weight and the stiffness of an upper sand layer are important parameters for determining the punch-through mechanism.

M.S. Hossain & Randolph (2010b) studied centrifuge model tests of vertical undrained penetration of a spudcan into stronger clay overlying weaker strata. Strength ratio between the soil layers, thickness of the upper layer, and strength gradient of the weaker layer are the varying properties in their study. Half-spudcan tests were conducted in order to capture the soil flow continuously through a transparent front window. Full-spudcan penetration was also conducted in order to determine the embedment resistance. Flow mechanisms (Figure 2.12) were observed in the order of:

- Soil moves vertically downwards, and layer interface deforms.
- Stronger upper material is trapped under the spudcan, and carried into weaker layer.
- Delayed backflow of the soil.
- Localized flow around the penetrated spudcan.

They investigated potential punch-through for every case they constructed with a peak resistance followed by a reduction. This reduction becomes more and more critical as the strength ratio of the weaker layer reduces with respect to the one of the stronger layer. Observed backflow onto the spudcan during the vertical penetration into double layered soil limits the cavity depth, and plays an important role in response of the spudcan not only for the vertical loading conditions but also for lateral loading, and moment applications, as well as during extraction.

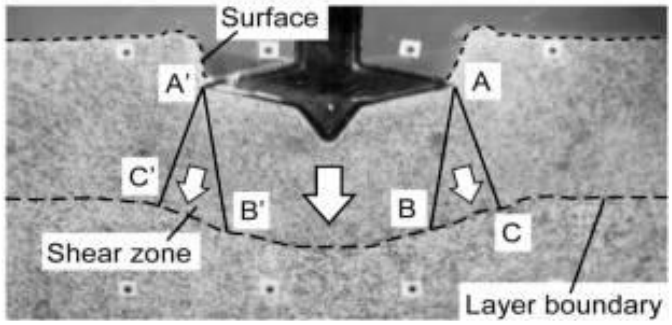

a)

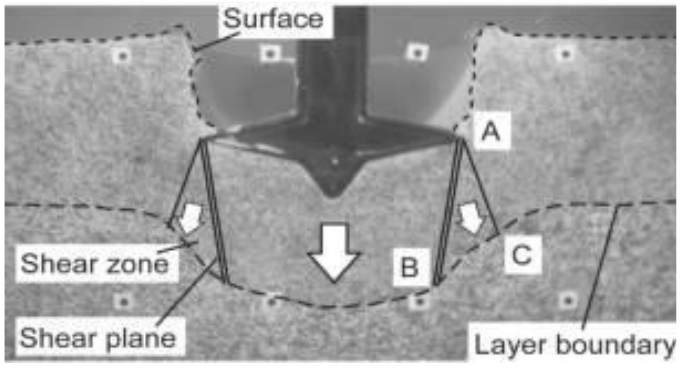

b)

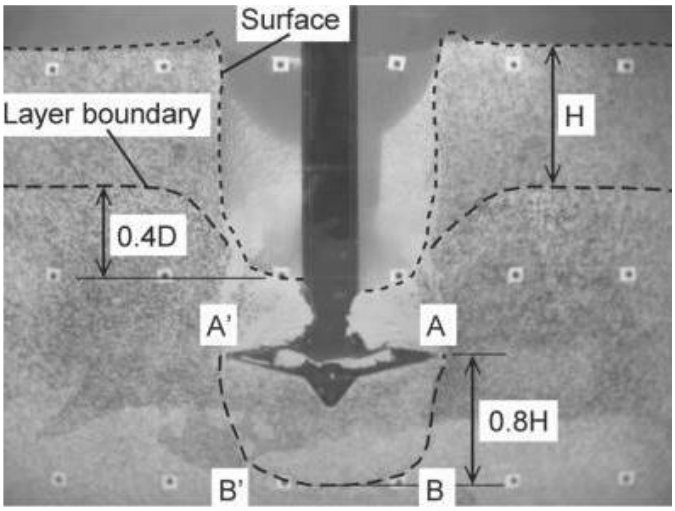

c)

Figure 2.12 Typical deformation mechanisms at different stages of punch-through (M.S. Hossain & Randolph, 2010b)

Leung, Purwana, Chow, & Foo (2005) studied the behavior of spudcans during the extraction process in order to estimate the uplift resistance by conducting some centrifuge model tests. They instrumented both the top and the bottom faces of the foundation with total and pore pressure transducers which read the total pressure and pore pressure changes in the soil during the lifetime of the spudcan from penetration to extraction. Their centrifuge model set-up is given in Figure 2.13.

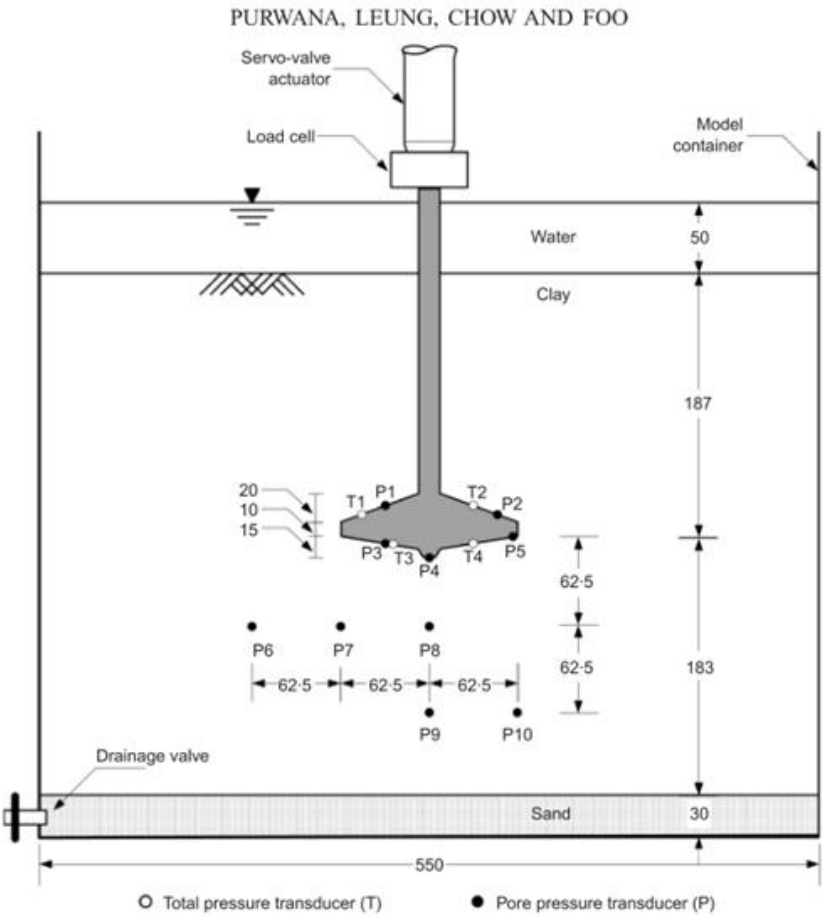

Figure 2.13 Centrifuge Model Set-up (all dimensions in mm.) (Leung et al., 2005)

In this study, between penetration, and extraction, operation stage is also simulated by keeping a constant vertical load on the spudcan. The results show that between the spudcan base and the soil, suction is developed, and it increases as the spudcan operation period gets longer. This contributes to the force that needs to be applied during the extraction. According to this study, four major results can be acquired:

- Process of spudcan penetration is an undrained process since similar magnitudes of total vertical and pore pressure at the foundation are observed while it is installed.
- The required breakout force for the extraction of a spudcan increases with the operation period.

- The total pressure transducers at the top of the spudcan show that, soil resistance does not change significantly during the extraction process. However, pore pressure transducers at the bottom of the spudcan shows negative pore pressure generation. This leads to requirement of a larger force to extract the spudcan.
- For the spudcans having similar installation load, and penetration depths, a larger ratio of operational load to penetration load requires more breakout force for spudcan penetration. However, this effect is not as significant as the operation duration.

Another study on vertical extraction of spudcan type foundations through single, and multilayer soils were conducted by M. S. Hossain & Dong (2014) Similar to the study of Leung et al. (2005), half-spudcan models were constructed in order to capture the soil flow by a digital camera, and full-spudcan models were established in order to obtain the resistance.

For all cases of the soil being modeled, suction that occurs at the base of the spudcan, shearing, and weight of the soil above the spudcan affect the extraction resistance. Maximum resistance against extraction can be seen in stiffer soil. For the soil that consists of soft clay with increasing shear strength with depth, peak resistance can be achieved at the beginning of the extraction process. Figure 2.14 shows soil failure mechanisms for these kind of layers.

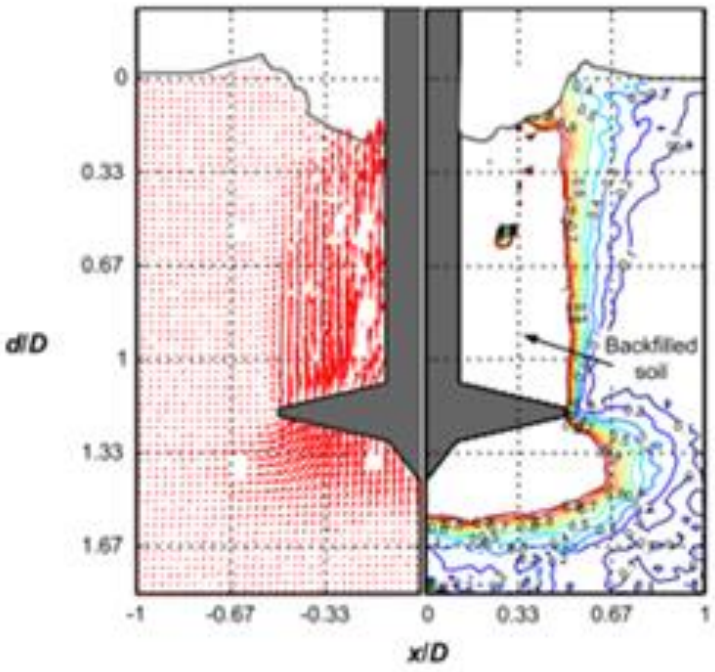

Figure 2.14 Soil-Failure Mechanisms for Spudcan Extraction in Nonhomogeneous Clay (Muhammad Shazzad Hossain & Dong, 2014)

In Figure 2.14, d/D represents ratio of embedment depth to spudcan diameter, while x/D stands for the ratio of horizontal length to spudcan diameter. In this kind of a soil layer, since the resistance against extraction remains constant all the way up to the mudline, for similar real cases, this process can be problematic. In these kind of situations, suction generated at the base should be released.

For stiff clay overlying a soft clay, peak resistance against extraction can be seen at a shallow depth in the stiff layer. This behavior is familiar since for these kind of soil where punch-through is a problem during installation, peak resistance is also caught around the same depth in stiff clay. Figure 2.15 shows the failure mechanism of such kind of soils.

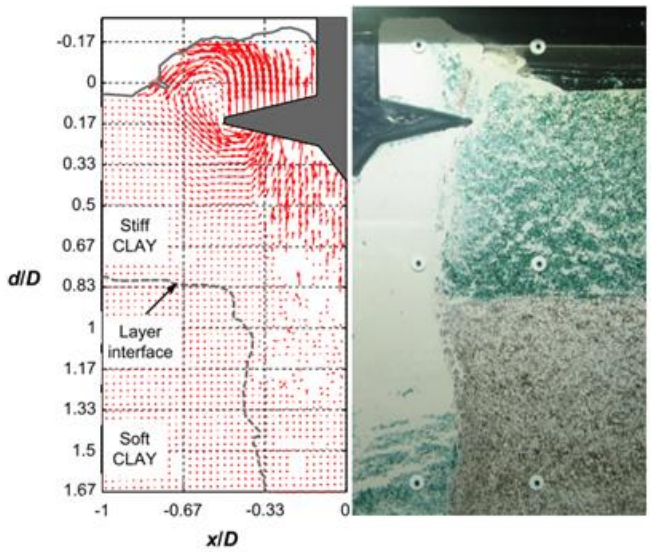

Figure 2.15 Soil-Failure Mechanisms for Spudcan Extraction in Stiff over Soft Clay (Muhammad Shazzad Hossain & Dong, 2014)

For soils having more than two layers of clay, the behavior is the combination of single, and double-layer soils. The resistance against extraction increases in the middle layer which is stronger compared to others. (Figure 2.16)

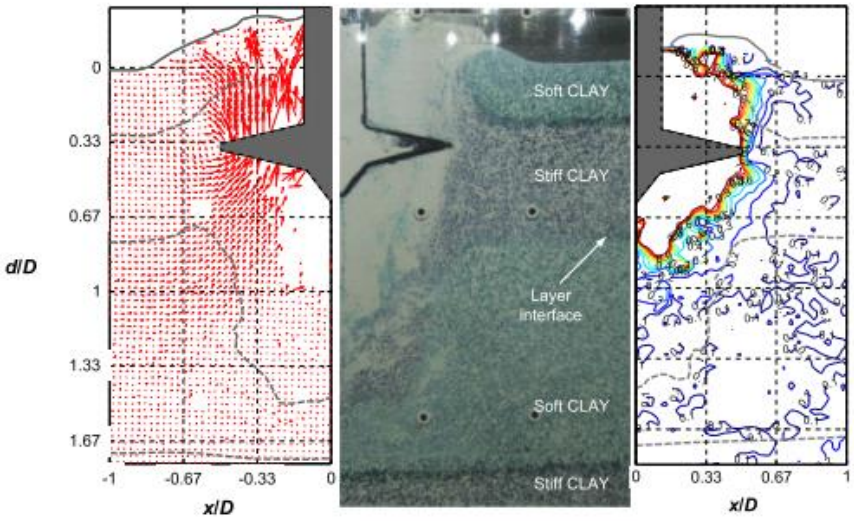

Figure 2.16 Soil-Failure Mechanisms for Spudcan Extraction in Multi-Layered Clay (Muhammad Shazzad Hossain & Dong, 2014)

Hu, Randolph, Hossain, & White (2005) conducted drum centrifuge model test, and finite element analysis in order to capture the soil failure mechanisms during penetration of a spudcan into uniform clay with constant shear strength. Numerical analysis is carried out to verify the model test findings. They focused on the conditions of the limiting stable cavity, instead of the spudcan resistance during penetration. From both methods, an open cavity can be observed during the initial penetration, where heave occurs on the mudline. After a certain depth, soil starts to flow back onto the spudcan. After it starts, existing open cavity stands stable.

The depth at which backflow of the soil begins above the spudcan can be taken as the stable cavity depth after deep penetration. This is a function of the soil shear strength (S_u), and the unit weight (γ'), as well as, the foundation size (D). It is found that back-flow is due to penetration of the spudcan rather than a wall failure.

By taking the results of both numerical, and experimental findings into account, the limiting cavity depth can be expressed simply by Equation 2.1

$$\frac{H}{D} = \left(\frac{S_u}{\gamma' * D}\right)^{0.55} \tag{2.1}$$

CHAPTER 3

METHODOLOGY

3.1 Introduction

In this study, numerical models have been generated in order to shed light on the factors affecting the spudcan penetration into clayey seabed. Since there are no well-instrumented and well-documented spudcan penetration case study in the literature, the methods depicted in InSafeJIP (Osborne et al., 2011) were used to validate the results obtained numerically (Chapter 4). The existing laboratory tests in the literature do not include sufficient detail about material properties and procedures in order to numerically model those cases in this thesis. After the verification of the numerical model, a systematic parametrical study was conducted (Chapter 5). Numerous factors affecting the bearing capacity during the penetration process such as the spudcan penetration depth, cone angle, and the diameter of the spudcan, material properties of clay, and the spacing between two adjacent spudcans were investigated. Three dimensional finite element method, (Abaqus 6.14 software) has been used in all the analyses. Since the problem we are dealing with is a large-strain problem, common finite element methodology with small strain assumption cannot be used (except with some approximations, e.g. press and replace technique by Engin, Brinkgreve, & van Tol (2015) In order to model the penetration of the spudcan into sea-bottom sediments, Coupled Eulerian Lagrangian (CEL) method available in Abaqus software was adopted. This method is briefly described with its assumptions and properties in this chapter.

In Abaqus software the problem is handled by first creating the geometry of the soil body and the spudcan, then generating finite element meshes, applying boundary conditions, defining the gravity loading and then prescribed displacements.

3.1.1 Brief Information about Coupled Eulerian Lagrangian (CEL) Method

In a Lagrangian analysis, as the material deforms, the finite elements also deform because the nodes of the elements are fixed within the material. These kind of elements are fully occupied by material at any time of the simulation. Therefore, the material boundary overlaps the boundary of the elements. On the other hand, nodes are fixed within space in an Eulerian analysis. Material flows inside the elements that do not deform. These kind of elements, therefore, do not need to be 100% full of material every time. Therefore, an Eulerian boundary does not correspond to an element boundary, and an Eulerian mesh typically extends beyond the material boundaries. If an Eulerian material escapes from the Eulerian mesh, it disappears from the simulation. Therefore, it is vital to describe predefined void meshes in which there is no Eulerian material, initially in order to simulate the material moves. (Figure 3.1)

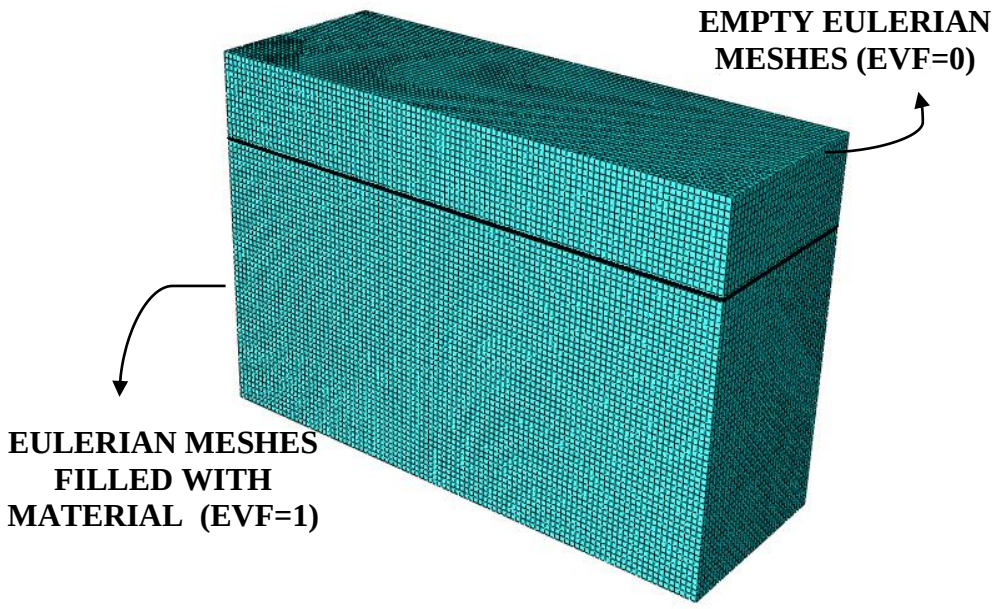

Figure 3.1 Eulerian Meshes used in this Study (EVF=Eulerian Volume Fraction)

Coupled Eulerian Lagrangian method, as can be understood from the name itself, contains both Lagrangian elements, and Eulerian material. An Eulerian material should contact with Lagrangian elements through Eulerian – Lagrangian contacts (called General Contact in Abaqus 6.14).

Coupled Eulerian Lagrangian analyses are especially effective for large deformation applications. Although, traditional Lagrangian elements distort excessively, and the analyses lose its accuracy, high damage analyses, liquid sloshing, or any penetration problem can be solved easily and effectively by Eulerian analysis.

For the analyses throughout this thesis, Explicit module of Abaqus 6.14 is used, and Eulerian implementation in this software is based on the volume of fluid method, in which, material as it flows inside the mesh is tracked by calculating its Eulerian volume fraction (EVF) for each element. In this method, EVF is equal to one if the element is full of a material, and is equal to zero if there is no material in the element. Single element can contain more than one material, and if the sum of the volume fractions of all materials in an element is less than one, the remainder is filled with "void material", automatically which has neither strength nor mass.

3.2 Model Properties

Abaqus/Explicit was used to demonstrate the spudcan penetration into seabed composed of clay layer(s). In order to conduct a systematic parametric study, a certain property is varied within a preset range while all other model parameters are kept constant.

Although more comprehensive constitutive models are available in the software, elastic – perfectly plastic Mohr Coulomb failure criterion was adopted in all the analyses. Mohr-Coulomb model is preferred since it is a simple model that is sufficient for the purposes of this study and since the input parameters of other constitutive models are much more in number and their values are relatively more difficult to estimate. The main objective of this study is to extend our understanding of the spudcan penetration

process using a minimum number of variables. For this purpose, the Mohr Coulomb failure criterion seems to be sufficient. Undrained analyses were conducted for the seabed consisting of clay.

Spudcans were modeled as rigid materials in all the analyses. Therefore, only the geometry of the spudcan is taken into account in this study. Generating traditional Lagrangian meshes and defining a reference point on the spudcans are required by the software. Any mechanical boundary condition including velocity, displacement, and rotation types should be defined on the reference point.

General contact algorithm based on "penalty contact method" with a friction coefficient was adopted between Eulerian and Lagrangian materials (SIMULIA, 2010). This type of contact does not enforce an interaction between the Eulerian and Lagrangian elements which means a Lagrangian body can move freely in an Eulerian mesh until it encounters an Eulerian material (where EVF is not zero). Lagrangian spudcan should be modelled inside the Eulerian mesh which is initially empty (EVF = 0) because there is no initial contact between these elements.

Before investigating the effects of different parameters on how the bearing capacity changes during spudcan penetration, it is important to specify the size of the model (geometry), mesh resolution, and spudcan penetration velocity which will be presented in detail in the following sections.

3.3 Model Size and Boundary Conditions

While doing three dimensional finite element calculations, one must select the size of the model (geometry) so that it is not affected by the geometrical constraints applied at the boundaries. Therefore, specifically for this problem, it is desirable to choose the limits of the model (the distance to boundaries) as far as possible from the penetration process but, on the other hand, as the size of the model increases, the computation time also increases. Therefore, one should find an optimal solution to this problem, and

select a size for the model so that while it is not affected by any geometrical constraints, it also does not consume excessive time to compute. A number of analyses to investigate this issue were conducted, and presented in this chapter of the thesis. It should also be noted that for the purpose of saving time, only the half of the model has been simulated for all the analyses using the symmetry condition.

In order to determine the size of the model, single spudcan penetration analyses were conducted, and the geometry of the spudcan as well as the soil properties were kept constant during this process. Soil properties and the geometrical properties of a typical real spudcan made of steel are given in Table 3.1 and Table 3.2, and illustrated in Figure 3.2.

Table 3.1 Soil Properties

Parameter		**Value**	**Unit**
General	Failure Criterion	Mohr - Coulomb	-
	Drainage Type	Undrained	-
	Unit Weight	19.62	kN/m^3
Strength Parameters	Ratio of Deformation Modulus / Undrained Shear Strength	500	-
	Poisson's Ratio	0.45	-
	Internal Friction Angle	0	degree
	Undrained Shear Strength	40	kPa
	Dilatancy Angle	0	degree

Table 3.2 Spudcan Properties

Parameter	**Value**	**Unit**
Diameter	10	m
Cone Angle	120	degree
Surface Roughness Coefficient	0.5	-
Cylindrical Height	5	m

The values in Table 3.2 are the spudcan properties that are used in the analyses for the determination of the boundary sizes, and fixities. In this table, surface roughness coefficient is a parameter that stands for the ratio of the maximum shearing strength which occurs on the spudcan surface to the shear strength of the soil that the foundation is embedded. More detailed explanations about the surface roughness coefficient will be made in Chapter 4.1

Figure 3.2 illustrates the geometric properties that are given in Table 3.2

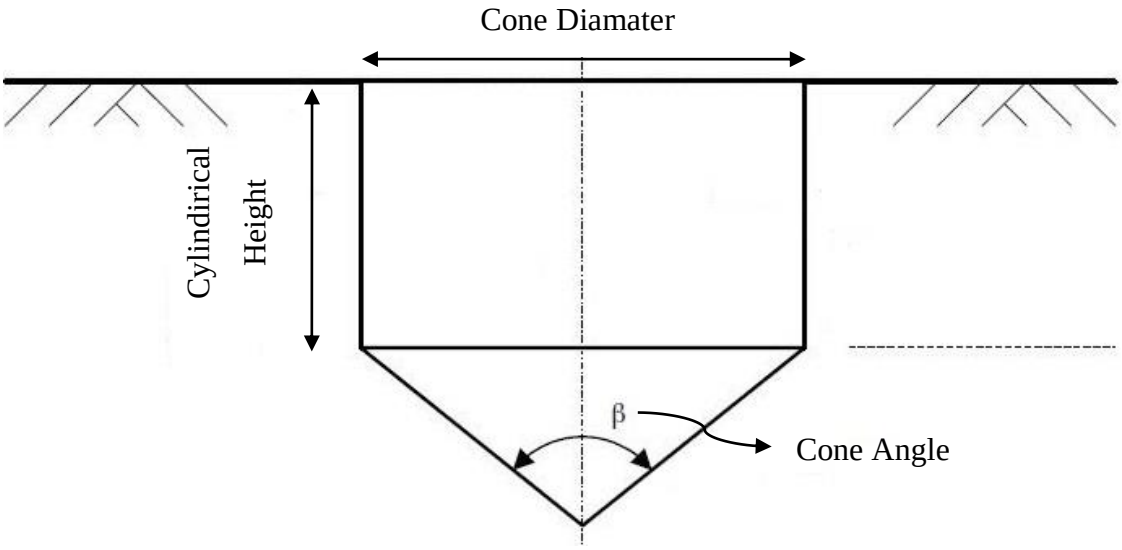

Figure 3.2 Spudcan Geometric Properties

Boundary conditions of the model have been chosen such that behavior of the movement of a cone foundation into a single layered cohesive soil can be simulated. Boundary condition at the very bottom of the model was selected so that the movement is prevented against all directions for all cases. For the sides of the geometry, boundary fixities were provided to the model such that translation in the directions which are

normal to the surfaces are fixed, and movement in other directions which are tangential to the surfaces are allowed. This situation is explained in Table 3.3, and in Figure 3.3 in order to clarify. Apart from these fixities, there are two boundary conditions working consecutively on the reference point of the spudcan. The spudcan is fixed in space while the gravity load is being applied to the ground. After that, this fixity is removed, and instead, there applied a prescribed velocity condition to the same point in order to simulate the penetration process.

Table 3.3 Boundary Conditions on the Surfaces

	Boundary Conditions		
Surface	**x-direction**	**y-direction**	**z-direction**
Front	Free	Free	Fixed
Rear	Free	Free	Fixed
Left	Fixed	Free	Free
Right	Fixed	Free	Free

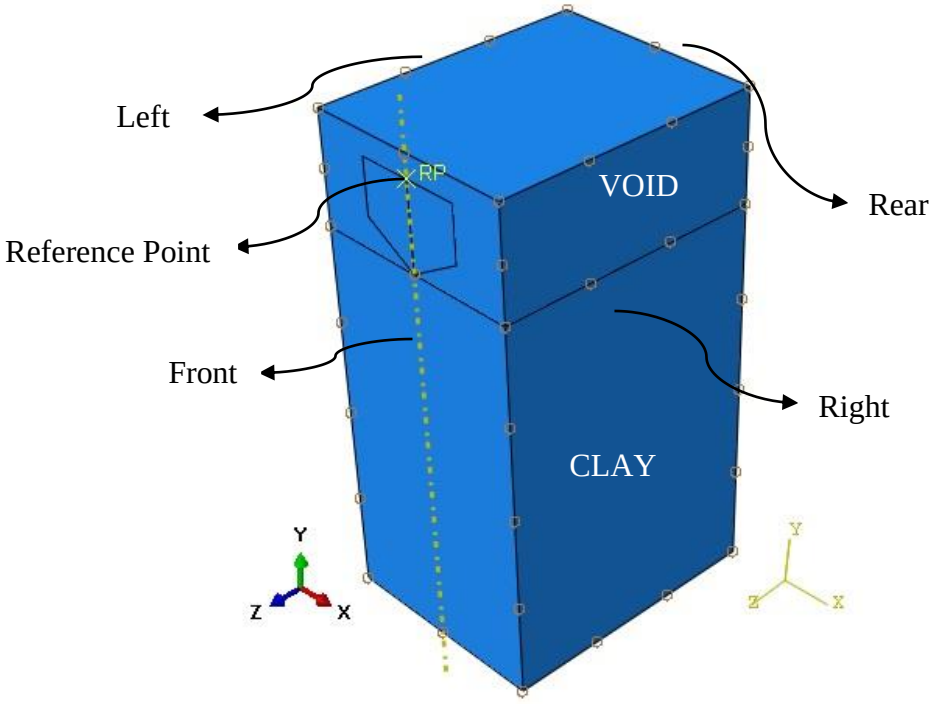

Figure 3.3 Boundary Surfaces of the model

With these boundary conditions, analyses for the selection of the size of the model have been conducted for different geometries by changing the ratio of the diameter of the spudcan, D, and the length of the soil parallel to the front side, S (Figure 3.3). The S/D ratios that are tried in the analyses are 2, 3, 4, and 5.

For the S/D ratios given in Figure 3.4, at a certain time during the penetration of the spudcan, vertical stress contour plots are given in Figure 3.5, Figure 3.6, Figure 3.7, and Figure 3.8, below with the same scales indicated in Figure 3.5. In these plots the vertical stress values shown in the legends are in Pascal.

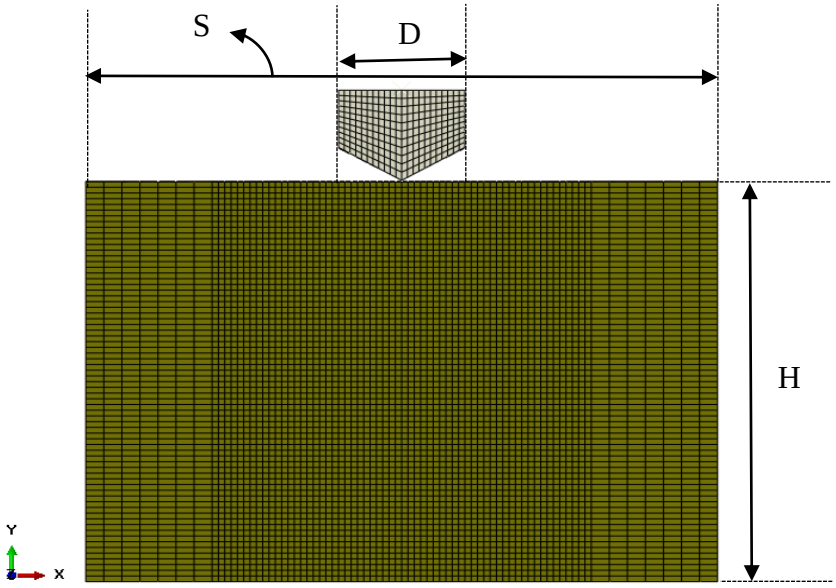

Figure 3.4 Model Dimensions: Length of the Model, S, and the Diameter of the Spudcan, D

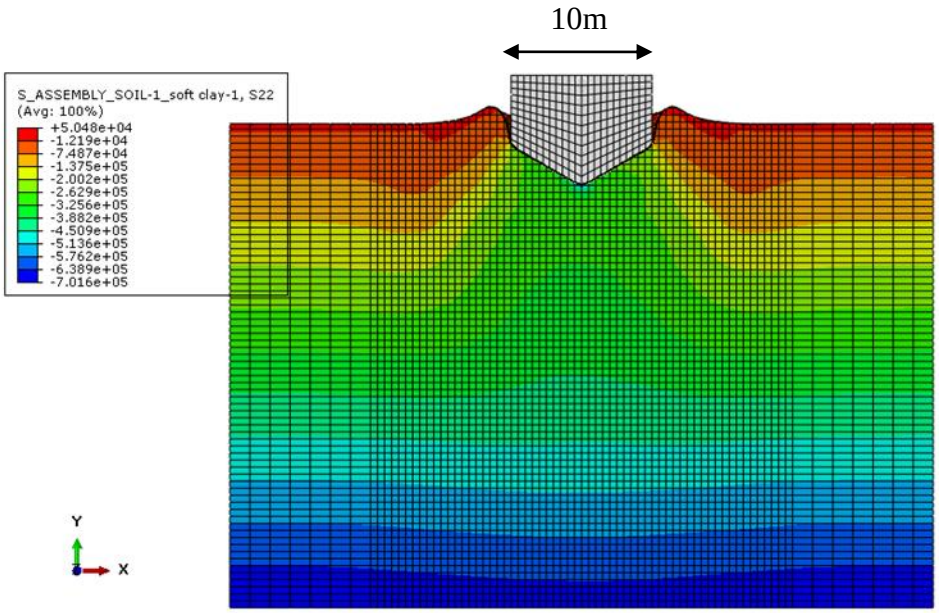

Figure 3.5 Vertical Stress Contours for S/D = 5

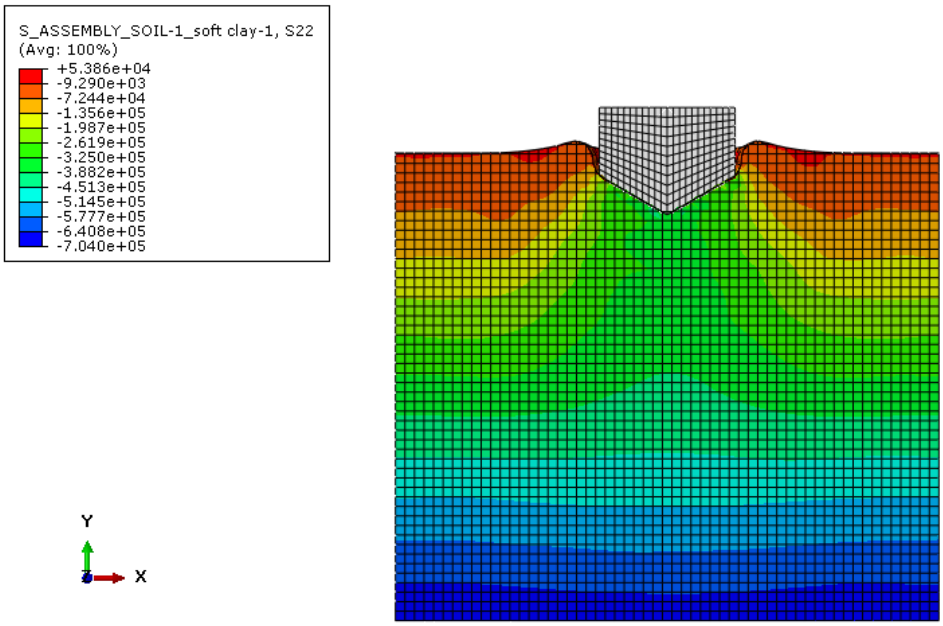

Figure 3.6 Vertical Stress Contours for S/D = 4

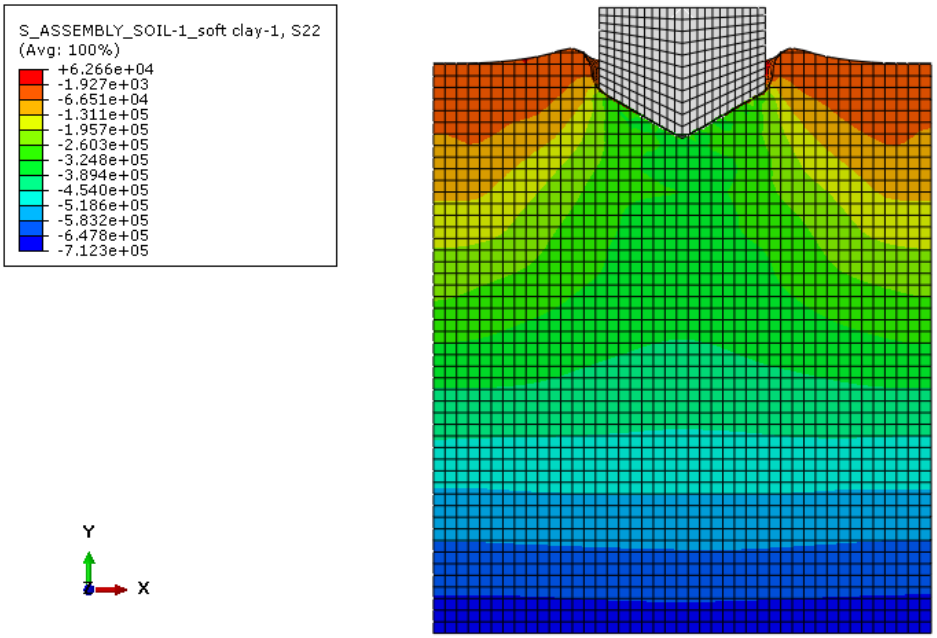

Figure 3.7 Vertical Stress Contours for S/D = 3

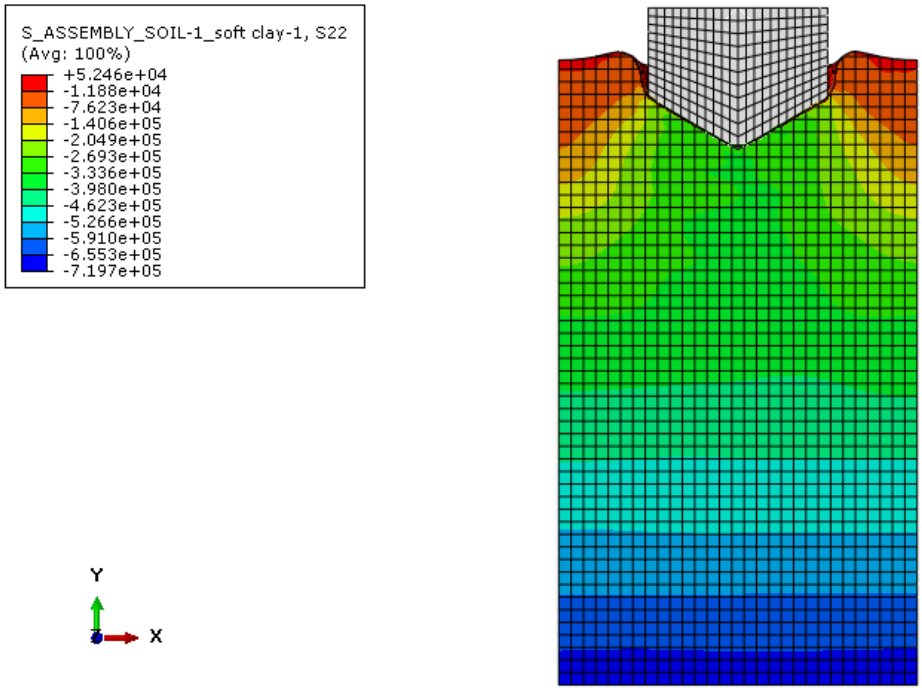

Figure 3.8 Vertical Stress Contours for S/D = 2

As can be observed from these figures the vertical stress values do not depend primarily on the lateral size of the soil geometry. We can see from Figure 3.8 that, for S/D ratio of 2, the lateral boundaries are very close to the zone of the soil that is affected from the spudcan penetration process, therefore this size should not be preferred because the soil should be allowed to freely deform without being affected from the lateral boundaries. In order to illustrate the effect of the size of the model in a clearer way, for these different S/D ratios, reaction force at the base of the spudcan versus penetration depth graphics are given in Figure 3.9. This reaction force is generally called “bearing capacity” in the literature; therefore, in order to use the same terminology, bearing capacity is used in order to address this force in this study.

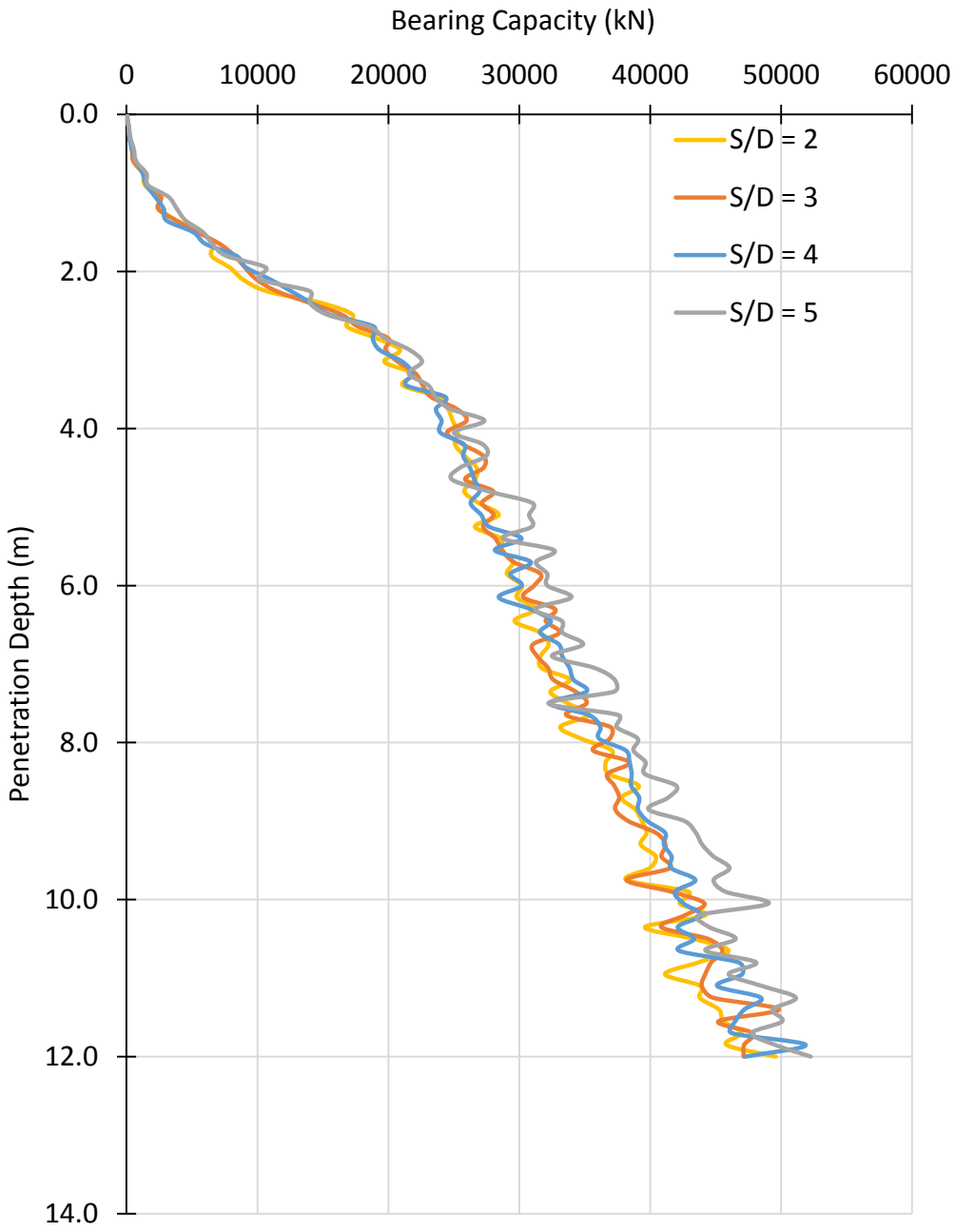

Figure 3.9 Penetration Depth (m) vs Bearing Capacity (kN) for 4 Different S/D Cases

It can be seen from the above graph that there is not a significant change in the bearing capacity for different sizes of the model. This may be because of the soil parameters that were used for these analyses, maybe Poisson's Ratio, or the geometry of the

spudcan that was used. In order to see the effect of the size of the model on the results, since it is expected that the differences in horizontal geometry in the soil body should affect the forces in lateral direction more, the horizontal forces generated at the base of the spudcan are also checked for S/D=2, and S/D=5, and the results are given in Figure 3.10. It can be seen in Figure 3.10, as the lateral size of the model decreases, the horizontal forces increase, in other words, in S/D=2 case, the boundaries are chosen so close to the spudcan penetration zone that it is affecting the results. Therefore S/D=2 should not be used, and a larger lateral size of the model should be preferred, to represent, in our numerical model, the reality in which lateral extent of the soil is infinite.

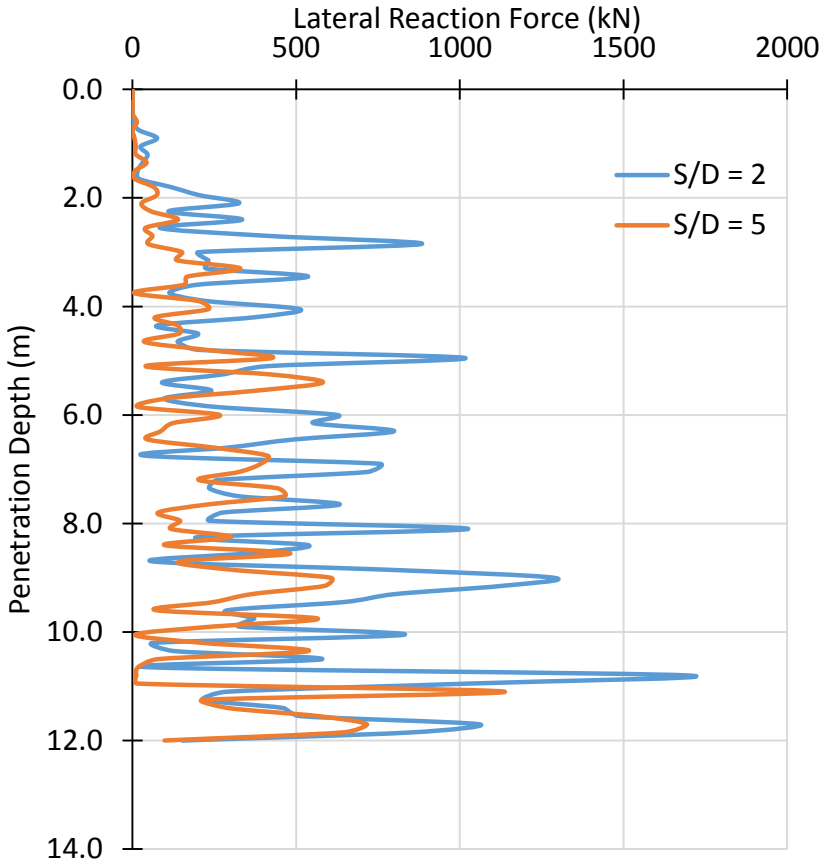

Figure 3.10 Penetration Depth (m) vs Lateral Reaction Force (kN) at the spudcan base for two different S/D (α=0.5)

3.3.1 Discussion of Results

By evaluating the vertical stress contours in Figures 3.5 through 3.8 together with the two graphs in Figure 3.9, and Figure 3.10, S/D = 5 case was chosen in order to be on the safe side since too close lateral boundaries to the zone of the soil affected by penetration would interfere with the results of the analyses

Furthermore, by inspecting Figure 3.9, there is not a significant change in the bearing capacity values with penetration depth. This also could mean that the vertical geometry chosen is also sufficient for the analyses, and no need to do any more simulations for this case. Therefore for the lateral extent of the model S/D = 5, and for the vertical extent of the model, H = 45 meters are used as the geometrical properties of the model for all analyses in this thesis.

3.4 Mesh Dependencev

Abaqus/Explicit module uses 8-noded 3D Eulerian elements with reduced integration for Eulerian analysis and these meshes are called EC3D8R in the software These are only type of available elements for these kind of analyses in Abaqus 6.14 to discretize the soil.

Abaqus 6.14 enables the user to generate as many mesh elements as possible, and one can divide the model into sub-models to use different fineness of mesh elements in different locations. This property can be used if computation time of an analysis takes too much time by coarsening the meshes far away from the spudcan in order to reduce the number of elements in the model.

Optimum number of elements was selected by investigating their effects on the reaction forces that occur under the spudcan. Model size and the boundary conditions determined as well as the soil parameters and the geometrical properties of spudcan selected in Chapter 3.3 were used for this purpose.

3.4.1 Discussion of Results

Six different analyses (Table 3.4) were conducted by changing the approximate element size, therefore, the number of the elements, in order to obtain the most accurate reaction force. It was obvious that the computation time changes drastically for different conditions. This variation may depend on the size of the model (Figure 3.11), material, and the interaction properties, precision of the calculations, and hardware of the used computer. One can also observe that the computation time increases as the number of elements increases. While for the elements having one dimension of 1.5 meters, the computation time is around 10 minutes, for the elements having 3 times shorter dimensions, the computation time increases up to 10 hours (60 times).

Table 3.4 Values used in the mesh effect analyses

Approximate Element Size (m)	**Number of Elements in the Mesh**
0.4	459684
0.5	308340
0.6	163950
0.7	107328
1	62325
1.5	18750

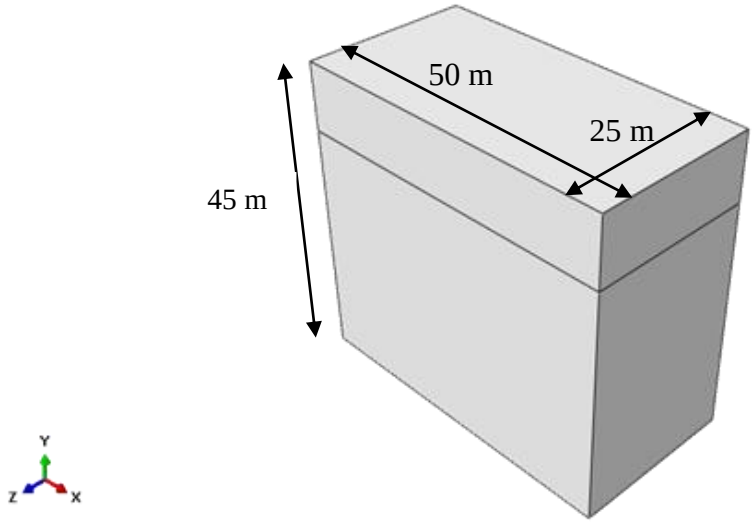

Figure 3.11 Model size used in the analyses

It was observed that by using elements having approximate size of 0.4 m and 0.7 m, there is a negligible difference in the reaction forces generated on the spudcan. On the other hand, using elements with larger size leads to a considerable difference in the reaction forces. In Figure 3.12, this result is given with respect to different approximate element sizes.

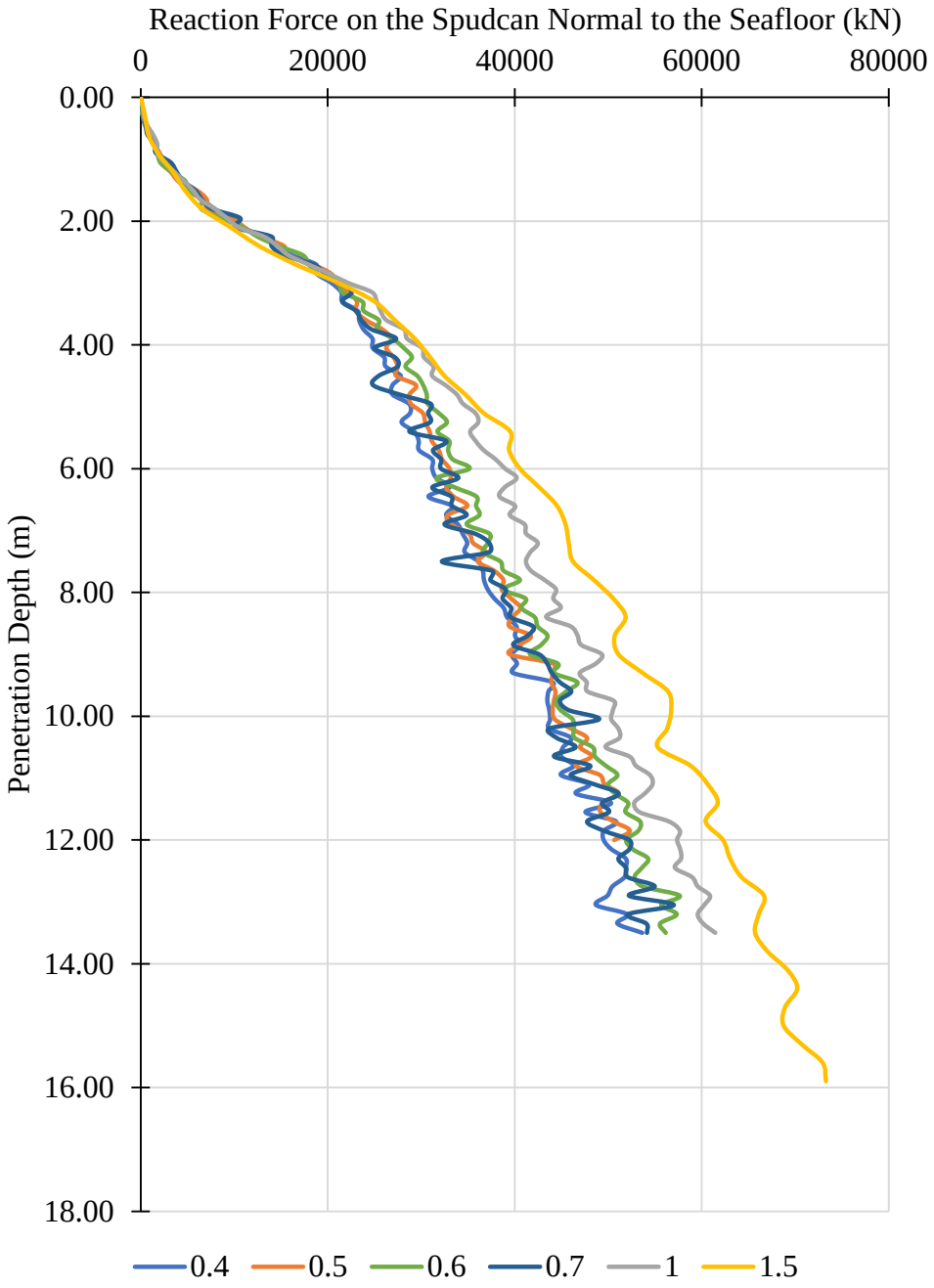

Figure 3.12 Effect of mesh element size on the vertical reaction force applied by the seafloor on the spudcan

In conclusion, it is determined that using elements with approximate size of 0.7 meters (Figure 3.13) is sufficient in order to catch the desired numerical accuracy. It also requires a quarter of the time with respect to the time required using the finest mesh that has been studied. Therefore, for all analyses in this thesis, this fineness of mesh element was used.

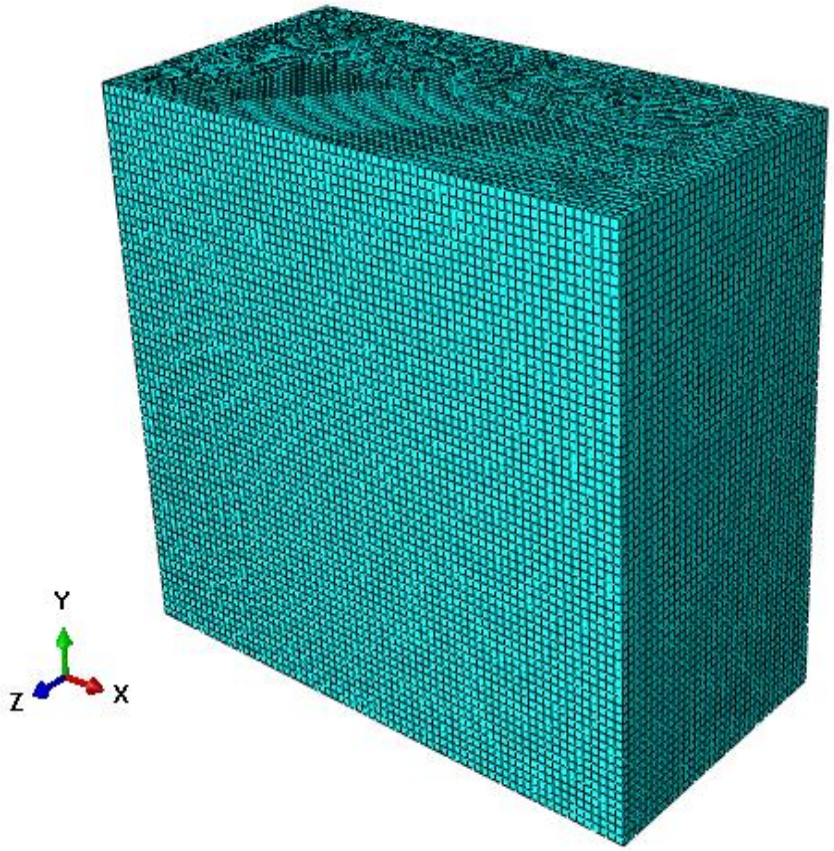

Figure 3.13 Mesh density of the model used in this study (for scale, height = 45 m)

3.5. Spudcan Penetration Velocity

Spudcan penetration velocity can be one of the factors that affect the results obtained; therefore, a study has been conducted for this issue also. In this part of the thesis, with the geometric parameters presented in Chapter 3.3 and in Figure 3.11, and the mesh size given in Chapter 3.4, analyses with different spudcan penetration velocities (10, 15, 30, 45 cm/s) are conducted. The numerical simulation times, in Abaqus, for these velocities are changing between approximately 8 hours for 10 cm/s to 1 hour for 45 cm/s penetration velocity. Some of the real reported penetration velocities of spudcans in the literature, as given in Chapter 1 of this thesis, range between 1 cm/s (*Maersk Interceptor*, n.d.) to 170 cm/s (Tho et al., 2012). For the selected velocities, the penetration depth vs bearing capacity values for each velocity are also shown in Figure 3.14.

3.5.1 Discussion of Results

When the graph in Figure 3.14 is inspected, it can be said that, although as the penetration velocity increases, the bearing capacity increases slightly, for these penetration velocities the effect is small. This might be because those four selected velocities are not too dramatically different from each other, and there might be some effect for very small and very large penetration velocities. On the other hand, it is very time consuming to simulate the slowest penetration velocity in Abaqus 6.14. Therefore from these velocities, V = 15 cm/s, was chosen to be the penetration velocity that was used for all the simulations conducted in the scope of this thesis.

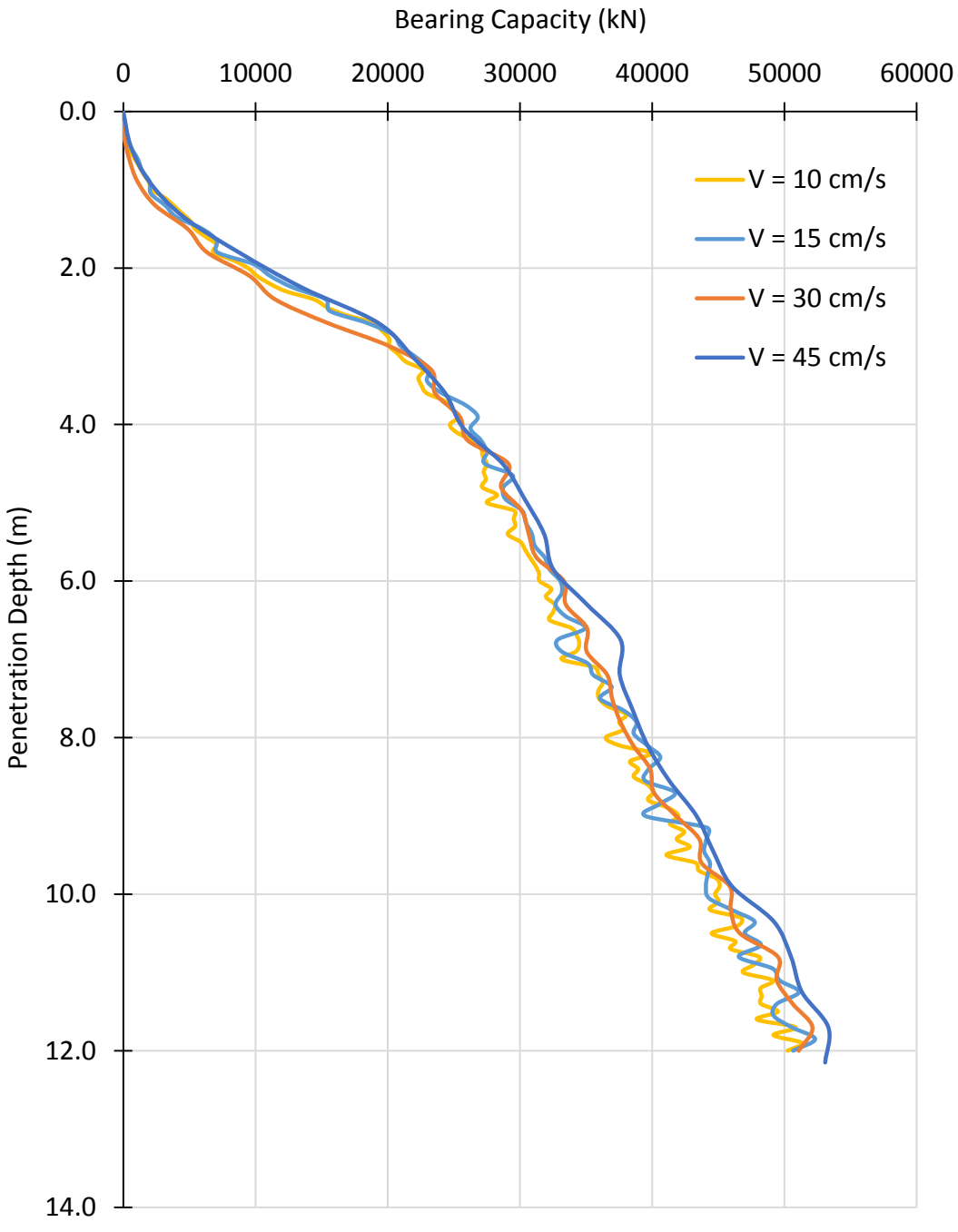

Figure 3.14 Penetration depth (m) vs bearing capacity (kN) for four different penetration velocities

CHAPTER 4

COMPARISON OF THE NUMERICAL MODEL

In this section, we compare our numerical simulations with the InSafeJIP Guideline (Osborne et al., 2011). For generic spudcan geometries and soil properties, 3D Coupled Eulerian-Lagrangian analyses are conducted and their results are compared with the approximate methods of this guideline. Since this thesis is mainly concerned with the penetration process of a spudcan into a homogeneous clayey soil profile, the comparisons of the numerical model were made by using the corresponding procedures given in the InSafeJIP guideline.

4.1 InSafeJIP (Osborne et al., 2011)

According to the guideline, before a jack-up type oil platform is installed at its position, spudcan penetration into sea-bottom should be made as a function of the applied loads. Prediction model requires the following information:

- Spudcan geometry
- Soil profile
- Maximum preload $F_{V,100}$, and light-ship load $F_{V,0}$ expected on each spudcan

After these values are gathered, one should obtain a load – penetration curve for a depth of z_1, which can be evaluated as the maximum of:

- At $F_{V,100}$, penetration depth plus 0.5 times the diameter of the spudcan
- Consistent penetration depth for the 1.5 times of $F_{V,100}$

In the guideline, bearing capacity calculations are used to obtain load-penetration predictions. It should be noted that this kind of bearing capacity calculations are typically performed for shallow foundations in geotechnical engineering. For the design of shallow foundations, bearing capacity calculations involve a factor of safety (typically 3.0), in addition to detailed site investigation on-site. Therefore, typically, a bearing capacity failure is not observed in geotechnical engineering, and most of the foundation problems are due to large settlement value. However, this is not the case for spudcan penetration in off-shore oil platforms. Since (i) carrying out detailed site investigations at the offshore sites is more expensive and difficult, (ii) the dynamic/cyclic loads can be unpredictable due to storms etc, and (iii) using a large factor of safety value for bearing capacity of spudcan could result in very expensive solutions, spudcan bearing capacity failures could be experienced in real life. Therefore, bearing capacity calculations' accuracy is very significant, especially for the offshore structures. Determining the soil profile correctly, understanding the soil behavior and correct numerical modeling could provide significant savings in the offshore foundation industry, due to the benefits such as reducing the required penetration depths of spudcans etc.

Foundation bearing capacity is calculated as the multiplication of the plan area of the foundation, and the bearing pressure, that is a function of soil strength, soil weight, and foundation depth. There are many variants of this theory that take geometry of the foundation, soil conditions, and many other factors into account.

The penetration depth (z in the InSafeJIP guideline) is defined as the distance between the tip of the spudcan and the mudline as shown in Figure 4.1.

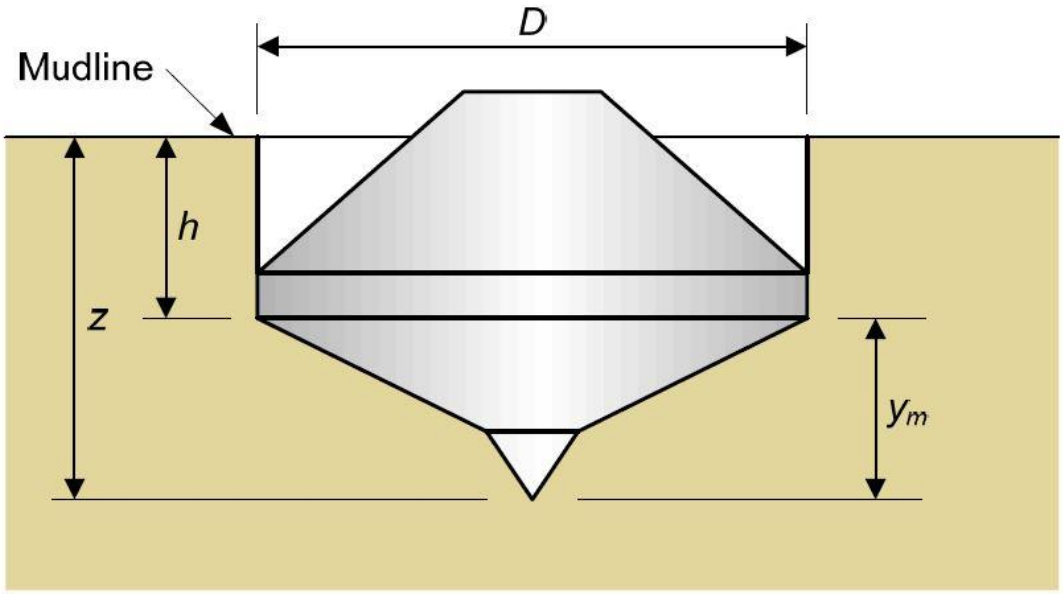

Figure 4.1 Penetration Depths z and h (Osborne, 2011)

Although z is the penetration depth, bearing capacity calculations require the use of h (Figure 4.1) as the penetration depth which can be defined as the lowest depth of the largest plan area of the spudcan.

Although most spudcans have polygonal geometry in plan view (Figure 4.2), for bearing capacity calculations, it is convenient to convert them into an equivalent circle having the same diameter D with the polygon. Therefore, a spudcan can be idealized with a few cones and cylinders on top of each other as shown in Figure 4.1.

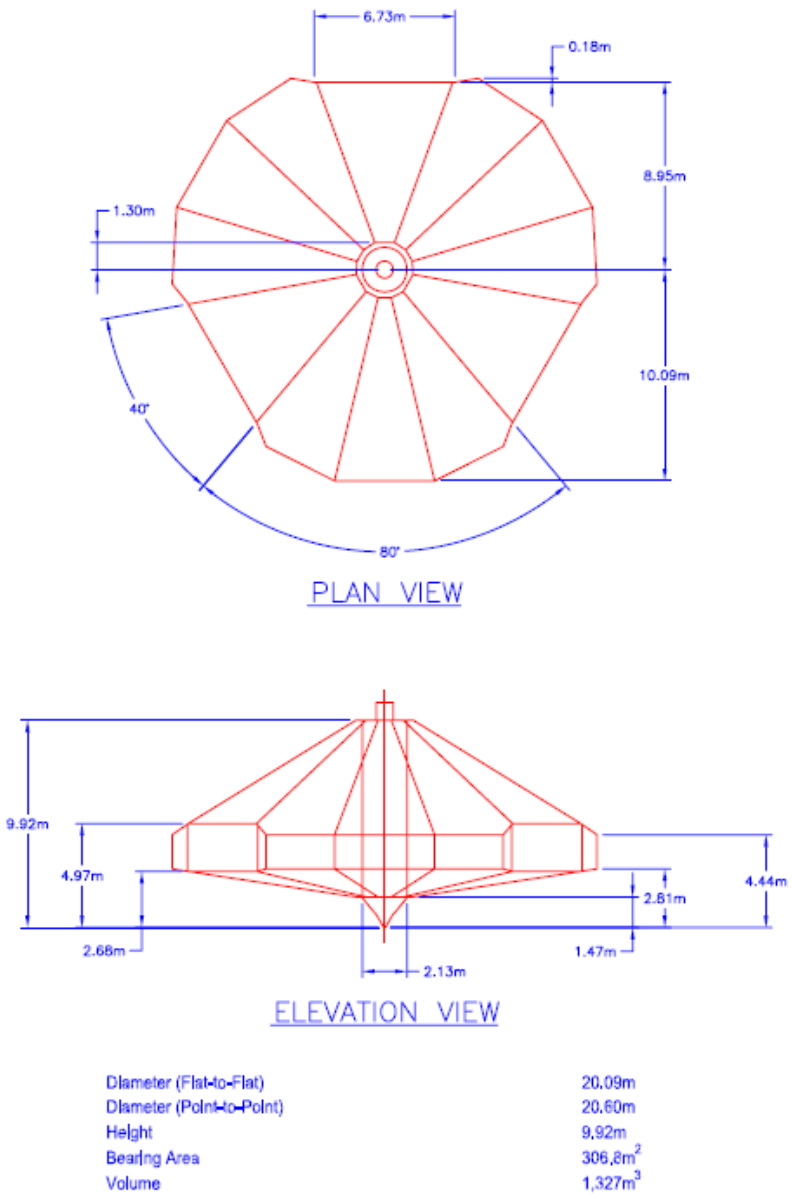

Figure 4.2 An example of a relatively large spudcan geometry and dimensions ("Letourneau Design, Super Gorilla XL," 2015)

Soil layers extending beyond the penetration depths should be known at each spudcan's location, and some idealization should be made for these layers. During the penetration process, fine-grained materials can be treated as undrained due to the relatively rapid penetration and the critical nature of the undrained case as compared to the drained one.

These kind of materials can be called clay; although, they may not be geologically classified as clay. For clays, unit weight as well as the undrained shear strength should be known. There are some studies in the literature that initially uses the peak value of the undrained shear strength and as the penetration of the spudcan continues the shear strength is dropped to a residual value related with the sensitivity of the clay. The sensitivity of the clay is defined as the ratio of the undrained shear strength in the undisturbed state to that in the remolded state. Sensitivity values for most clays range from 2 to 4; sensitive clays have values in the range of 4 to 8; and quick clays can have sensitivity values larger than 16 (Terzaghi, Peck, & Mesri, 1996). The sea-bottom cohesive sediments are typically deposited in marine (salty) environment, and therefore they display a random fabric, in a flocculated / aggregated nature, and they do not exhibit significant strength anisotropy, as opposed to lacustrine clays (which are deposited in lake environment). Undrained shear strength of clays can be taken as constant or as linearly increasing as a function of depth. (Figure 4.3) Examples of soft clay undrained shear strength profiles can be seen in Figure 4.4. The rate of increase of the undrained shear strength with depth can typically be expected to be in the order of 1.5 – 3 kPa/m depth, which is also in good agreement with the empirical relation of cu = 0.22 σ'_v for normally consolidated clays (for overconsolidated clays, 0.22 σ'_p for vertical stresses less than preconsolidation pressure, and 0.22 σ'_v for vertical stresses larger than preconsolidation pressure). For 1 m increase in depth, the in-situ effective vertical stress (σ'_v) increases approximately by 10 kPa, and cu increases approximately by 2,2 kPa per meter depth.

Figure 4.3 Sketches for describing the undrained shear strength with depth in seabed (Morrow & Bransby, 2011)

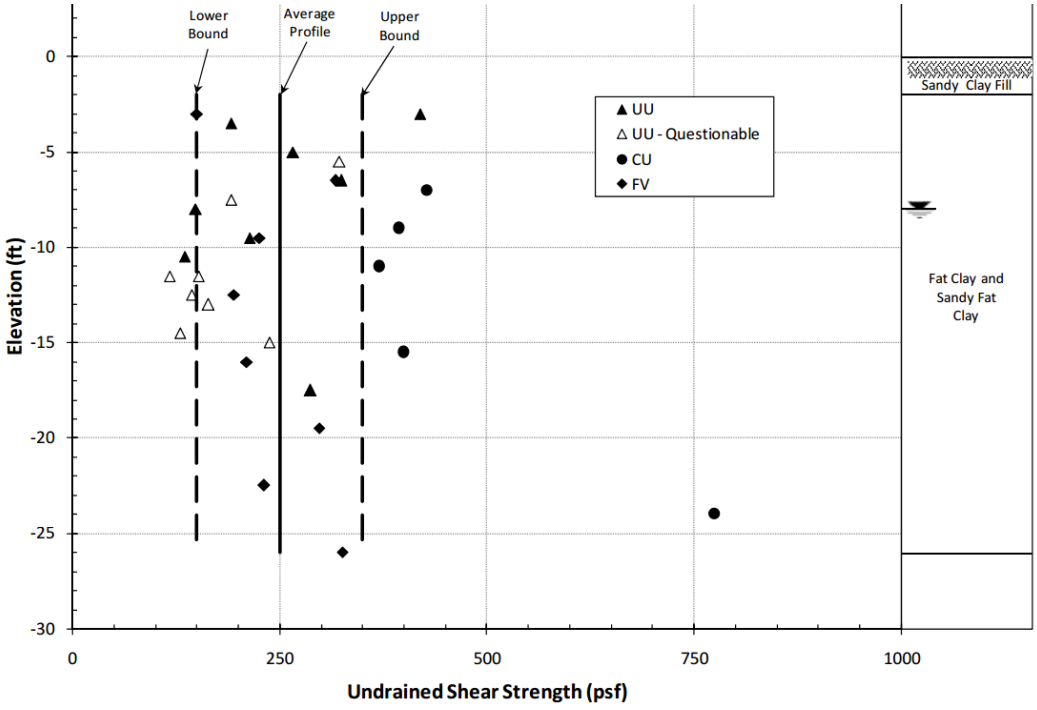

(a)

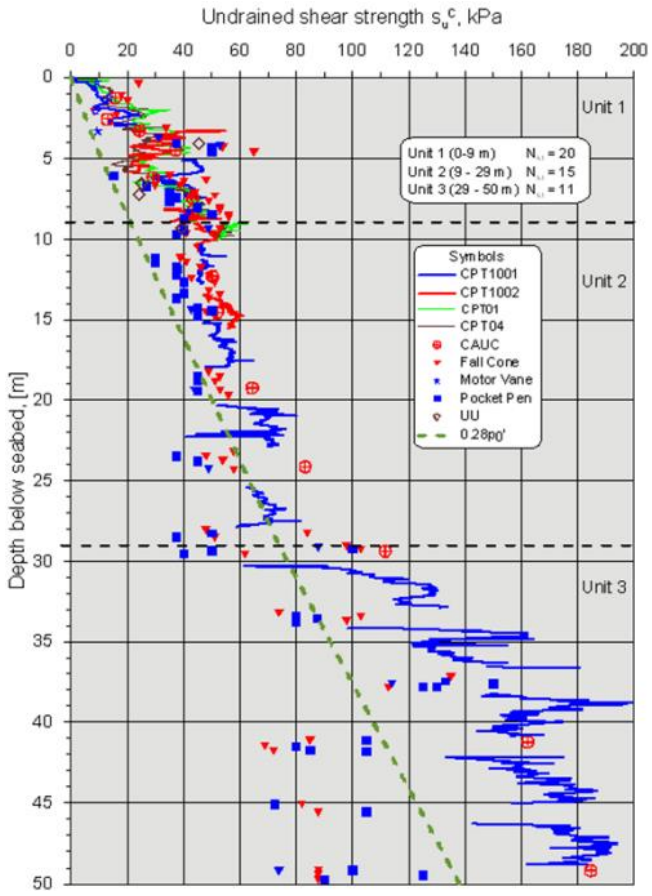

(b)

Figure 4.4 Examples of undrained shear strength profiles (a) from a site near the shore in Texas ("Characterization of Undrained Shear Strength Profiles for Soft Clays at Six Sites in Texas," 2008) (b) from a site in Norwegian Sea (De Groot, 2011)

After determining the penetration depth, spudcan geometry, and the soil parameters, one should be aware of the backflow process. Since the spudcan type foundations are continuously being pushed into the seabed by displacing the soil as it penetrates, it results in differences in the soil's displacement mechanism. Therefore, after a certain depth, the soil may start to flow back onto the spudcan.

Last of all, apart from these parameters, spudcan roughness factor, or surface roughness coefficient, which is denoted as α in InSafeJIP is one of the main properties which is used in the determination of bearing capacity factor. This factor can be defined as the ratio between maximum shear strength that can occur on the surface of the spudcan and

shear strength of the soil. This value should be in between 0 and 1, and this guideline suggests using 0.5 for clay if there is no evidence that supports any other value.

4.1.1 Spudcan Penetration in Clay

As mentioned earlier, homogeneous clay layer was taken into account in this chapter and in this thesis. Although the clay can be idealized with a strength that is linearly increasing as the depth increases, in all simulations presented in this chapter, it is kept constant.

In order to calculate the bearing capacity, change in the geometry as the spudcan penetrates into seabed should be taken into account. On the other hand, since there is no change in the soil profile, there is no need to concern about it.

If the maximum plan area of the spudcan does not penetrate into ground, it means that the spudcan is "partially penetrated". In other words, $z < y_m$ is satisfied (see Figure 4.5).

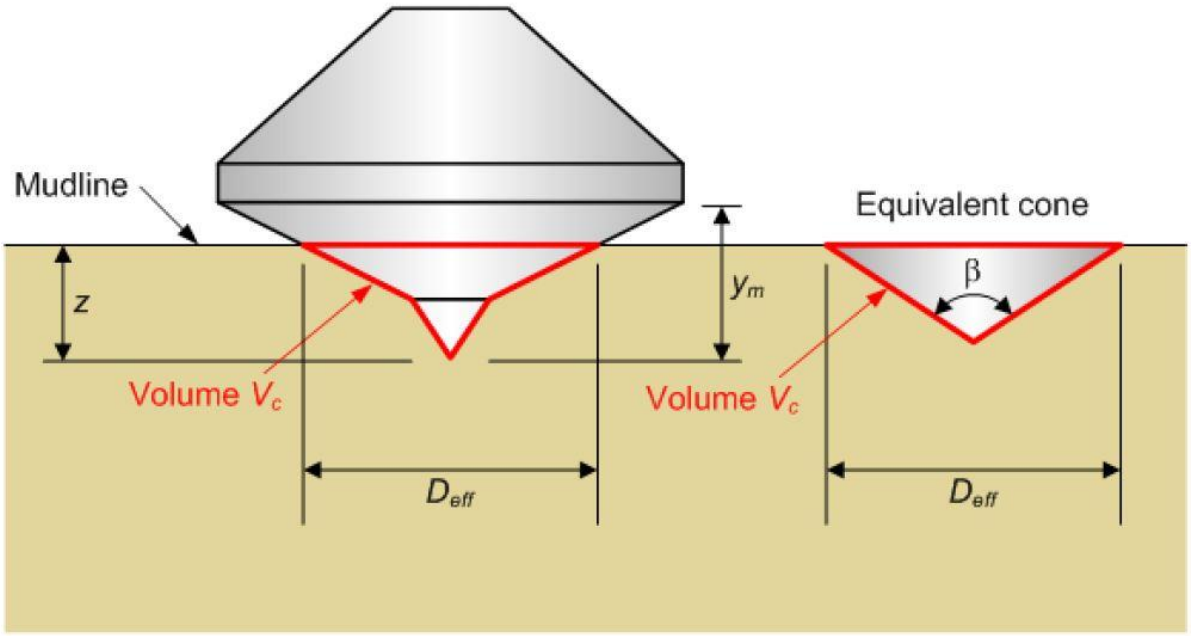

Figure 4.5 Equivalent Cone Definition (Osborne et al., 2011)

In case of a partial penetration, one should calculate the plan area by using the intersection between spudcan profile and mudline. Equivalent cone angle β can be calculated so that the equivalent cone covers the same volume with the original geometry of the spudcan embedded while they have the same plan area that is in contact with the surface of the soil layer.

Then, volume of the embedded part of the spudcan can be calculated with Equation 4.1:

$$V_c = \frac{1}{3} * \frac{\pi * D_{eff}^2}{4} * \frac{D_{eff}}{2} * \tan\left(\frac{\beta}{2}\right) = \frac{\pi * D_{eff}^3}{24} * \tan(\frac{\beta}{2}) \quad (4.1)$$

In which,

- β represents the equivalent cone angle
- D_{eff} represents the diameter of spudcan in contact with the mudline.

After calculating the volume of the embedded part of the spudcan, as stated in Chapter 4.1, the depth at which the embedment mechanism changes should be considered. At the critical cavity depth, which is denoted as h_c in the guideline, flow pattern changes from from "flow onto the surface" to "flow around the foundation". This depth is calculated from the following equation which is derived by (Hu et al., 2005):

$$\frac{h_c}{D} = \left(\frac{S_{uh}}{\gamma' * D}\right)^{0.55} - \frac{1}{4} * (\frac{S_{uh}}{\gamma' * D}) \quad (4.2)$$

Where S_{uh} is the local strength value at the critical depth which is equal to the undrained shear strength of the soil in our case.

After determining these values, the bearing capacity can be calculated for the three difference cases as follows

1. If $z \leq y_m$, (See Figure 4.1 and Figure 4.2) this is "partial penetration" case, and there is no backfill. In this case the following equation (Equation 4.3) can be used to estimate the bearing capacity:

$$Q_v = S_{u0} * N_C * A_{eff} + \gamma' * V_c \quad (4.3)$$

where,

- A_{eff} is the circular effective area which is in contact with the mudline,
- N_c is inclusive of the circular foundation shape factor,
- S_{u0} is the undrained shear strength of the clay layer.

The bearing capacity factor N_c is given by (Martin & Houlsby, 2003)as it is recommended in the guideline by the use of some factors related with the soil properties, and spudcan diameter. This subject will be discussed after all aforementioned cases are presented.

2. If $z \geq y_m$ and $h \leq h_c$, this means that the spudcan is fully penetrated into the ground, and there is no backfill, and in this case, the following equation (Equation 4.4) is used in the guideline.

$$Q_v = S_{u0} * N_c * A + \gamma'(V_C + A * h) \quad (4.4)$$

where

- V_C represents the volume of the conical part of the spudcan below the level h (See Figure 4.2 and Figure 4.3) Therefore, $V_c = V_C$ when $z = y_m$

3. If $z \geq y_m$ and $h \geq h_c$, this means that for the full penetration case there is a backfill, and the following equation (Equation 4.5) is recommended by the guideline.

$$Q_v = S_{u0} * N_c * A + \gamma'(V_C + A * h_c) \quad (4.5)$$

where,

- h_c represents critical cavity depth at which backfilling starts.

Before going deeper into these equations, and working on some examples, determination of the undrained bearing capacity factors for different conditions should be practiced from (Martin & Houlsby, 2003) as stated in InSafeJIP guideline. These factors are presented in the corresponding study as a function of various variables, and these are:

- The cone angle (β)
- The Dimensionless Penetration Depth (h/D) (See Figure 4.1)
- The Surface Roughness Factor (α)
- The Dimensionless Definition of the Rate of Increase of Strength with Depth ($\rho D/S_{um}$) which is taken to be zero in all analyses presented here.

For the determination of the factors, there are some assumptions that may result in some deviations in the bearing capacities that are calculated in this study. First of all, Martin & Houlsby (2003) treat soil as rigid-plastic with yield governed by Tresca condition with an S_u. On the other hand, in this study, Mohr-Coulomb failure criteria is used as stated in Chapter 3. Furthermore, the soil is assumed to be weightless in their study which makes the undrained bearing capacity factors independent of the specific weight of the soil; however, this is not the case in the analyses conducted in this thesis. Finally, it is assumed in their study that the space above the conical footing is occupied by a rigid, perfectly smooth shaft (Figure 4.6). As illustrated in Figure 4.6, shear stress on the vertical sides of the cylindrical shaft is assumed to be zero; therefore, for the analysis presented in this study, after the conical footing is penetrated into ground, there may be a deviation in the bearing capacity values.

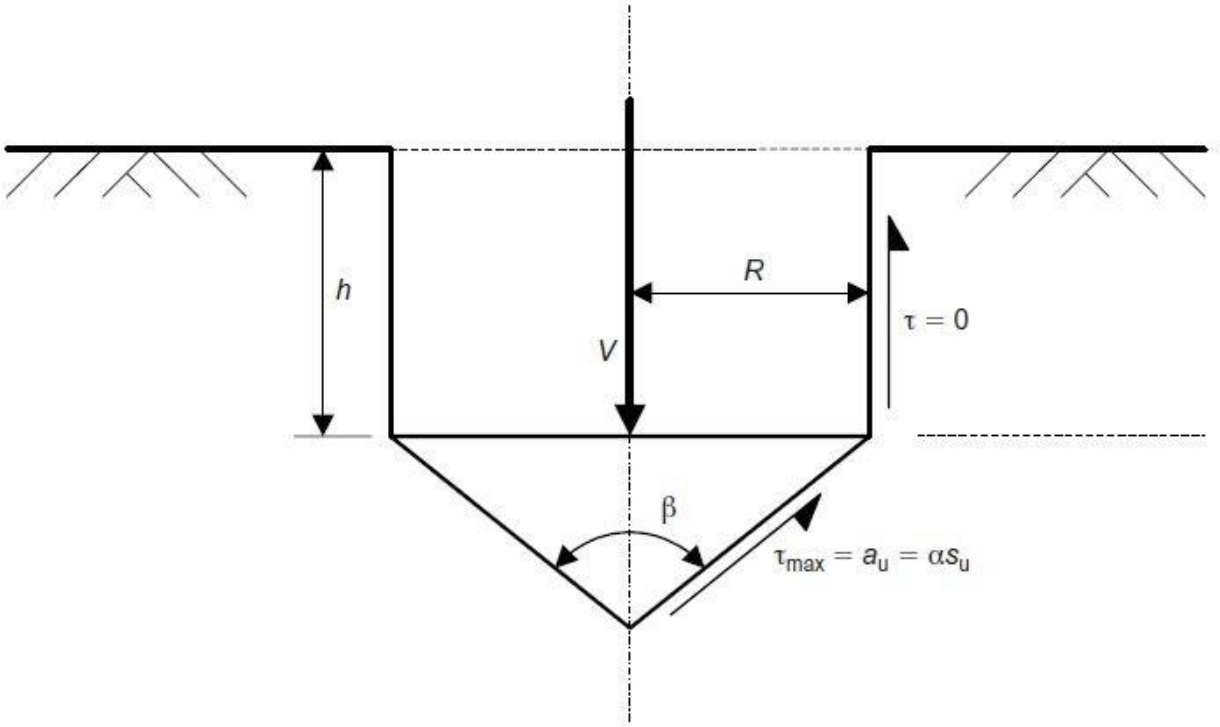

Figure 4.6 Footing Outline (Martin & Houlsby, 2003)

In their study, Martin & Houlsby (2003) presented 6 different undrained bearing capacity factor tables with six different cone angles, roughness factors, and dimensionless embedment depths. For illustration purposes, the table given for the case in which the cone angle is 120 degrees is given in Table 4.1.

Table 4.1 Undrained Bearing Capacity Factors for Conical Footings on Clay for $\beta = 120^{\circ}$ (Martin & Houlsby, 2003)

Values of $N_{c0} = V/\pi R^2 s_{u0}$ for $\beta = 120^{\circ}$

$2R\rho/s_{um}$	$h/2R$	Roughness factor, α					
		0·0	0·2	0·4	0·6	0·8	1·0
0·0	0·0	4·959	5·253	5·509	5·732	5·918	6·053
	0·1	5·228	5·516	5·769	5·987	6·170	6·298
	0·25	5·570	5·852	6·100	6·312	6·489	6·617
	0·5	6·037	6·310	6·550	6·756	6·934	7·047
	1·0	6·737	7·006	7·243	7·441	7·614	7·718
	2·5	8·068	8·322	8·551	8·746	8·899	8·988
1·0	0·0	5·687	6·043	6·362	6·646	6·893	7·092
	0·1	5·887	6·237	6·547	6·824	7·065	7·259
	0·25	6·117	6·454	6·756	7·022	7·258	7·451
	0·5	6·393	6·719	7·010	7·266	7·485	7·659
	1·0	6·797	7·097	7·367	7·615	7·816	7·970
	2·5	7·521	7·817	8·080	8·294	8·493	8·615
2·0	0·0	6·375	6·787	7·161	7·495	7·795	8·038
	0·1	6·413	6·803	7·155	7·473	7·751	7·973
	0·25	6·465	6·833	7·167	7·461	7·719	7·935
	0·5	6·561	6·909	7·220	7·493	7·741	7·918
	1·0	6·805	7·119	7·396	7·654	7·867	8·034
	2·5	7·427	7·721	7·989	8·207	8·411	8·534
3·0	0·0	7·043	7·509	7·932	8·312	8·658	8·930
	0·1	6·838	7·267	7·653	7·998	8·307	8·570
	0·25	6·710	7·094	7·447	7·761	8·046	8·271
	0·5	6·658	7·018	7·340	7·625	7·882	8·077
	1·0	6·805	7·115	7·407	7·671	7·890	8·062
	2·5	7·385	7·680	7·948	8·173	8·376	8·507
4·0	0·0	7·696	8·217	8·685	9·108	9·488	9·814
	0·1	7·201	7·657	8·071	8·441	8·771	9·031
	0·25	6·876	7·285	7·654	7·985	8·274	8·525
	0·5	6·721	7·085	7·416	7·715	7·971	8·178
	1·0	6·805	7·117	7·413	7·681	7·902	8·078
	2·5	7·385	7·658	7·925	8·152	8·356	8·487
5·0	0·0	8·349	8·911	9·429	9·894	10·310	10·668
	0·1	7·521	7·991	8·427	8·819	9·176	9·450
	0·25	7·012	7·433	7·814	8·153	8·453	8·718
	0·5	6·765	7·134	7·471	7·775	8·034	8·250
	1·0	6·804	7·119	7·417	7·687	7·910	8·088
	2·5	7·341	7·643	7·911	8·139	8·343	8·475

In order to use the values given in Table 4.1, some assumptions are also made in this study. The table is linearly interpolated to obtain intermediate values. This interpolation is done not only for the roughness factor, but also for the dimensionless embedment depth. This may also result in some deviations between the hand calculations, and numerical study of the bearing capacities.

It should also be noted that, for this thesis study, the undrained shear strength of the clay is assumed to be constant everywhere. Therefore only the first row of the N_c factor will be used in the calculations.

4.1.1.1 Theoretical Calculations

Spudcan cone angle and diameter are taken as 120 degrees and 10 meters, respectively. Two different surface roughness coefficients of 0.5 and 1.0 are chosen, and undrained shear strength of clay layer is taken as 40 kPa. Furthermore, as stated in Chapter 3, Poisson's Ratio is taken to be 0.45 (almost incompressible) for undrained conditions.

As stated in Chapter 4.1.1, after the penetration depth, diameter and cone angle of the spudcan, and soil properties are defined, the next step is to calculate the partial volumes of the spudcan as it is embedded into seabed. Then, the critical cavity depth is estimated, and three different bearing capacity equations are used to calculate the reaction force that occurs on the foundation.

For these two cases, the undrained bearing capacity factors are tabulated in Table 4.2. For $\alpha = 0.5$, the values are linearly interpolated between given values for 0.4 and 0.6.

Table 4.2 Undrained Bearing Capacity Factors for β = 120°

β = 120°		
h/2R	**α=1**	**α=0.5**
0	6.053	5.6205
0.1	6.298	5.878
0.25	6.617	6.206
0.5	7.047	6.653
1	7.718	7.342
2.5	8.988	8.6485

As indicated in Chapter 4.1.1, the bearing capacity should be calculated for the embedment depth of y_m (Figure 4.1). The critical cavity depth is, also found from Equation 4.2. These dimensions for the spudcan having a cone angle β = 120° are given in Table 4.3

Table 4.3 Necessary Dimensions for Bearing Capacity Calculation of the Spudcan with β = 120°

Parameter	**Value**	**Unit**
D	10.00	m
hc	4.12	m
ym	2.89	m
zc	12.01	m

It should also be noted that,

$$z_c = h_c + y_m \tag{4.6}$$

Last of all, in Table 4.2, the bearing capacity factors are given for different h/2R values. In between these values, linear interpolation should also be made in order to catch more

realistic results of bearing capacities. The calculations are conducted according to these assumptions, and all bearing capacity values at certain depths are calculated.

Bearing capacity – penetration curves for the two roughness coefficient combinations are given in Figure 4.7. In these figures, at the depth for which maximum diameter of cone is in contact with the ground, and at the critical cavity depth, there are sudden changes in the trend of the graphs. It is stated in InSafeJIP (Osborne et al., 2011) that these sudden changes occur smoothly in practice.

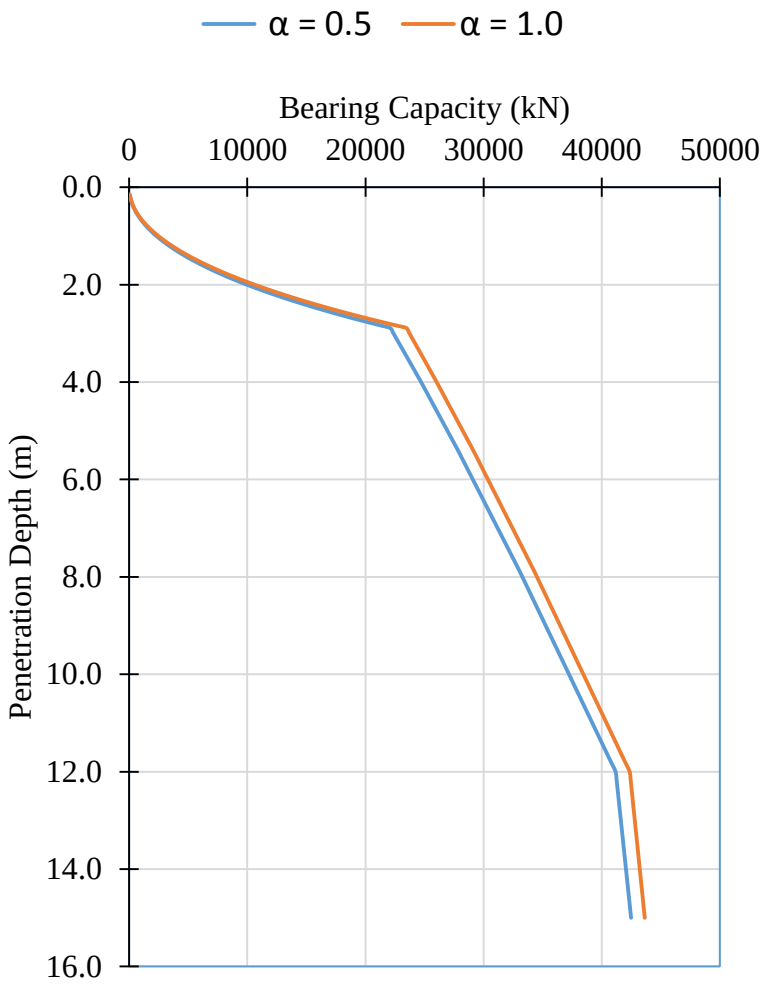

Figure 4.7 Bearing Capacity (kN) – Penetration Depth (m) Curves obtained from InSafeJIP Bearing Capacity Calculation Techniques

4.2 Numerical Model

For the same dimensions presented in Chapter 4.1, numerical models were constructed in 3D finite element software (Abaqus 6.14) for comparison with the theoretical calculations.

First, in order to accurately define the initial stress conditions on the soil profile, gravitational field was applied with a linearly increasing amplitude (Figure 4.8) in 15 seconds to eliminate the generation of stress waves on the ground which may affect the results.

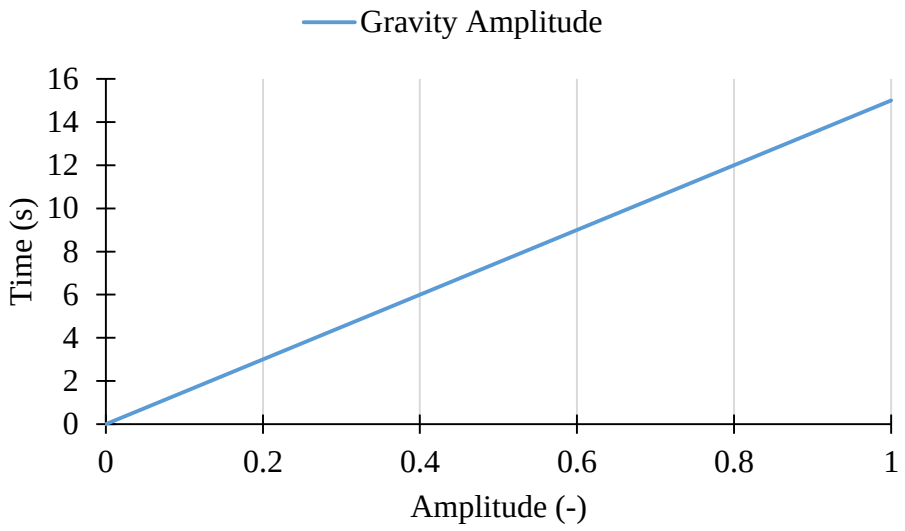

Figure 4.8 Application of the gravity amplitude

After initialization of the stress profile, penetration of the spudcan into the seabed starts, and the following bearing capacity vs penetration depth sketches are obtained. (Figure 4.9)

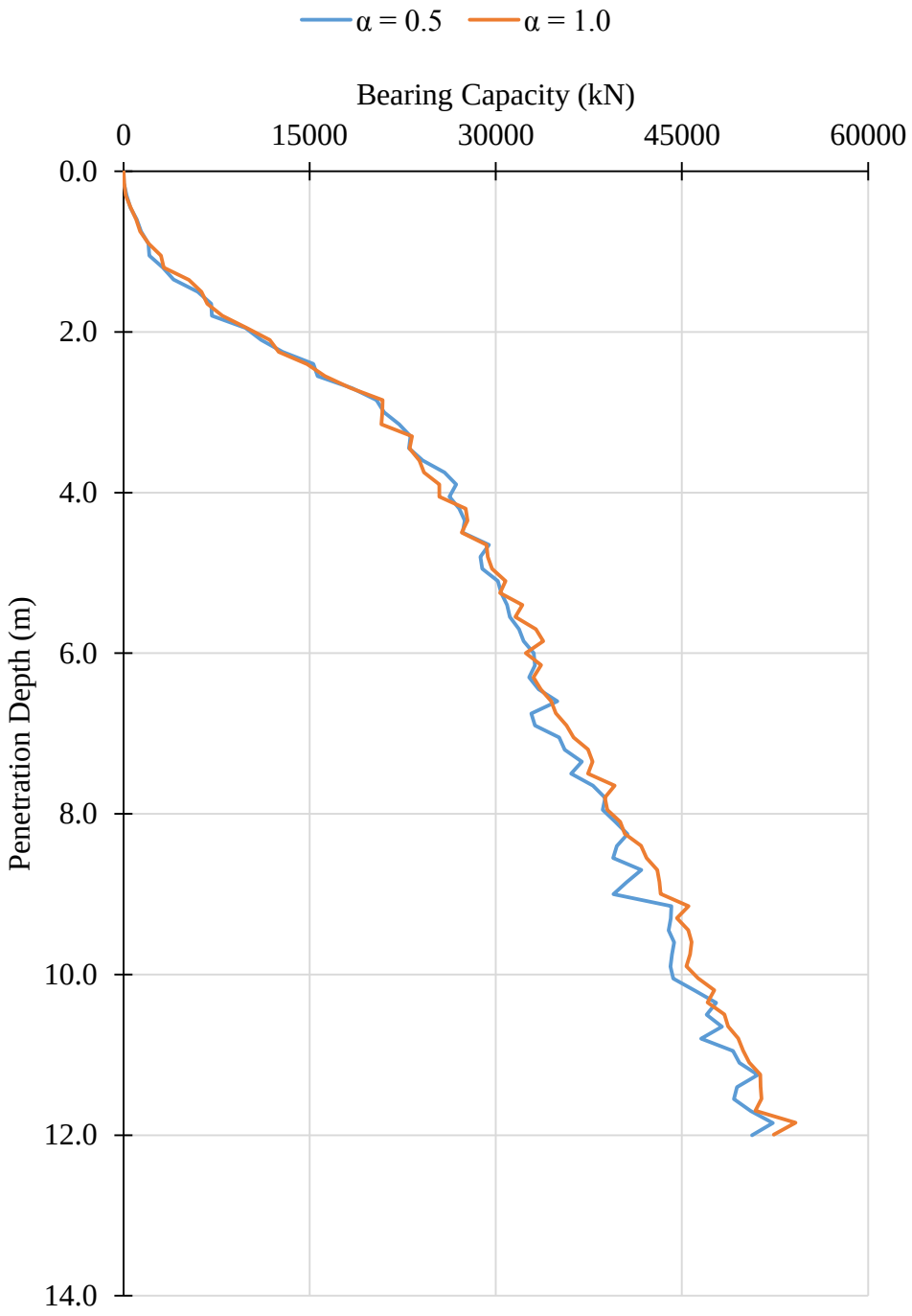

Figure 4.9 Bearing Capacity - Penetration Depth Curves obtained from Abaqus 6.14 Software

Figure 4.9 shows that the roughness coefficient has a small effect on the bearing capacity values; however, as expected, as it increases, the reaction forces on the spudcan in vertical direction also increase. Figure 4.10 and Figure 4.11 shows a direct comparison of the numerical and theoretical results for the two values of surface friction considered.

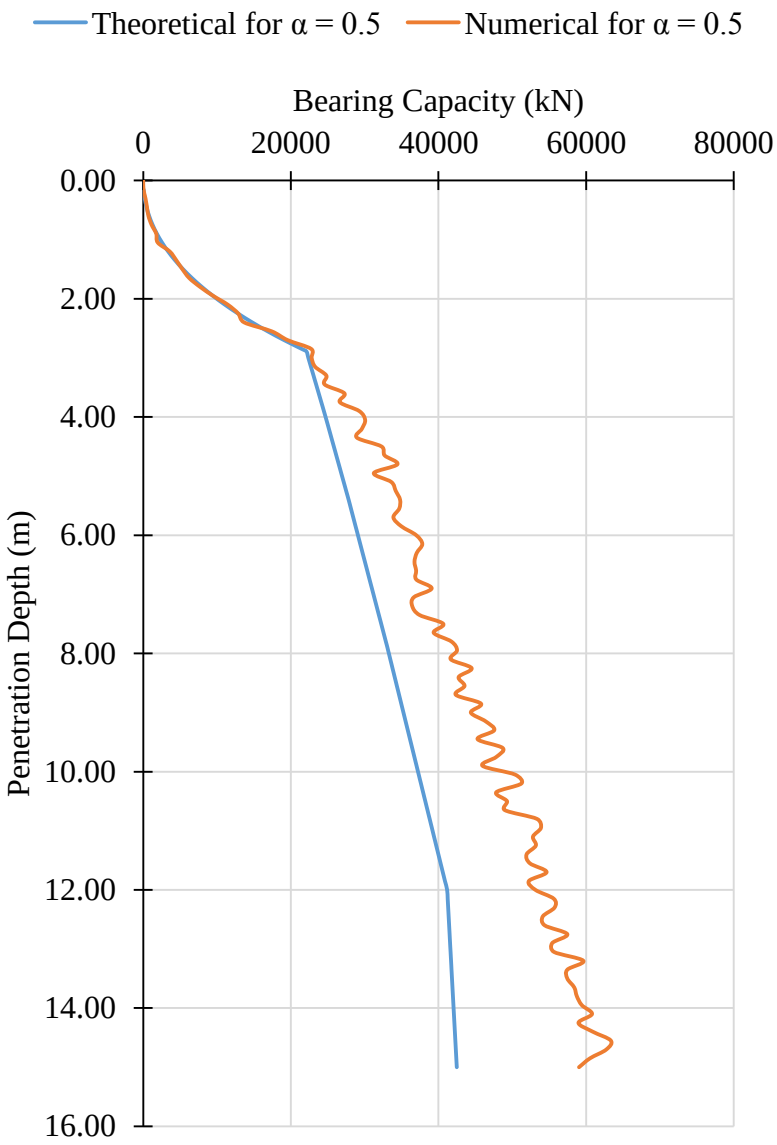

Figure 4.10 Bearing Capacity - Penetration Depth Curves Comparison for α = 0.5

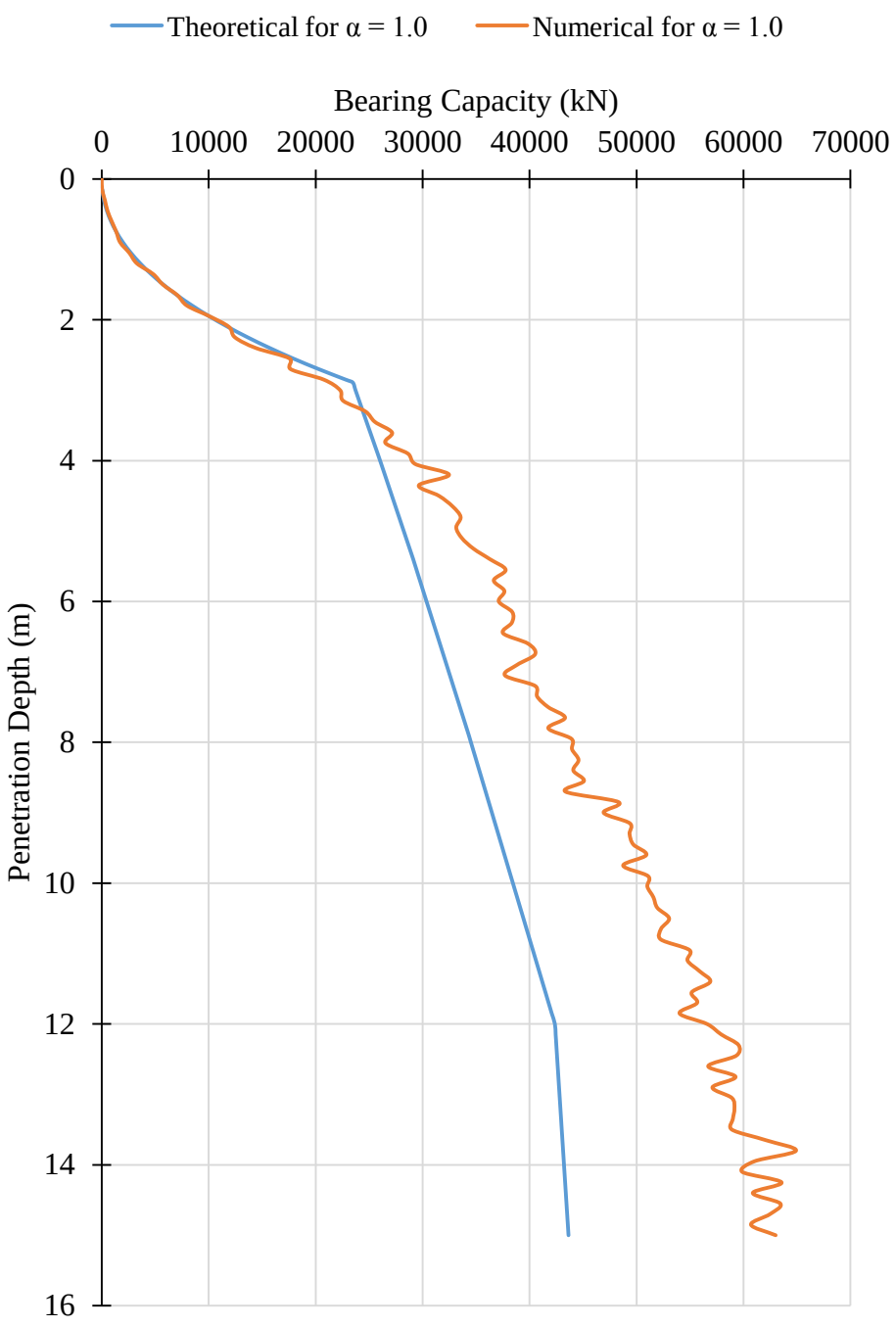

Figure 4.11 Bearing Capacity - Penetration Depth Curves Comparison for α = 1.0

4.3. Discussion of Results

In this chapter, numerical and theoretical penetration dependence of the bearing capacity were computed and compared against each other. InSafeJIP uses the undrained bearing capacity factors which are presented by Martin & Houlsby (2003). These numerical models from which these factors are evaluated in the corresponding paper are subjected to some restrictions as stated in Chapter 4.1.1. The assumptions used in both methods are the same for the spudcan cone; therefore, the results were found to be pretty similar to each other. However, since the shearing stress that occurs on the walls of the spudcan is assumed to be zero in (Martin & Houlsby, 2003), as stated in Chapter 4.1.1 the bearing capacities found with the use of this method are smaller than the ones of the numerical models.

As a general approach, the numerical models used within the scope of this thesis can be considered to be similar with the methods used in InSafeJIP, and can be used in order to obtain the bearing capacity - penetration depth values of the spudcan penetration. It was not possible to validate the numerical results with the measured penetration-depth graphs of real spudcans, since (1) due to the competitive and patentable nature of the technological developments in the offshore industry, many companies do not publicly share their real measured penetration resistance versus depth data, (2) it is not always easy to accurately measure these values due to various different loading conditions existing in the field and uncertainties involved in the problem, (3) for the laboratory studies that measured these data, numerical modelling could not be carried out to duplicate their results because of some of the missing (not reported) information, in the laboratory studies as well.

From Figure 4.10, and Figure 4.11, it can be seen that trend of the graphs start to change at the predicted cavity depths. As it is previously stated, this change is not abrupt as it is in InSafeJIP but occurs smoothly. After that depth, as the penetration proceeds, clay tends to flow onto the spudcan, and this results in the reduction of the rate of change of the upwards reaction forces generated at the spudcan surface with respect to depth.

Some of the stresses and deformations in the numerical study will be presented in the following chapter.

CHAPTER 5

PARAMETRIC STUDY

Reaction forces developed at the base of the spudcans during penetration process are affected by several factors. In this chapter, a parametric study on a number of factors is carried out to examine their effects on spudcan penetration through cohesive materials. After the verification of the numerical method with the hand calculations given in InSafeJIP (Osborne et al., 2011) in the previous chapter, numerical models were constructed. In Table 5.1, major factors affecting the vertical reaction force on the spudcan during penetration into seabed are listed. In this chapter, effects of spudcan embedment depth, undrained shear strength of cohesive seabed, spudcan diameter, cone angle and surface roughness of the spudcan, were investigated by changing one parameter at a time while keeping the rest of the parameters constant. Furthermore the spacing between two adjacent spudcans is also investigated to see the effect on penetration resistance during installation.

Table 5.1 Parametric Study Variables and Their Values

Property	Values	Property	Values
Cone Angle (˚)	90	Undrained Shear Strength of the clay (kPa)	20
	120		40
	150		80
Spudcan Diameter (m)	7.5	Surface Roughness (-)	0
	10		0.5
	12.5		1
	15	Spacing / Diameter Ratio (-)	1.5
Embedment Depth (m)	3		2.0
	12		2.5
	20		3.0

5.1 Description of the Numerical Model

Except for the case where we analyzed two adjacent spudcans together, the geometry of the computational domain was kept constant in all of the simulations. As mentioned in the preceding section, while checking the effect of one parameter on the penetration resistance, the others were kept constant, and these constant values are tabulated in Table 5.2.

Table 5.2 Typical values that are kept constant when the others are varied

Property	Value	Unit
Embedment Depth	12	m
Spudcan Diameter	10	m
Cone Angle	120	°
Undrained Shear Strength	40	kPa
Surface Roughness	0.5	-

Boundary conditions were the same for every analysis, and they were clearly defined in Chapter 3.3. For the parametric analyses, predescribed penetration velocity was taken as 15 cm/s. A discussion on the effect of penetration velocity on the results was presented in Chapter 3.

Characteristic finite element size was taken as 0.7 m in all simulations based on our findings presented in Chapter 3.4. In the finite element mesh, 8-noded Eulerian elements with reduced integration (called EC3D&R in Abaqus 6.14) was the selected finite element type.

5.2 Parametric Analyses

Six series of analyses were conducted as given in Table 5.1. These are carried out in order to see the effect of the following factors on the spudcan penetration resistance (bearing capacity):

- the size (diameter) of the spudcan,
- the cone angle of the spudcan,
- the embedment depth of the spudcan.
- the undrained shear strength of the seabed soil
- the surface roughness of the spudcan
- the spacing between two adjacent spudcans.

5.2.1 The Effect of the Cone Angle

Cone angle of the spudcan type foundations affect the bearing capacity, critically. By changing this angle, and keeping the diameter of the spudcan constant (Figure 5.1), height of the cone can be reduced. This may enable the foundation to reach high bearing pressures faster, i.e., during the penetration process the desired preload can be achieved with lesser embedment. Figure 5.2, Figure 5.3, and Figure 5.4 show the vertical stress contours of these three spudcans (having cone angles of 90, 120 and 150 degrees), when their cone sections are fully penetrated into the sea bottom.

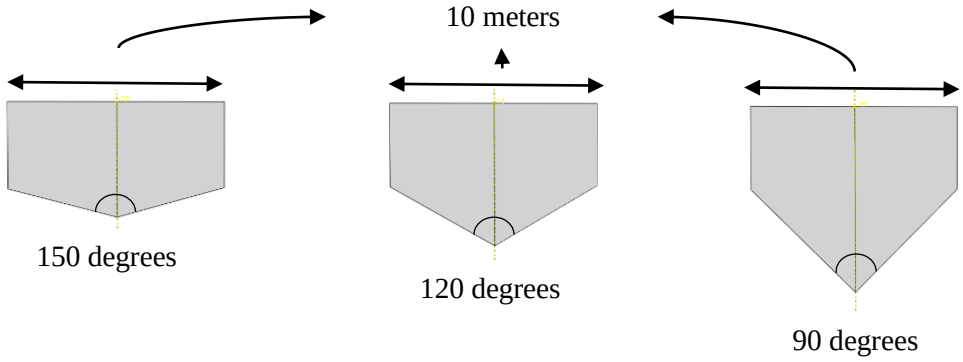

Figure 5.1 Spudcan Cross Sections with Different Cone Angles

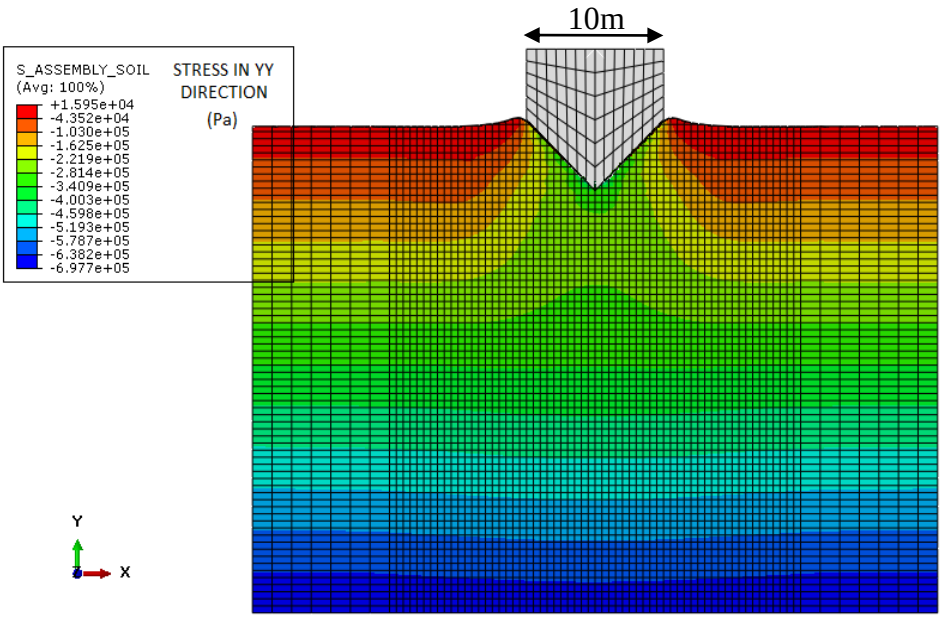

Figure 5.2 Vertical Stress Contours of Spudcan with 90 Degrees Cone Angle Penetrating into Seabed

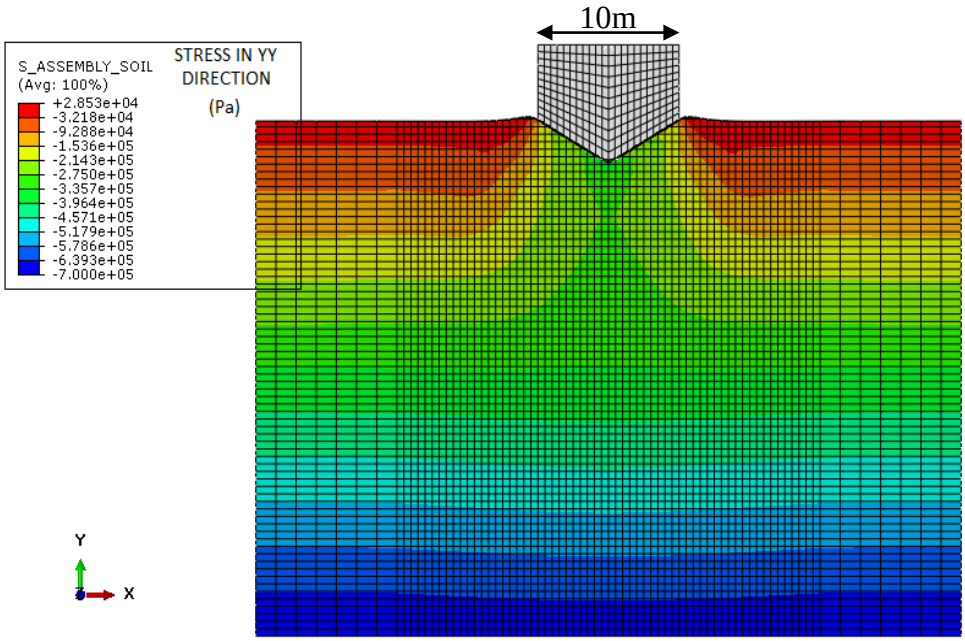

Figure 5.3 Vertical Stress Contours of Spudcan with 120 Degrees Cone Angle Penetrating into Seabed

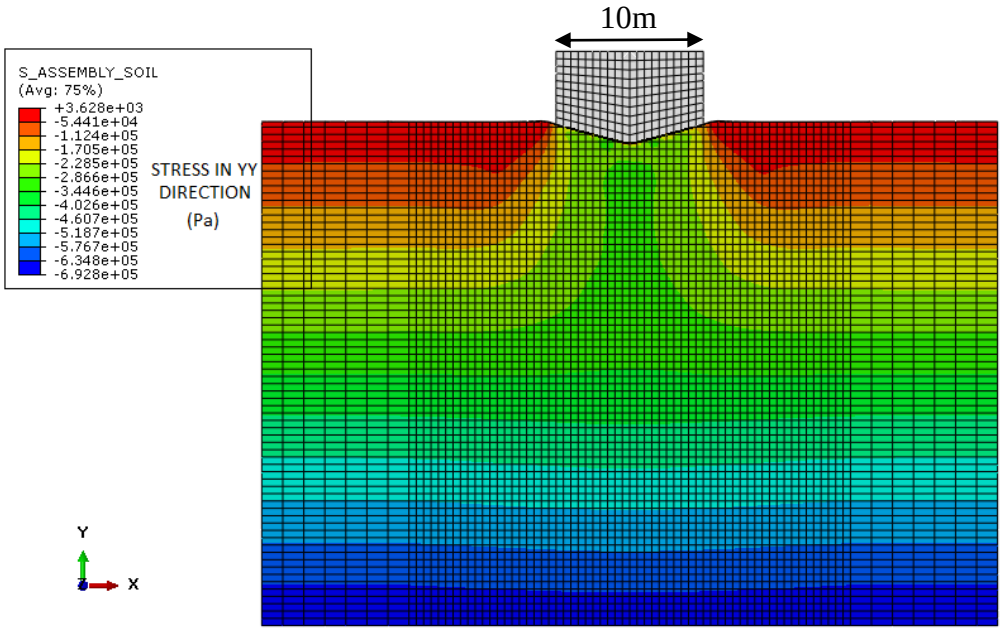

Figure 5.4 Vertical Stress Contours of Spudcan with 150 Degrees Cone Angle Penetrating into Seabed

As mentioned before, other properties related with this model were kept constant (Table 5.2) in order to see the true effect of cone angle change. Table 5.3 shows how the bearing capacity was reached as the spudcan penetrates into seabed for the first 5 meters of embedment. The spudcan with a cone angle of 90 degrees reached 21.5 MN bearing capacity at a penetration depth of 5.10 meters whereas the spudcan with a cone angle of 150 degrees reached 35.4 MN force at the same depth.

Furthermore, it is possible to see from Figure 5.2 through Figure 5.4 that for all three spudcans, the maximum vertical stresses that occurred in the soil underneath the spudcan tip are equal to each other since the spudcans have the same diameters.

An increase in the cone angle while keeping the diameter constant decreases the required penetration depth to reach the desired bearing capacity. Therefore, when deep penetration is hard due to the existence of deep-water or uncertainties due to insufficient site data for deeper soil strata, it is sensible to use spudcans with high cone angles. Sometimes, softer soil layers could be present under the upper stiffer layers, and for

these kinds of cases, punch-through may present itself as a major problem during penetration. This can also be viewed as a loss of stability of the spudcan due to the collapse of the underlying weak layer. For these cases, it is also better to reach the desired bearing capacity at shallow embedment depths with larger cone angle values. For better illustration, the values given in Table 5.3 are sketched in an x-y graph for 12 meters of embedment in Figure 5.5.

Table 5.3 Bearing Capacity vs Depth Values for Different Cone Angles

90 degrees		**120 degrees**		**150 degrees**	
Depth (m)	**Qv (kN)**	**Depth (m)**	**Qv (kN)**	**Depth (m)**	**Qv (kN)**
0.00	0	0.00	0.00	0.00	0.00
0.30	73	0.30	263.40	0.30	467.41
0.45	118	0.45	539.94	0.45	1484.85
0.60	217	0.60	1075.92	0.60	2721.78
0.75	287	0.75	1418.13	0.75	4022.81
0.90	433	0.90	2002.30	0.90	6509.98
1.20	1130	1.20	3181.21	1.20	11666.19
1.50	2017	1.50	5980.56	1.50	19207.81
1.80	2750	1.80	7119.90	1.80	21654.08
1.95	3253	1.95	9841.64	1.95	21745.79
2.10	4057	2.10	11099.34	2.10	21933.50
2.40	4872	2.40	15309.34	2.40	24676.71
2.55	5725	2.55	15633.23	2.55	25829.81
2.70	6048	2.70	18404.61	2.70	26738.17
3.00	7162	3.00	20995.40	3.00	28003.80
3.30	9664	3.30	23136.36	3.30	29809.32
3.45	10809	3.45	22992.45	3.45	29523.35
3.60	11642	3.60	24104.53	3.60	28756.37
3.90	13570	3.90	26811.46	3.90	30344.92
4.20	16659	4.20	27049.67	4.20	32588.86
4.50	18577	4.50	27336	4.50	31969.18
4.80	19862	4.80	28751	4.80	33107
4.95	20038	4.95	28899	4.95	34800
5.10	21463	5.10	30169	5.10	35367

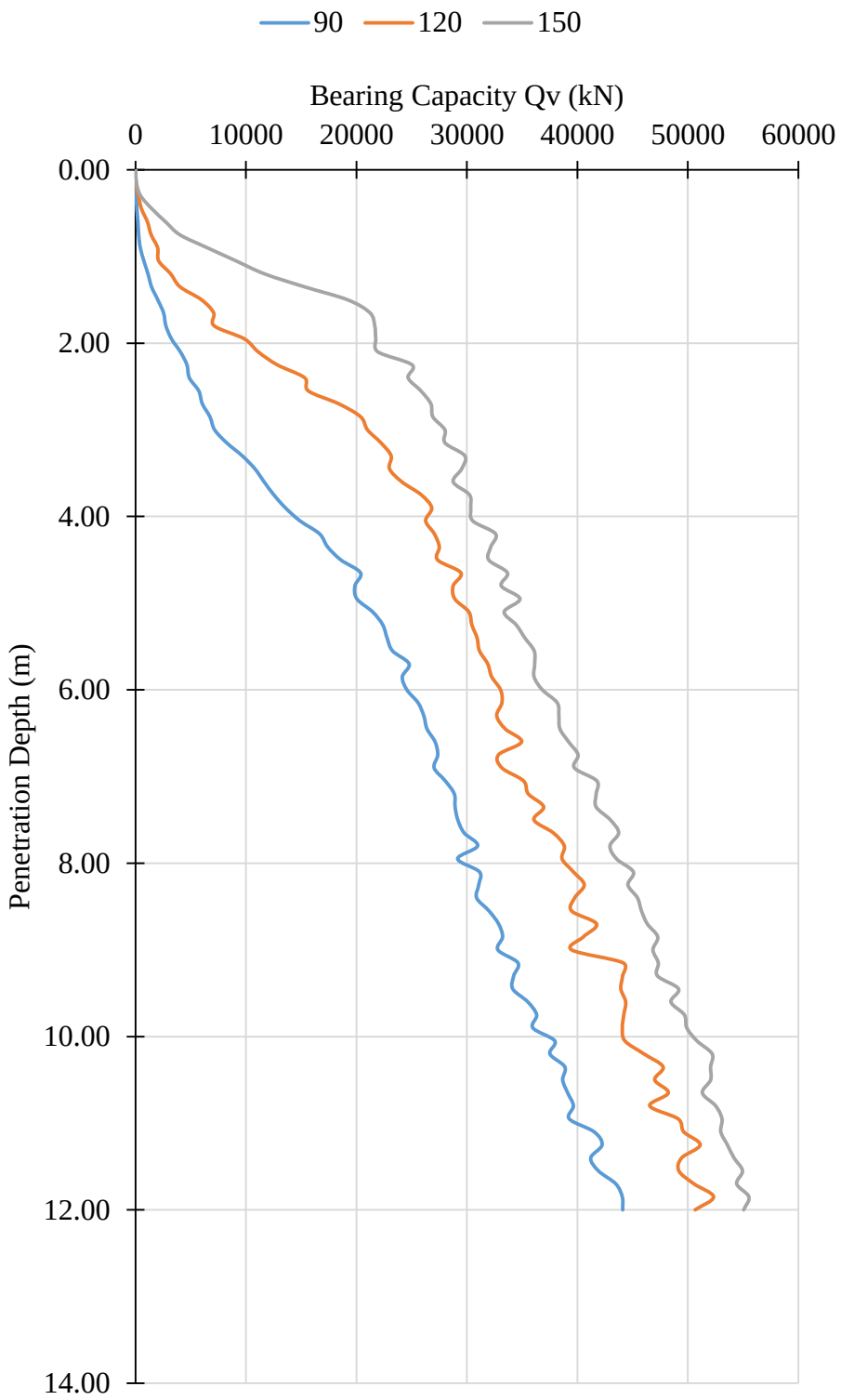

Figure 5.5 Embedment Depth vs Bearing Capacity Variety for Different Cone Angles

5.2.2 Effect of the Spudcan Diameter

It is inevitable that, the diameter of the spudcan will affect the bearing capacity significantly, as in the case of footing size effect for bearing capacity of the foundations of buildings. In this study, this effect is quantified by using four common spudcan diameters (ranging from 7.5 to 15 m) found in the literature as shown in Table 5.1. The rest of the simulation parameters are kept constant at their given values in Table 5.2. For a constant cone angle, this change in the diameter results in an increase in the height of the cone, which means that when the cone of the foundation is fully penetrated into the soil, bearing capacity becomes larger than bearing capacity of smaller dimensions. One should, therefore, choose diameter of the spudcan based on the availability of depth of penetration, and the level of the required bearing capacity. The results of bearing capacity versus penetration depth for the first 5 meters are tabulated in Table 5.4, and sketched in Figure 5.9 for 12 meters of penetration.

Table 5.4 Bearing Capacity versus Depth Values for Different Cone Diameters

D = 15m		**D = 12.5m**		**D = 10m**		**D = 7.5m**	
Depth (m)	**Qv (kN)**	**Depth (m)**	**Qv (kN)**	**Depth (m)**	**Qv (kN)**	**Depth (m)**	**Qv (kN)**
0.90	1799	0.90	1675	0.90	2002	0.90	1572
1.20	3396	1.20	3051	1.20	3181	1.20	3467
1.50	5334	1.50	4755	1.50	5981	1.50	5516
1.80	7773	1.80	6014	1.80	7120	1.80	6090
2.10	10367	2.10	10199	2.10	11099	2.10	9657
2.40	13955	2.40	13948	2.40	15309	2.40	11417
2.70	17696	2.70	19769	2.70	18405	2.70	12006
3.00	22185	3.00	22690	3.00	20995	3.00	14512
3.30	27464	3.30	27681	3.30	23136	3.30	13455
3.60	32704	3.60	33546	3.60	24105	3.60	16592
3.90	39344	3.90	33514	3.90	26811	3.90	15418
4.20	46143	4.20	35212	4.20	27050	4.20	17200
4.50	50974	4.50	40276	4.50	27336	4.50	19027
4.80	53876	4.80	33762	4.80	28751	4.80	16245
5.10	58360	5.10	42373	5.10	30169	5.10	19165

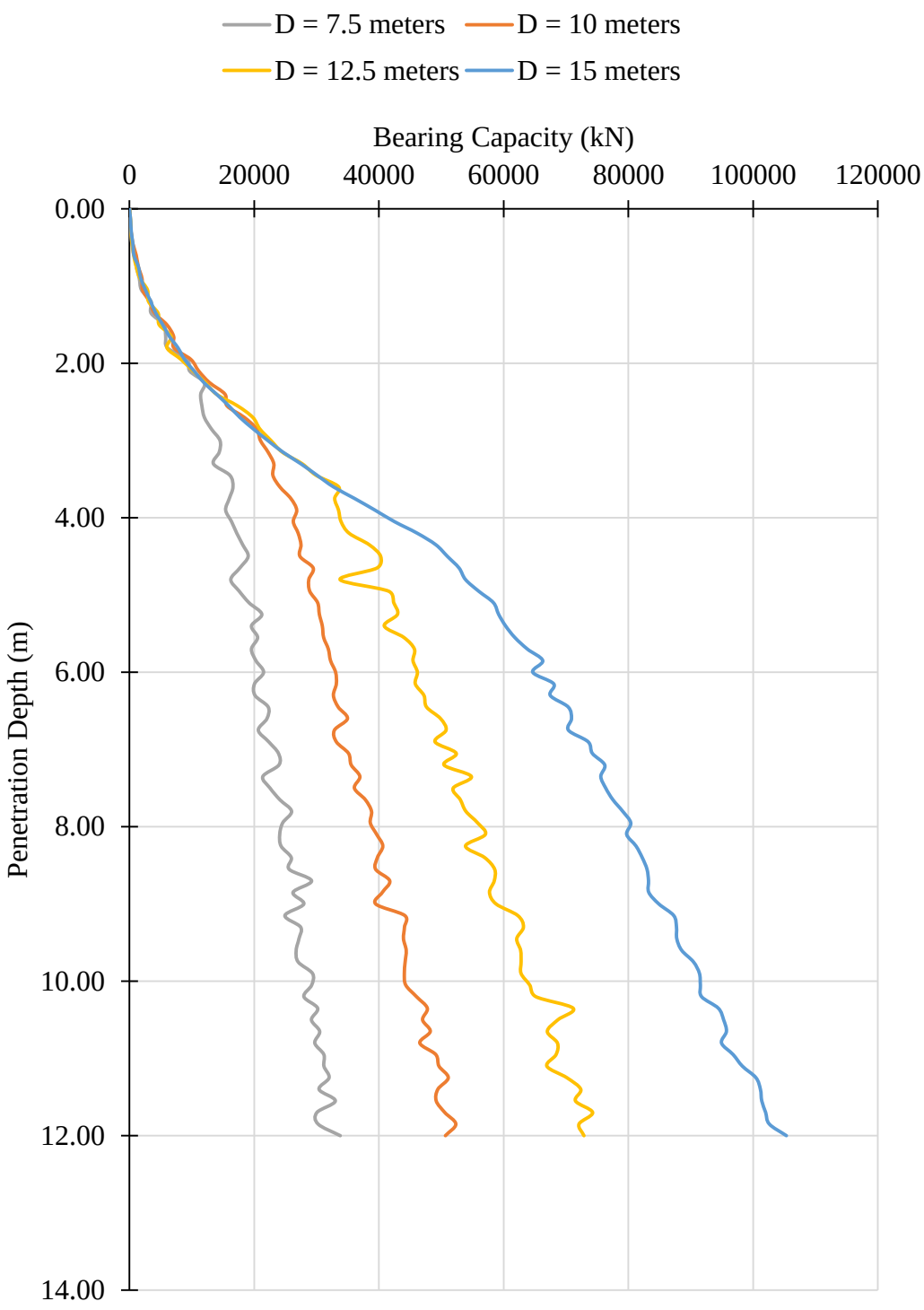

Figure 5.6 Embedment Depth vs Bearing Capacity Variety for Different Cone Diameters

5.2.3 Effect of the Embedment Depth

Embedment, or penetration, depth is one the main factors that affects the magnitude of the reaction forces developed on the spudcan foundations. For clayey strata, as the cone penetrates deeper into the soil, vertical forces increase. This increase is sharper until the cone fully penetrates into soil, in other words, maximum cone diameter meets the mudline. After it reaches the mudline, and penetrates into the soil with constant diameter, the trend of the increase in the vertical reaction forces slows down. These stages can be seen in all parametric studies presented in Chapter 5. However, as indicated in Chapter 4, a concept called “critical cavity depth” is one of the main factors that affects the reaction force variation. Here, analyses were conducted to understand the true effect of embedment.

Height of the cone is taken as 2.9 m whereas the cylindrical part at the top of the cone is taken as 5 m as shown in Figure 3.2. Three different embedment depths are chosen by taking the geometric properties of the spudcan, and the expected cavity depth into account. In order to capture the behavior at the desired level, the spudcan was penetrated into to soil for more than the preselected value of 12m embedment depth. In order not to be affected by the geometrical size of the model, vertical depth of the clay layer was extended for 10m while the horizontal extent was kept constant. Furthermore, characteristic element size, and mesh density were taken to be same as in the other analyses; however the number of elements increased due to the change in the geometry. Since the model size, and the penetration depth increased, computational time also increased.

Following figure (Figure 5.7) shows the results of the bearing capacity generated at the spudcan with respect to the depth of penetration.

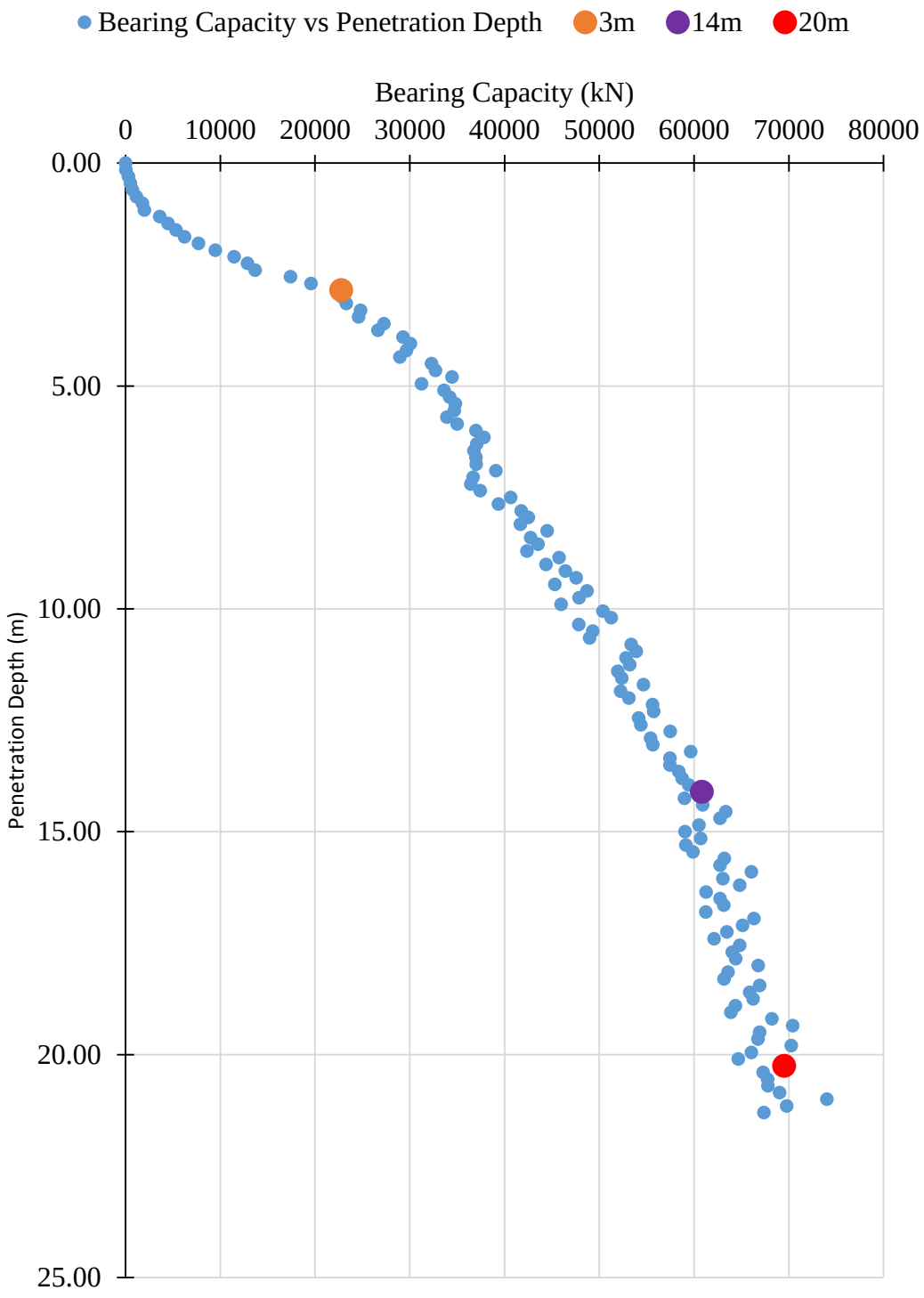

Figure 5.7 Penetration Depth vs Bearing Capacity Variety for 20m Embedment

On the graph, three different penetration depth – bearing capacity values are marked. Between (0,0) point, and orange mark (z = 3m), cone part of the spudcan penetrates into the ground, and as larger diameter meets the mudline, the reaction forces increase, tremendously. Figure 5.2, Figure 5.3, and Figure 5.4 show the vertical stress contours when the cone fully penetrates into the soil for different spudcan diameters. After the maximum diameter reaches the ground level, and the penetration goes on with a constant diameter, from orange mark (z = 3m) to purple mark (z =14m), the trend of increase changes. During this stage, the soil flows onto the mudline, and the vertical stress contours are shown in Figure 5.8, below

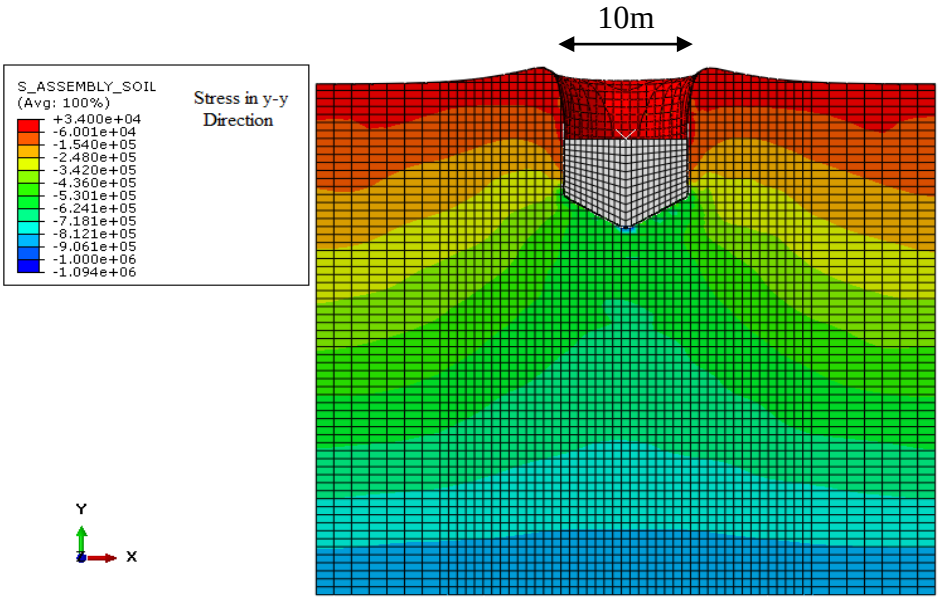

Figure 5.8 Vertical Stress Contours between 3m and 14m Depth of Penetration

As seen in Figure 5.8 as the spudcan penetrates into the ground, the flow takes place through the mudline, and surface heave occurs. The soil does not fall onto the spudcan at the edges (as it was also observed in Figure 2.11, in centrifuge model tests of M.S. Hossain & Randolph (2010b).

From Figure 5.7, another portion that needs some attention is the one between the purple mark (z = 14m) and red mark (z = 20m). In here, the increment in the bearing capacity slows down since the soil flow is around the spudcan instead of onto the mudline. (Figure 5.9.)

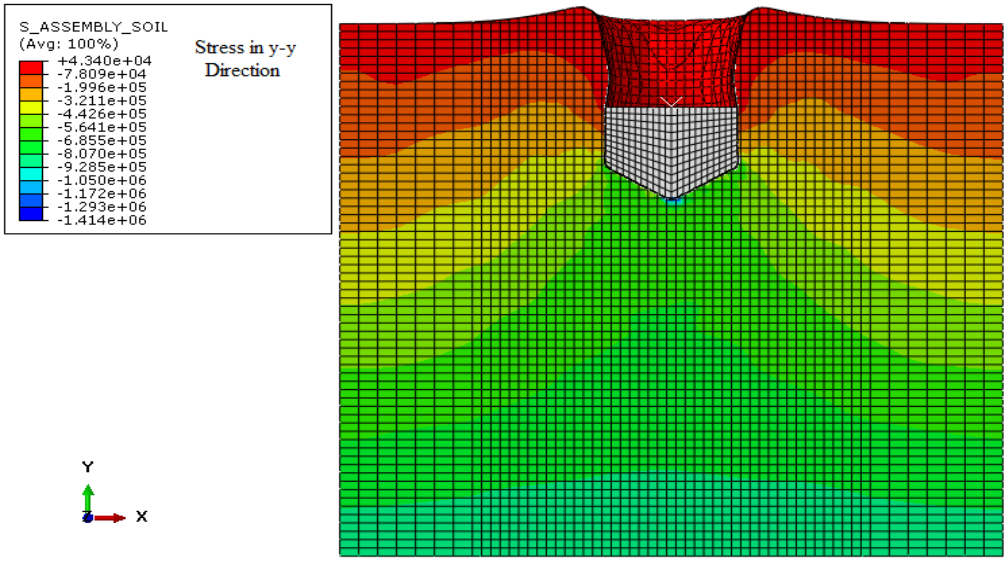

Figure 5.9 Vertical Stress Contours after 14m Depth of Penetration

As can be seen from the figure above, the soil at the edges where the spudcan enters, starts to flow onto the foundation. The depth that this behavior occurs can be defined as the critical cavity depth as stated in Chapter 4. This depth was found to be around 12m from the techniques given in InSafeJIP. By looking at the graph, however, it is around 14m.

InSafeJIP assumes that the change of the bearing capacity trend at the critical cavity depth is abrupt. However, same guide also states that in real life, this is not the case, and this change occurs smoothly (Osborne et al., 2011).

As the penetration continues, the soil also goes on flowing onto the foundation. Figure 5.10 shows how soil flows at the 21m depth onto spudcan from top view.

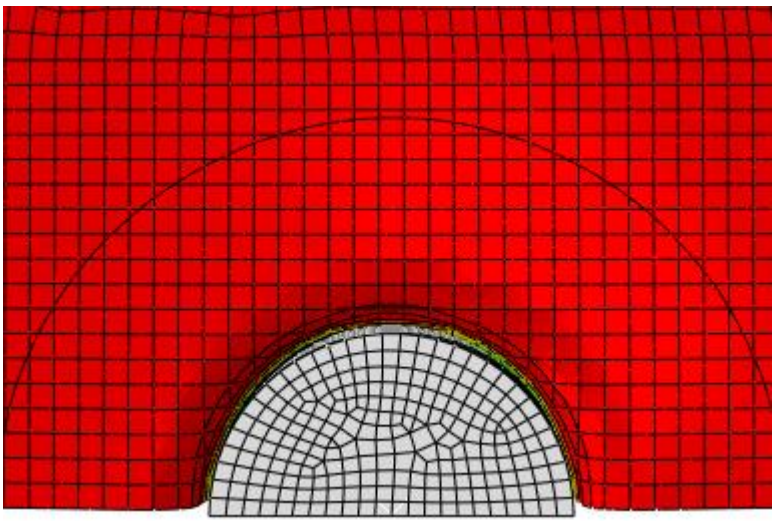

a)

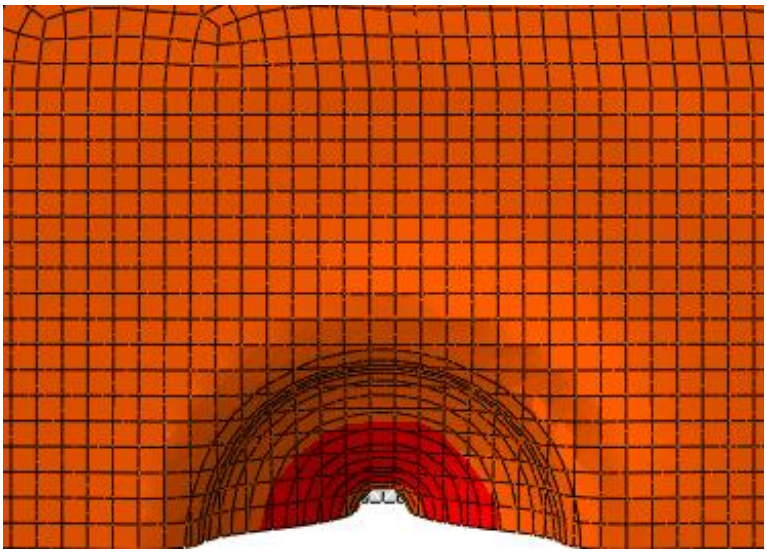

b)

Figure 5.10 Top View of the Penetration Area at a) 3m depth b) 21m depth

5.2.3.1 Discussion of Results

Since after the cavity depth, the increase in the vertical reaction forces occurs at a slower rate, one needs to take this into account in order to achieve the desired spudcan resistance. If the preload can be achieved after that depth, other factors affecting the bearing capacity can be considered to be changed to reduce required depth of penetration (since as this depth increases, there exist more risks because of the uncertainty in the behavior of soil and it is more expensive to penetrate spudcans into deeper zones).

5.2.4 Effect of the Undrained Shear Strength of the Soil

As indicated in (Knappett & Craig, 2012), base resistance of deep foundations, such as piles, can be calculated by treating them as embedded shallow foundations in deep strata, one can calculate the bearing capacity of a shallow foundation in undrained conditions by Equation 5.1

$$q_f = s_c * N_c * c_u + \sigma_q \tag{5.1}$$

where

- σ_q indicates the surcharge pressure on the foundation,
- N_c is the bearing capacity factor,
- s_c is the shape factor,
- c_u is the undrained shear strength of the soil.

Also, in the same book, it is stated that the shaft resistance can be found by Equation 5.2

$$\tau_{int} = \alpha * c_u \tag{5.2}$$

where

- c_u is the undrained shear strength of the soil,
- α is the adhesion factor that is in between 0 (fully smooth interface) and 1 (fully rough interface),

Therefore, the total bearing force will be the summation of these. (Equation 5.3)

$$Q_v = q_f * A_P + \tau_{int} * A_S \quad (5.3)$$

where

- A_P represents the base area of the foundation,
- A_S represents the side (skin) area of the pile foundation.

Equation 5.3 shows that the reaction force generated on the spudcan is directly proportional to the undrained shear strength c_u. Therefore it is expected that as it increases, the bearing pressure should also increase in our analyses.

In this part, three undrained shear strength values were used in order to demonstrate the effect. Undrained modulus of elasticity is also calculated for each model using the expression $E_U / C_U = 500$. Although this value changes depending on the plasticity and the overconsolidation state of the clay, it is assumed constant at 500 for simplicity

During the simulations, apart from the bearing resistance, one of the most important results is the change in the critical cavity depth. For softer clay, this depth is shallower than the stiffer clays as it is expected in Chapter 5.2.3. Figure 5.11 shows this depth for the clay having 20 kPa undrained shear strength.

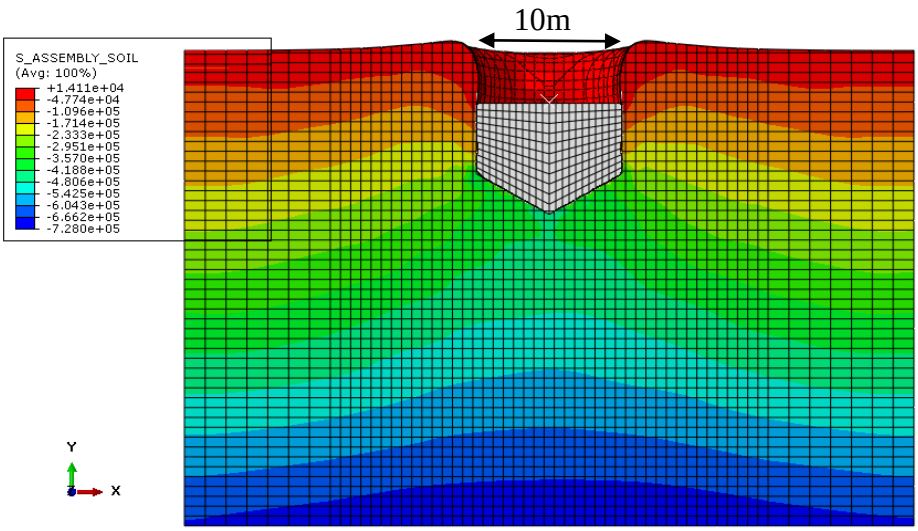

Figure 5.11 Cavity Depth for Cu = 20 kPa Clay

Figure 5.12 shows load-penetration curves for different undrained shear strength values.

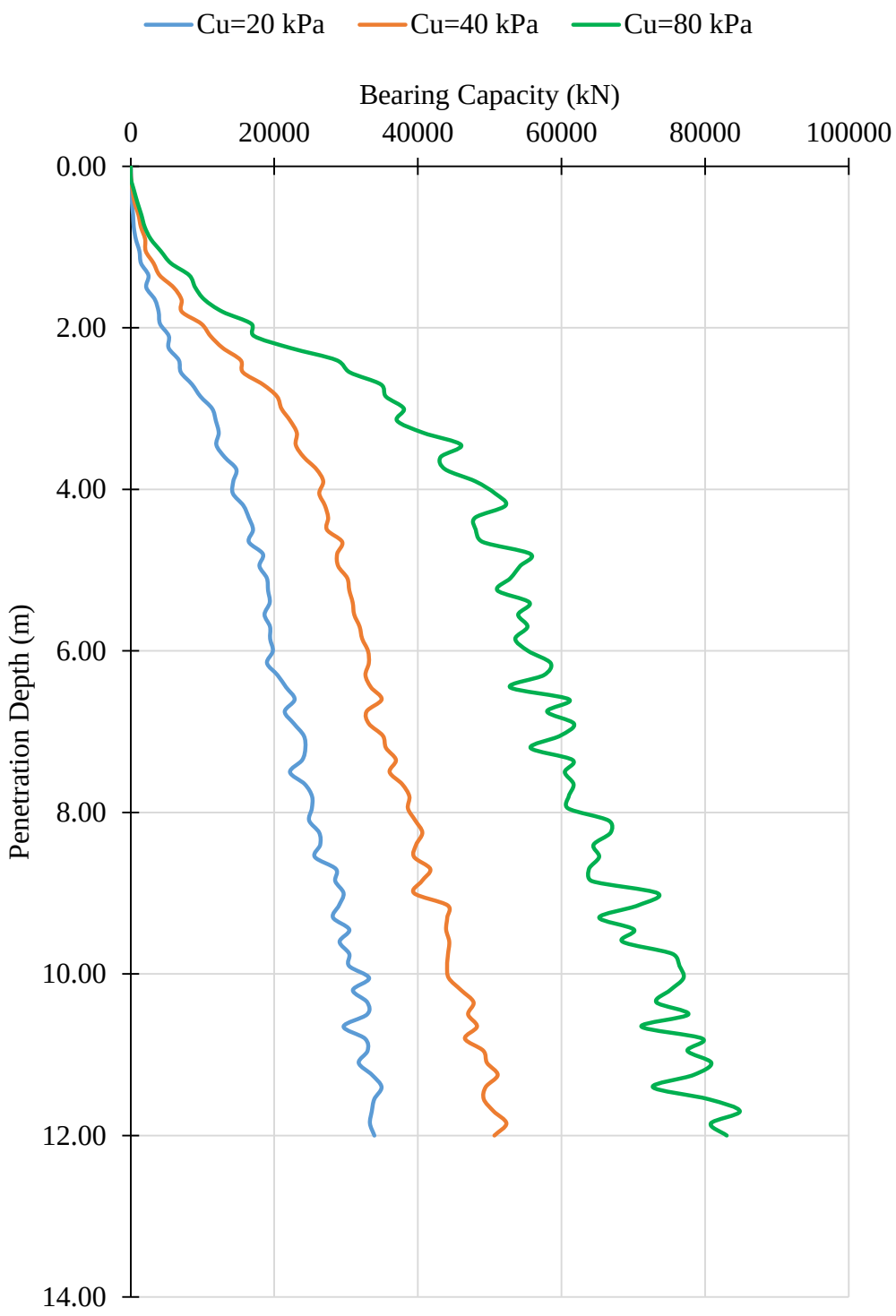

Figure 5.12 Vertical Load – Penetration Curves for Different Undrained Shear Strength

5.2.4.1 Discussion of Results

As it is indicated above, when undrained shear strength is 20 kPa, critical cavity depth reduces. In the graph in Figure 5.12, for the blue line (Cu = 20 kPa case), it can clearly be seen that around 10 meters of penetration depth, the line breaks, and changes its trend of increase due to backflow of the soil.

Furthermore, as it is expected, the penetration resistance increases as the undrained shear strength increases. Therefore, for stiffer soils, the preload capacity can be achieved at shallower depths, and for soft soils, it is possible not to reach that load by the spudcan with 10 m diameter. Increase in the diameter may be necessary.

5.2.5 Effect of the Surface Roughness Coefficient

Surface roughness coefficient is a property that governs the reaction forces on the spudcan foundation. This coefficient is affected by undrained shear strength of the soil, and the geometry and the material of the foundation (Knappett & Craig, 2012).

Since it affects the shear forces on the spudcan as stated in Equation 5.2, as it increases, an increase in the bearing capacity is expected. In this part of the study, three different surface roughness parameters were used.

It should also be noted that, as stated in Chapter 4, InSafeJIP (Osborne et al., 2011) suggested the use of $\alpha = 0.5$ for clayey soils unless there is information that enables the determination of it.

Figure 5.13 shows the vertical load – penetration curves for the spudcans with different roughness coefficients.

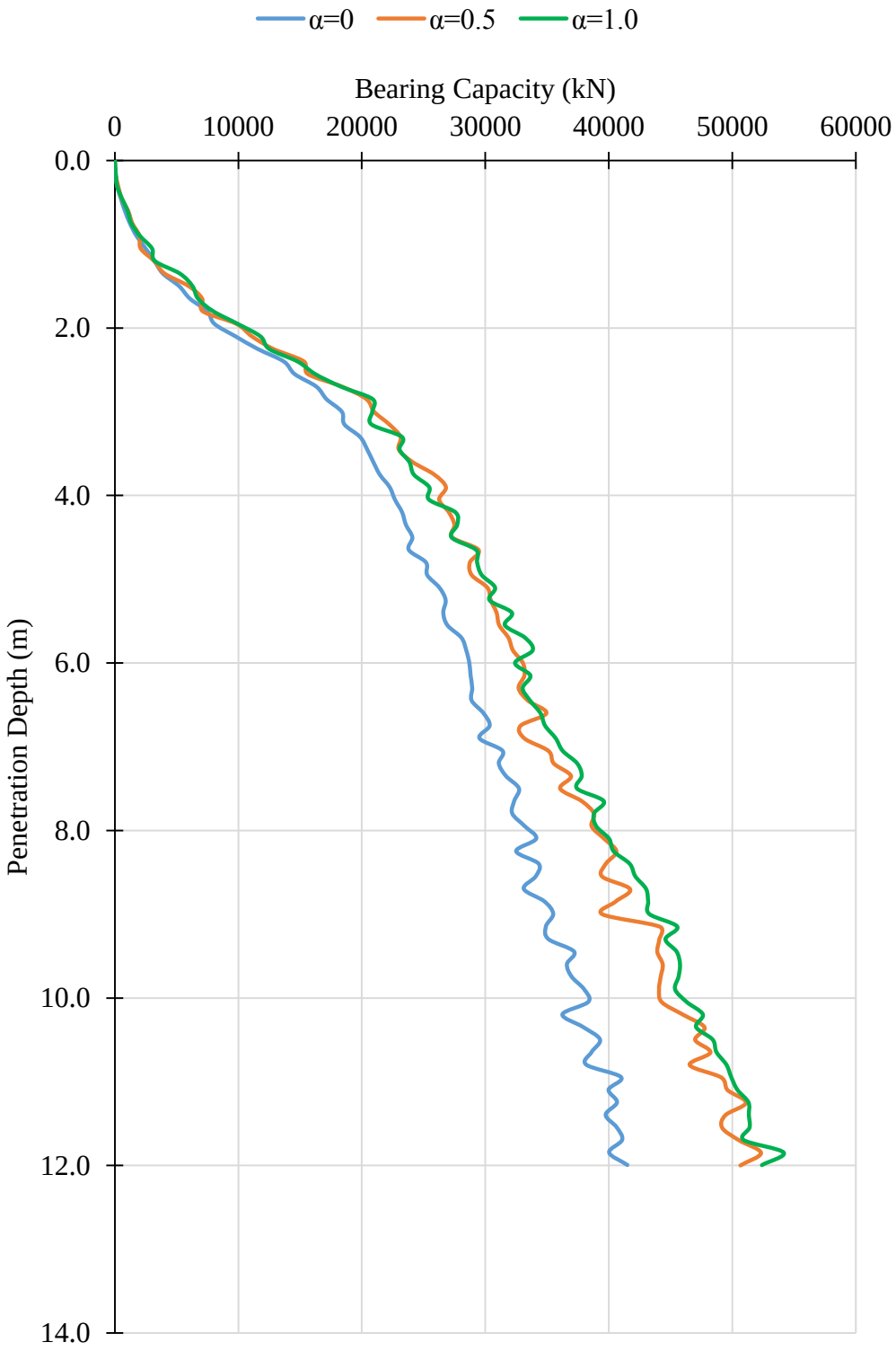

Figure 5.13 Vertical Load – Penetration Curves for Different Surface Roughness Coefficients

5.2.5.1 Discussion of Results

Figure 5.13 clearly states the effect of the surface roughness coefficient (α) on the vertical load – penetration behavior of the spudcans. For fully smooth case (α = 0), penetration resistance is much smaller than the other two cases. Although, there is a slight difference in between other two cases, they are very close to each other, giving almost the same bearing capacities. Therefore, this shows that "assumption of InSafeJIP about the roughness coefficient selection stating that for clayey layers, unless there is no information provided, α = 0.5 can be chosen for the calculation" is logical, and can be applicable to the calculations.

5.2.6 Effect of the Spacing/Diameter Ratio

One of the types of offshore oil platforms are jack-up rigs having generally three legs that are embedded onto the mudline as stated in Chapter 1. These legs touch the sea-bottom with giant spudcans in order to distribute the loads coming from the platform to larger areas. Since these spudcans can be embedded deeply into the soil, their behavior may be affected by the penetration process and the existence of each other.

This part of the study focuses on this issue. Spacing is defined from center-to-center of spudcans. Two spudcans with four different spacing/diameter ratios were penetrated into the clayey soil, simultaneously. The geometry of the model was adjusted so that the results were not affected by the boundary conditions.

Figure 5.14 shows the case where gravity load is applied just before the spudcans are penetrated into the soil. (S/D = 3)

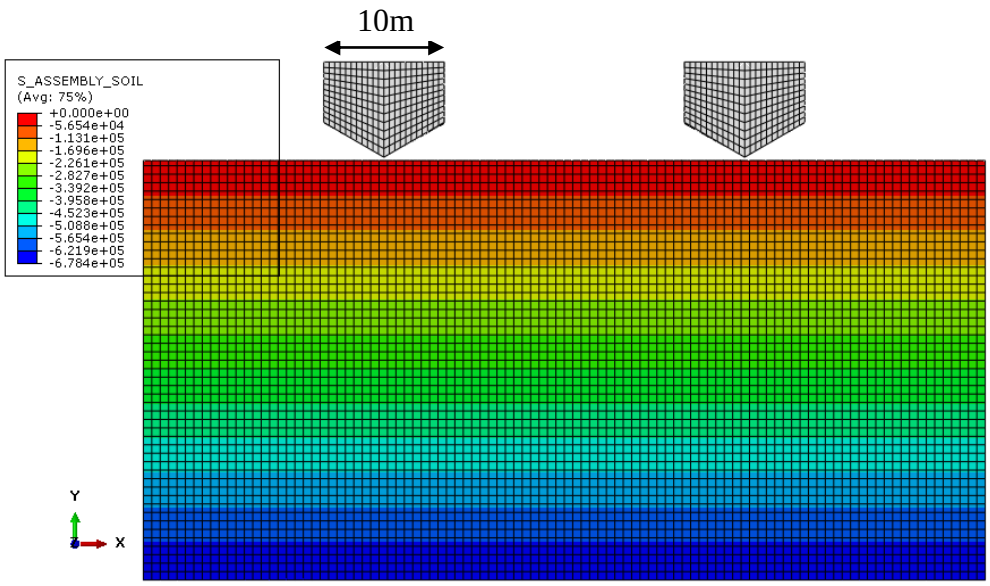

Figure 5.14 Initial Vertical Stress Conditions

Figure 5.15 shows the vertical stress contours when the cones of two spudcans are penetrated. (S/D = 3)

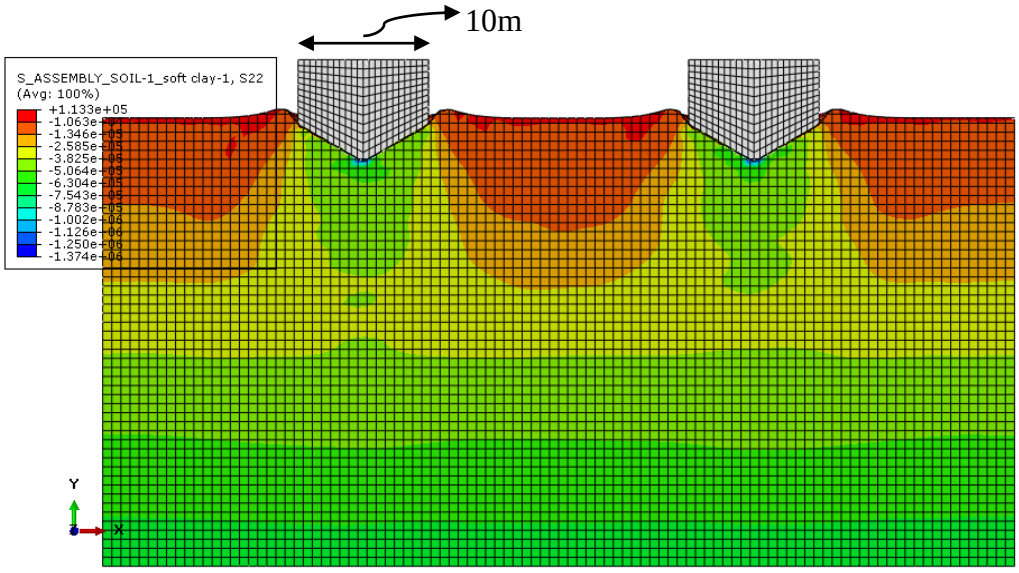

Figure 5.15 Vertical Stress Contours at the beginning of the Penetration

Vertical load – Penetration curves for each case are given in Figure 5.16. It can be seen that the results are not affected, critically. In order to give better idea about the change, trendlines are constructed for S/D=1.5, and S/D=3.0, and are shown in Figure 5.17

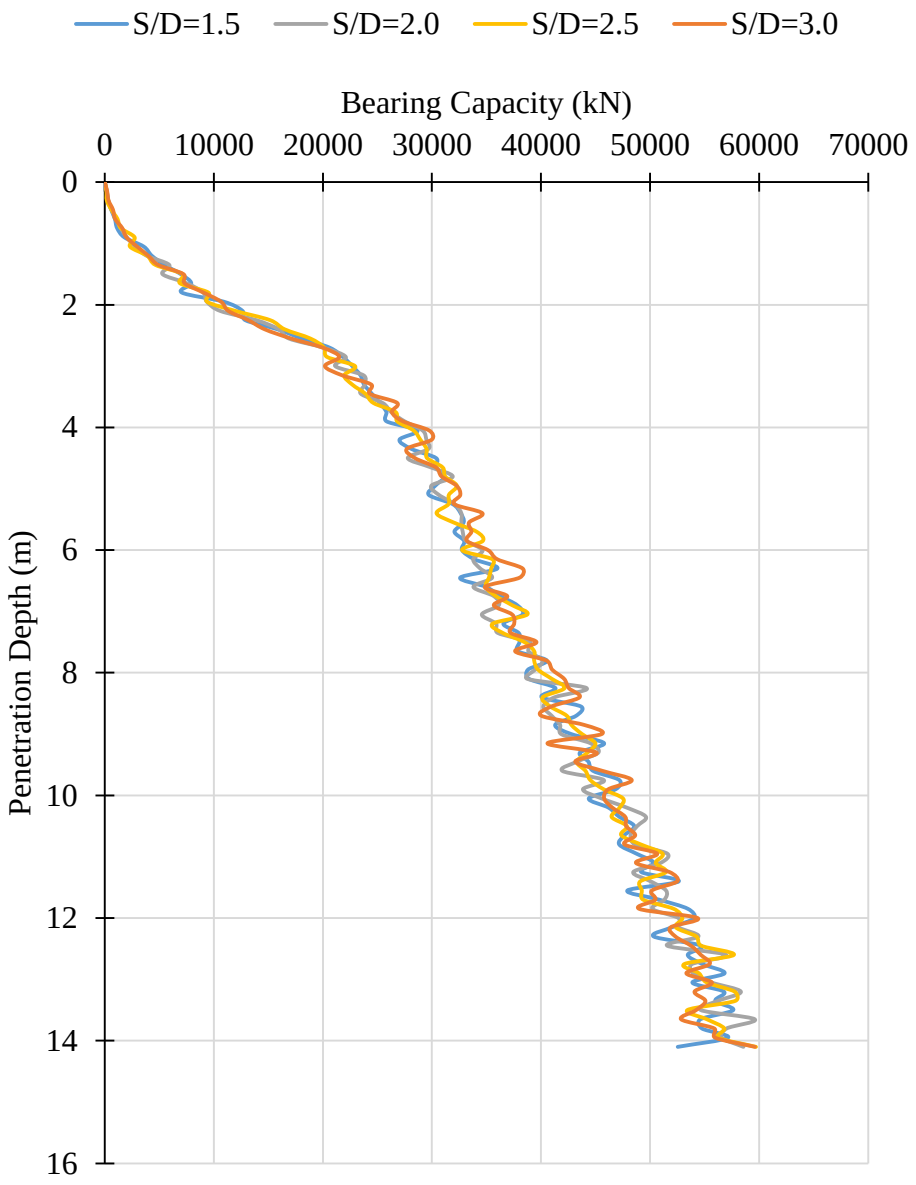

Figure 5.16 Vertical Load – Penetration Curves for Different S/D Ratios

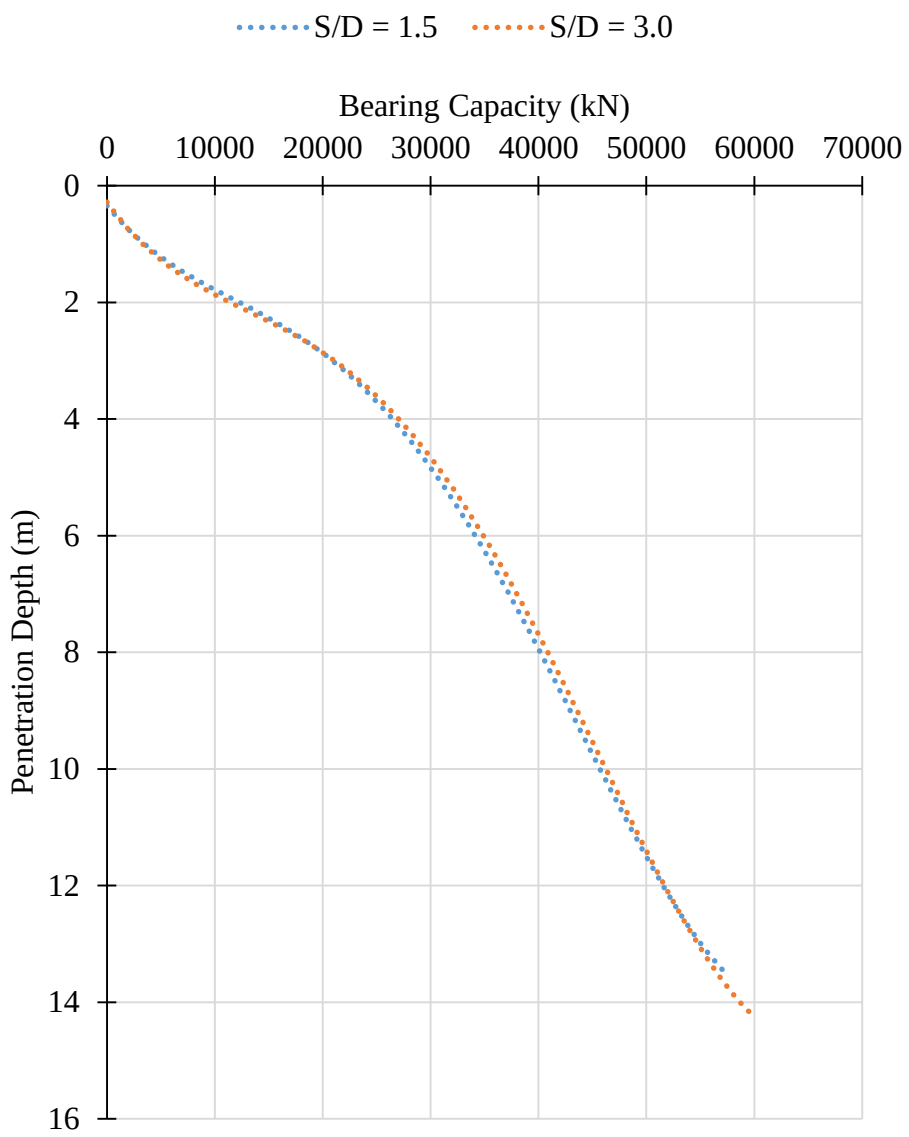

Figure 5.17 Vertical Load – Penetration Curves for S/D=1.5 and S/D=3.0

As it can be seen, the bearing capacity decreases for S/D=1.5 case; however, the change is negligibly low. Therefore, spacing of the spudcans is not an issue up to this value.

CHAPTER 6

DISCUSSION OF RESULTS AND CONCLUSIONS

In this thesis, the penetration of a foundation (spudcan) for "jack-up rig"-type offshore oil platform into a uniform clayey seabed is studied with three dimensional finite element modeling. Most of the failures observed in offshore oil platforms is not related with the superstructure but with the foundations of the platform. Typically, a bearing capacity failure is not observed in geotechnical engineering practice. However, this is not the case in offshore oil platforms. Therefore, in order to prevent any disasters, bearing capacity calculations' accuracy is very significant, especially for the offshore structures. Determining the soil profile correctly, understanding the soil behavior and correct numerical modeling could provide significant savings in the offshore foundation industry, due to the benefits such as reducing the required penetration depths of spudcans.

Although there exists some analytical methods (SNAME, InSafeJIP etc.) in the literature for calculation of the spudcan bearing capacity, they frequently underestimate or overestimate the bearing capacity due to simplifications involved in them. Therefore, the results based on such simplistic guidelines can sometimes be on the unsafe side (e.g. can result in disasters) or they could be on the very safe side (e.g. resulting in uneconomical designs, i.e. requiring too much penetration for developing sufficient bearing capacity). Furthermore, although there are numerous experimental and numerical studies in this topic in the literature, an understanding of the factors influencing the process and a study on determination of the required safe/economical penetration depth to achieve certain load bearing capacity of the spudcan was still missing. For analyses, 3D FEM software Abaqus 6.14 is used with Coupled Eulerian

Lagrangian (CEL) method. Methodology and steps followed in the study and related conclusions can be summarized as below:

- At the very beginning some of the questions we had were related with the setting up of the numerical model. For example: What should be the size of the model to use in 3D FEM? What should be the boundary conditions? What is the proper size for mesh elements considering the computation time and required / sufficient accuracy of the results? What should be the penetration velocity of the spudcan to be used in the numerical model etc. These issues are handled initially and the proper geometry model size, boundary conditions, mesh fineness etc are studied and determined. The total width of the numerical model space is selected as 5×diameter of the spudcan, the height of the model is almost 5×diameter of the spudcan, and FE mesh element size is chosen as 0.7 m (7% of the diameter of the spudcan) and penetration velocity is chosen as 15 cm/s.

- The next question to be answered was, whether our 3D FE CEL solution could accurately calculate the spudcan penetration resistance value and the resistance behavior with depth. Since there are no well-instrumented and well-documented spudcan penetration case studies in the literature, the methods depicted in InSafeJIP (Osborne et al., 2011) were used to validate our results obtained numerically. The existing laboratory model tests in the literature do not include sufficient detail about material properties and testing procedures (some of the information is missing/not reported) in order for us to numerically model those cases. It was not possible to validate the numerical results with the measured penetration-depth graphs of real spudcans. Because, many companies do not publicly share their real measured penetration resistance versus depth data due to the competitive nature of the technological developments in the offshore industry.

- Undrained analyses were conducted for the seabed consisting of clay since this condition is more critical as compared to long term drained behavior. Although more comprehensive constitutive models are available in the FE software, elastic – perfectly plastic Mohr Coulomb failure criterion was adopted in all the analyses in this thesis.

Mohr-Coulomb model is preferred since: (1) it is a simple model that is sufficient for the purposes of this study. The main objective of this study is to extend our understanding of the spudcan penetration process using a minimum number of variables. For this purpose, the Mohr Coulomb failure criterion seems to be sufficient. (2) The number of input parameters required for other constitutive models are much more, and their values are relatively more difficult to estimate based on typical offshore geotechnical site investigations and lab testing. Of course more sophisticated sampling and lab testing carried out in research labs can provide those constitutive model parameters if preferred. (3) This methodology (3D FE CEL) could be used by practicing engineers; therefore, choosing a simpler constitute model such as Mohr-Coulomb would make the usability of the method and determination of the material properties of that constitutive model relatively easier.

- 3D FEM CEL methodology (with Abaqus 6.14) can predict bearing capacity of spudcans, similar to InSafeJIP, however with certain differences. As compared to simplified calculation methods presented in guidelines such as InSafeJIP (which typically consider N_c bearing capacity factor), use of FEM provides significant benefits for variable/complex site soil and spudcan geometrical conditions. Hand-calculations using InSafeJIP guidelines and 3D FEM CEL methods give very similar spudcan penetration resistance values, up to where the cone is fully penetrated. After this depth, as compared to InSafeJIP, 3D FEM calculations seem to be giving larger penetration resistance at the same depth. The difference between the two predictions is on the order of 50%. This could also be interpreted in terms of the required penetration depth for a target bearing capacity. Comparing the calculations presented in Chapter 4, for example, up to a depth of 6 m, 3D FEM calculations indicate a savings in the required penetration depth, on the order of 2 m, whereas after about 6 m depth, the savings could be on the order of 4 m or more. Therefore, the benefit is much stronger, i.e. savings is larger especially for deeper penetrating spudcans. Furthermore, the rate of increase of the spudcan bearing capacity with depth is larger in 3D FEM calculations as compared to InSafeJIP method (e.g. rate of increase of spudcan penetration is 2100 kN/m in

InSafeJIP, and 3800 kN/m using 3D FEM solution). Therefore 3D FEM CEL method can successfully be used to predict the spudcan penetration resistance with depth as well as the deformations developing in the soil (if needed).

- The other question we had was related with the factors affecting the penetration resistance of the spudcan and their effects. Therefore, a systematic parametric study was conducted. Because of the complexity of the interaction between the penetrating spudcan and the seabed, the problem involves a considerable number of variables. Some of the variables that are investigated in this thesis were spudcan diameter (7.5, 10, 12.5 and 15 m), spudcan cone angle (90, 120, 150 degrees), roughness of spudcan surface (roughness coefficient of 0, 0.5 and 1.0), undrained shear strength of clay (20, 40, 80 kPa), spudcan penetration depth (3, 12, 20 m), and the spacing between two adjacent spudcans (spacing/diameter ratio of 1.5, 2.0, 2.5, 3.0).

- An increase in the spudcan cone angle, while keeping the diameter constant, decreases the required penetration depth to reach the desired bearing capacity. Using a 150-degree cone angle can provide savings in the penetration depth of the spudcan on the order of 2 to 4 m, as compared to a 90-degree cone, for a given target bearing capacity to achieve. Therefore, when deep penetration is hard due to the existence of deep-water or uncertainties due to insufficient site data for deeper soil strata, it is sensible to use spudcans with high cone angles. Sometimes, softer soil layers could be present under the upper stiffer layers, and for these kinds of cases, punch-through may present itself as a major problem during penetration. This can also be viewed as a loss of stability of the spudcan due to the collapse of the underlying weak layer. For these cases, it is also better to reach the desired bearing capacity at shallow embedment depths with larger cone angle values.

- It is inevitable that, the diameter of the spudcan will affect the bearing capacity significantly, as in the case of footing size effect for bearing capacity of the foundations of buildings. In this study, this effect is quantified by using four common spudcan diameters (ranging from 7.5 to 15 m) found in the literature. For a constant cone angle, change in the diameter results in an increase in the height of the cone, which means that

when the cone of the foundation is fully penetrated into the soil, bearing capacity becomes larger than bearing capacity of smaller dimensions. This can also be interpreted in terms of the penetration depth required for a target bearing capacity. For example, for a target bearing capacity of 50000 kN, a penetration depth of 7 m is required for a spudcan diameter of 10 m, whereas 11 m is required for a spudcan diameter of 12.5 m. In other words, 1.5 times more bearing capacity can be achieved for a given depth of penetration (for example 5 m) when we use a spudcan with a diameter of 12.5 m instead of 10 m. As the diameter of the spudcan increases, the height of the cone increases (in this study, from approximately 2 meters to 4.5 meters for spudcan diameters of 7.5 and 15 m, respectively). Since this is the critical depth at which the rate of increase of resistance decreases, it is beneficial to have this "critical depth" at a deeper point, therefore it is beneficial to use larger diameter spudcan.

- As the undrained shear strength of the clay increases, the bearing capacity increases, as expected. For a 4 times increase in C_U value, approximately 2 times increase in bearing capacity is calculated for a given depth of penetration (for Cu in the range of 20 and 80 kPa). For a given target bearing capacity, the required depth of penetration could be saved by 4 m or more, when comparing a clay with C_U value of 20 kPa and 40 kPa. For very soft clays, it may not be possible to reach to a desired target load unless diameter or other factors are changed as well. For softer clay, as compared to stiffer clays, critical cavity depth is shallower than the stiffer clays.

- For fully smooth spudcan surface case (roughness coefficient, $\alpha = 0$), penetration resistance is much smaller than the rough surfaces ($\alpha = 0.5$ and 1.0). Although, there is a slight difference in between other two cases, they are very close to each other, giving almost the same bearing capacities. Therefore, this shows that "assumption of InSafeJIP about the roughness coefficient selection stating that for clayey layers, unless there is no information provided, $\alpha = 0.5$ can be chosen for the calculation" is logical, and can be applicable to the calculations. As the surface roughness increases, the spudcan penetration resistance increases as expected, however very slightly. This can be obtained by InSafeJIP method and with 3D FEM study via Abaqus in this thesis.

- Offshore jack-up rigs typically have three legs inserted in close proximity to each other. In this thesis, two spudcans with four different spacing/diameter ratios (1.5 to 3) were penetrated into the clayey soil, simultaneously to observe the effects. The penetration depth versus bearing capacity plots did not seem to be significantly affected by the spacing, for the spacings used in this parametric study.

- The results of this study is only valid for the spudcan geometry and soil properties used in this study. They should not be generalized.

- Investigation of the aforementioned factors and understanding the relations between them will provide a significant step in enhancing the safe and economical design and successful penetration operation of spudcans. It should not be forgotten that, the key element with utmost importance is to have extensive and correct information and interpretation about the subsoil profile and their material properties.

Possible future study topics:

- Typical properties of undrained shear strength of sea-bottom clayey soils could be further studied to develop an understanding of the sensitivity, anisotropy, rate effects, peak/residual shear strength, whether the undrained shear strength is typically constant (uniform) or increasing with depth, the rate of increase of shear strength with depth etc. and the effects of all of these issues on the spudcan penetration process could be studied.

- Spudcan penetration process for sandy / silty seabed soils could be investigated. Furthermore, multi-layer soil profiles with different stiffnesses could be studied especially dealing with the common “punch through” problem in strong over weak seabed soils.

- Effect of the soil constitutive model used in FE modeling could be investigated further.

- Shape & geometry effects of the spudcan on the resistance could be investigated to develop an optimum shape.

- Detailed laboratory (1g and centrifuge) spudcan penetration physical models with extensive instrumentation and real life spudcan penetration data are very valuable and should be conducted and presented to provide an advancement in offshore geotechnical studies.

REFERENCES

Arabdrill 19 AD19 - Oil Rig Disasters - Offshore Drilling Accidents. (2002). Retrieved June 4, 2015, from http://home.versatel.nl/the_sims/rig/ad19.htm

Characterization of Undrained Shear Strength Profiles for Soft Clays at Six Sites in Texas. (2008). Retrieved July 7, 2015, from http://www.utexas.edu/research/ctr/pdf_reports/0_5824_2.pdf

Chi, C., Aubeny, C. P., & Zimmerman, E. H. (2009). Stability assessment of spudcan foundation. *OCEANS 2009, MTS/IEEE Biloxi - Marine Technology for Our Future: Global and Local Challenges*, (Table 1).

Craig, W. H. (1991). Deep penetration of spud-can foundations, (4), 541–556.

De Groot, D. J. (2011). Geotechnical Site Characterization: Cohesive Offshore Sediments. Amherst.

Dean, E. T. R. (2010). *Offshore geotechnical engineering. Principles and practice*.

Elkadi, A. S. K., Lottumand, H. van, & Luger, H. J. (2014). A 3D coupled Eulerian-Lagrangian analysis of the dynamic interaction of jack-up legs with the seabed. *Numerical Methods in Geotechnical Engineering*, 1255–1259.

Engin, H. K., Brinkgreve, R. B. J., & van Tol, F. (2015). Simplified numerical modelling of pile penetration – the press-replace technique. *International Journal for Numerical and Analytical Methods in Geomechanics*.

Hossain, M. S., & Dong, X. (2014). Extraction of Spudcan Foundations in Single and Multilayer Soils. *Journal of Geotechnical & Geoenvironmental Engineering*, *140*(1), 170–184. http://doi.org/10.1061/(ASCE)GT.1943-5606.0000987

Hossain, M. S., & Randolph, M. F. (2009). New Mechanism-Based Design Approach for Spudcan Foundations on Single Layer Clay. *Journal of Geotechnical and Geoenvironmental Engineering*, *135*(9), 1264–1274. http://doi.org/10.1061/(ASCE)GT.1943-5606.0000054

Hossain, M. S., & Randolph, M. F. (2010a). Deep-penetrating spudcan foundations on layered clays: centrifuge tests. *Géotechnique*, *60*(3), 171–184. http://doi.org/10.1680/geot.8.P.040

Hossain, M. S., & Randolph, M. F. (2010b). Deep-penetrating spudcan foundations on layered clays: numerical analysis. *Géotechnique*, *60*(3), 171–184. http://doi.org/10.1680/geot.8.P.040

Hu, Y., Randolph, M. F., Hossain, M. S., & White, D. J. (2005). Limiting cavity depth for spudcan foundations penetrating clay. *Géotechnique*, *55*(9), 679–690. http://doi.org/10.1680/geot.2005.55.9.679

Jack-up rigs. (n.d.). Retrieved June 14, 2015, from http://www.eurasiadrilling.com/operations/offshore/jack-up-rigs/

Knappett, J. A., & Craig, R. F. (2012). *Craig's Soil Mechanics* (8th ed.). Oxon: Spon Press.

Lee, J., & Randolph, M. (2011). Penetrometer-Based Assessment of Spudcan Penetration Resistance. *Journal of Geotechnical and Geoenvironmental Engineering*, *137*(6), 587–596. http://doi.org/10.1061/(ASCE)GT.1943-5606.0000469

Letourneau Design, Super Gorilla XL. (2015). Retrieved July 7, 2015, from http://www.issmge.org/en/technical-committees/applications/154-offshore-geotechnics

Leung, C. F., Purwana, O. a., Chow, Y. K., & Foo, K. S. (2005). Influence of base suction on extraction of jack-up spudcans. *Géotechnique*, *55*(10), 741–753. http://doi.org/10.1680/geot.2005.55.10.741

Maersk Interceptor. (n.d.). Retrieved from http://www.maerskdrilling.com/en/drilling-rigs/jack-ups/maersk-interceptor

Martin, C. M., & Houlsby, G. T. (2003). Undrained bearing capacity factors for conical footings on clay. *Géotechnique*, *53*(5), 513–520. http://doi.org/10.1680/geot.2003.53.5.513

McLendon, R. (2010). Types of offshore oil rigs | MNN - Mother Nature Network. Retrieved June 6, 2015, from http://www.mnn.com/earth-matters/energy/stories/types-of-offshore-oil-rigs

Morrow, D. R., & Bransby, M. F. (2011). Pipe-soil interaction on clay with a variable shear strength profile. *Frontiers in Offshore Geotechnics II*, 822.

Osborne, J. J., Teh, K. L., Houlsby, G. T., Cassidy, M. J., Bienen, B., & Leung, C. F. (2011). *"InsafeJIP" Improved Guidelines for the Prediction of Geotechnical*

Performance of Spudcan Foundations During Installation and Removal of Jack-Up Units. Surrey.

Punch-Through of Jack-Up Spudcan Foundation in Sand Overlying Clay. (2008). Retrieved June 3, 2015, from http://www.eng.nus.edu.sg/EResnews/0806/rd/rd12.html

Qiu, G., & Henke, S. (2011). Controlled installation of spudcan foundations on loose sand overlying weak clay. *Marine Structures*, *24*(4), 528–550. http://doi.org/10.1016/j.marstruc.2011.06.005

SIMULIA. (2010). Formulation of Eulerian-Lagrangian contact. In *Abaqus 6.10 Analysis User's Manual Volume II: Analysis* (p. 1079).

SNAME. (2008). *Guidelines for Site Specific Assessment of Mobile Jack-Up Units*. Jersey City.

Terzaghi, K., Peck, R. B., & Mesri, G. (1996). *Soil Mechanics in Engineering Practice*.

Tho, K. K., Leung, C. F., Chow, Y. K., & Swaddiwudhipong, S. (2012). Eulerian Finite-Element Technique for Analysis of Jack-Up Spudcan Penetration. *International Journal of Geomechanics*, *12*(1), 64–73. http://doi.org/10.1061/(ASCE)GM.1943-5622.0000111

UWA team to investigate new footings for mobile drilling rigs | Energy and Minerals Institute. (n.d.). Retrieved July 11, 2015, from http://www.emi.uwa.edu.au/news/uwa-team-investigate-new-footings-mobile-drilling-rigs-0

WIND CARRIER - SPUDCAN. (2011). Retrieved May 6, 2015, from http://www.nash-eng.com/projects.html#!prettyPhoto

Yi, J. T., Lee, F. H., Goh, S. H., Zhang, X. Y., & Wu, J. F. (2012). Eulerian finite element analysis of excess pore pressure generated by spudcan installation into soft clay. *Computers and Geotechnics*, *42*, 157–170. http://doi.org/10.1016/j.compgeo.2012.01.006

Yu, L., Hu, Y., Liu, J., Randolph, M. F., & Kong, X. (2012). Numerical study of spudcan penetration in loose sand overlying clay. *Computers and Geotechnics*, *46*, 1–12. http://doi.org/10.1016/j.compgeo.2012.05.012

Zhang, J., Tang, W., Su, S., Qin, W., Wang, J., & Liu, R. (2013). Numerical analysis and verification of pile penetration into stiff-over-soft clay. *Petroleum Exploration and Development*, *40*(4), 526–530. http://doi.org/10.1016/S1876-3804(13)60068-3

Zhang, Y., Wang, D., Cassidy, M. J., & Bienen, B. (2014). Effect of Installation on the Bearing Capacity of a Spudcan under Combined Loading in Soft Clay. *Journal of Geotechnical and Geoenvironmental Engineering*, (2013), 1–12. http://doi.org/10.1061/(ASCE)GT.1943-5606.0001126.